HARVESTING ELECTRICITY FROM FUNGAL FUEL CELL FED WITH LIGNOCELLULOSIC WASTE

BY

WAN NUR ASIAH BINTI WAN MOHD SUKRI

A thesis submitted in fulfilment of the requirement for the degree of Doctor of Philosophy in Engineering

Kulliyyah of Engineering

International Islamic University Malaysia

OCTOBER 2024

ABSTRACT

Microbial fuel cell (MFC) suffers from low energy gain yield (output/cost) and is unsuitable for most practical implementations. Microbial zinc/air cell employing freely suspended white rot fungal *Phanerochaete chrysosporium* fed with empty fruit bunch (EFB) has demonstrated promising prospects as a sustainable MFC. This work aimed to increase the energy gain yield of the system by minimizing external control features, implementing low-cost design, and increasing the energy output. To fulfil the power output for most low-power applications, multiple MFCs need to be connected in a stacking configuration. However, the variation in individual MFC's electromotive force (e.m.f) due to living microbes activities induces parasitic currents in parallel configuration. This work introduced a novel open-parallel unit-cell configuration for MFC stacking. All unit cells were connected in parallel configuration but hydrodynamically connected i.e. they shared a common electrolyte. Using this configuration, the discharge capacity of the MFC stack was extended 3.4 times, the total power output was increased by 2.6 times compared to the common parallel configuration, and the parasitic current was effectively eliminated. The microbial zinc/air cell is an air-cathode MFC. The air cathode is the most expensive component in an air-cathode MFC and, in most cases, requires an air aeration system. Therefore, this work designed and fabricated a low-cost and easy-to-fabricate air cathode. It is low cost because it is non-catalytic and the fabrication did not require special processes, only mere mechanical press of the cell holders. Further, the air cathode components of carbon felt, carbon fibre sheet and nickel mesh, were designed for operating under submerged conditions and depending only on dissolved oxygen. Therefore, air aeration is not required. The proposed air cathode was capable of sustaining a discharge current of 1 mA for 42 days (1008 mAh) under submerged conditions thus supporting its viability. Aside from the low-cost design, the cylindrical air cathode configuration also offers the advantage of compact multipolar design. Since the microbial zinc/air cell was fed with lignin rich EFB as a substrate for *Phanerochaete chrysosporium*, this work assessed its efficacy as a lignin rich agrowaste degradation cell. The rates of lignin degradation were evaluated under self-generated current and externally supplied current. It was found that electric current stimulus enhances the lignin degradation. Externally supplied current induced higher lignin degradation. However, when the current supplied was 5 mA or higher, it disrupted the lignin degradation rates.

ملخص البحث

تعاني خلايا الوقود الميكروبية (MFC) من انخفاض إنتاجية اكتساب الطاقة (الناتج / التكلفة) وهي غير مناسبة لمعظم التطبيقات العملية. أظهرت خلايا الزنك / الهواء الميكروبية التي تستخدم فطريات العفن الأبيض المعلقة بحرية – تعرف باسم *Phanerochaete chrysosporium* – والتي تتغذى على عاقيد الفاكهة الفارغة (EFB) آفاقا واعدة باعتبارها خلايا وقود ميكروبية مستدامة. يهدف هذا العمل إلى زيادة إنتاجية اكتساب الطاقة للنظام عن طريق تقليل ميزات التحكم الخارجي الى الحد الأدنى ، وتنفيذ تصميم منخفض التكلفة ، وزيادة إنتاج الطاقة. لتحقيق مخرجات الطاقة لمعظم التطبيقات منخفضة الطاقة، يجب توصيل العديد من MFCs في تكوين تكديس. ومع ذلك ، فإن الاختلاف في القوة الدافعة الكهربائية الفردية (e.m.f) لخلايا MFC بسبب أنشطة الميكروبات الحية يحفز التيارات الطفيلية في التكوين المتوازي. قدم هذا العمل تكوينًا جديدًا لخلية وحدة متوازية ومفتوحة لتكديس MFC. كانت جميع خلايا الوحدة متصلة في تكوين متوازي ولكنها متصلة هيدروديناميكيًا أي أنها تشترك في إلكتروليت مشترك. باستخدام هذا التكوين، تم تمديد سعة التفريغ لمكدس 3.4 MFC مرة، وتم زيادة إجمالي انتاج الطاقة بمقدار 2.6 مرة مقارنة بالتكوين المتوازي المشترك، وتم القضاء على التيار الطفيلي بشكل فعال. إن خلية الزنك / الهواء الميكروبية هي عبارة MFC بكاثود هوائي. الكاثود الهوائي هو أغلى مكون في الكاثود الهوائي MFC، وفي معظم الحالات، يتطلب نظام تهوية الهواء. لذلك، في هذا العمل تم تصميم وتصنيع كاثود هوائي منخفض التكلفة وسهل التصنيع. يرجع انخفاض نكلفته لأنه غير محفز ولم يتطلب التصنيع عمليات خاصة ، فقط مجرد ضغط ميكانيكي لحاملي الخلايا. علاوة على ذلك ، تم تصميم مكونات كاثود الهواء من لباد الكربون وألواح ألياف الكربون وشبكة النيكل للعمل في ظل ظروف مغمورة والاعتماد فقط على الأكسجين المذاب. لذلك ، تهوية الهواء غير مطلوبة. كان كاثود الهواء المقترح قادرا

على الحفاظ على تيار تفريغ قدره 1 مللي أمبير لمدة 42 يوما (1008 مللي أمبير في الساعة) في ظل ظروف مغمورة مما يدعم صلاحيته. بصرف النظر عن التصميم منخفض التكلفة ، يوفر تكوين كاثود الهواء الأسطواني أيضا ميزة التصميم المدمج متعدد الأقطاب. نظرًا لأن خلية الزنك / الهواء الميكروبية تم تغذيتها بمركب EFB الغني بالليجنين كركيزة لـ *Phanerochaete chrysosporium*، فقد قيم هذا العمل فعاليته كخلية تحلل زراعي غنية بالليجنين. تم تقييم معدلات تدهور اللجنين في ظل التيار المولد ذاتيًا والتيار المورد خارجيًا. وجد أن تحفيز التيار الكهربائي يعزز تدهور اللجنين. أدى التيار المورد خارجيًا إلى تحلل أعلى للجنين. ومع ذلك، عندما كان التيار المورد 5 مللي أمبير أو أعلى، فقد عطل معدلات تحلل اللجنين.

APPROVAL PAGE

The thesis of Wan Nur Asiah Binti Wan Mohd Sukri has been approved by the following:

……..
Raihan Bin Othman
Supervisor

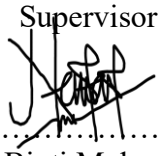

……..
Noraini Binti Mohamed Noor
Co-Supervisor

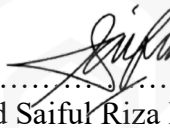

……..
Mohd Saiful Riza Bin Bashri
Co-Supervisor

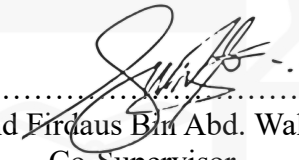

……..
Mohd Firdaus Bin Abd. Wahab
Co-Supervisor

……..
Mohammed Saedi Jami
Internal Examiner

……..
Ahmad Azmin Mohamad
External Examiner

……..
Adamu Abubakar Ibrahim
Chairman

DECLARATION

I hereby declare that this thesis is the result of my own investigations, except where otherwise stated. I also declare that it has not been previously or concurrently submitted as a whole for any other degrees at IIUM or other institutions.

Wan Nur Asiah Binti Wan Mohd Sukri

Signature…… Date 24/01/2024……...

INTERNATIONAL ISLAMIC UNIVERSITY MALAYSIA

DECLARATION OF COPYRIGHT AND AFFIRMATION OF FAIR USE OF UNPUBLISHED RESEARCH

HARVESTING ELECTRICITY FROM FUNGAL FUEL CELL FED WITH LIGNOCELLULOSIC WASTE

I declare that the copyright holder of this thesis are jointly owned by the student and IIUM.

By signing this form, I acknowledge that I have read and understand the IIUM Intellectual Property Right and Commercialization policy.

Affirmed by Wan Nur Asiah Binti Wan Mohd Sukri

…….. 24/01/2024

Signature Date

ACKNOWLEDGEMENTS

All glory is due to Allah, the Almighty, whose Grace and Mercies have been with me throughout the duration of my programme. Although, it has been tasking, His Mercies and Blessings on me ease the herculean task of completing this thesis.

I would like to express my greatest gratitude to my project supervisor Dr. Raihan Othman for his patience, kindness, and willingness to spend his precious time in guiding me throughout this project. I would also like to express my thankfulness to my co-supervisors, Dr. Noraini Mohamed Noor, Dr. Mohd Saiful Riza Bin Bashri, and Dr Mohd Firdaus Bin Abd. Wahab for their advice and support in making this research an accomplishment.

Besides that, I would like to express my deepest love and thanks to my beloved mother and siblings who have continuously given their support throughout this project. I also would like to thank my beloved late father for the teachings he left and for laying the foundation of what I turned out to be in life.

Finally, many thanks to all individuals who's not mentioned here for their direct or indirect help for completion of this work.

TABLE OF CONTENTS

LIST OF TABLES

LIST OF FIGURES

LIST OF ABBREVIATIONS

AgNP	Silver nanoparticles
APAP	Acetaminophen
BFC	Biofuel cell
CCV	Closed circuit voltage
CE	Coulombic efficiency
COD	Chemical oxygen demand
DO	Dissolved oxygen
DIC	Dissolved inorganic carbon
DBL	Diffusion boundary layer
DET	Direct electron transfer
EFB	Empty fruit bunch
GDL	Gas diffusion layer
KCL	Kirchhoff's current law
KVL	Kirchhoff's voltage law
LiP	Lignin peroxidase (LiP)
MET	Mediated electron transfer
MFC	Microbial fuel cell
MnPs	Manganese peroxidase
OCV	Open circuit voltage
OPF	Oil palm fond
OPKS	Oil palm kernel shell
OPT	Oil palm trunk
ORR	Oxygen reduction reaction
PACF	Polyacrylonitrile carbon felt
PAP	4-aminophenol
PDA	Potato dextrose agar
PDB	Potato dextrose broth
PDMS	Poly(dimethylsiloxane)
PEM	Proton exchange membrane
PMU	Power management unit
POME	Palm oil mill effluent
PTFE	Polytetrafluoroethylene
PVC	Polyvinyl chloride
PVDF	Poly(vinylidene fluoride)
SEM	Scanning electron microscope
VP	Versatile peroxidase
WRF	White rot fungi

LIST OF SYMBOLS

Pt	Platinum
Cr	Chromium
O_2	Oxygen
H	Hydrogen
e^-	Electron
H_2O	Water
H	Hour
mA	Milliampere
mW	Milliwatt
Ω	Ohm
V	Voltage
W	Weight
T	Temperature
A	Ampere
R	Internal resistance
E	Electromotive force

CHAPTER ONE

INTRODUCTION

1.1 BACKGROUND STUDY

Microbial fuel cell (MFC) is one of the two types of biofuel cell (BFC) which utilizes the electrons derived from biochemical reactions that are catalysed by microbes to generate electricity (Ruscalleda Beylier et al., 2019). MFC can be operated with several substrates, from pure to complex compounds. Pure compounds include acetate and glucose, while complex compounds include lignocellulosic waste and wastewater (Pant et al., 2010). Other than generating electricity, MFC has also been widely studied for bioremediation. A notable example of bioremediation of industrial effluent using MFC is the removal of chromium by converting Cr(IV) to Cr(III) (Tandukar et al., 2009). Furthermore, MFC also has been used for the decomposition of agricultural waste including its wastewater and crop residues, for example, empty fruit bunch (EFB), palm kernels, and palm shells from the palm oil industry (Rohma et al., 2021).

Generally, microbes in MFC have two functions, degradation of substrates and generation of electrons which are then being transferred to the electrode. It may also act as a catalyst for the air cathode to assist oxygen reduction reaction (ORR) (Sukri et al., 2021). To ensure an efficient degradation of substrates, the selection of microbes used are important. Each substrate requires a different set of enzymes for degradation. For example, ligninolytic enzymes such as laccase and peroxidases catalyse lignin degradation, while hydrolytic enzymes such as cellulases, hemicellulases, pectinase, and lipases, catalyse the degradation of cellulose and hemicellulose (Qi et al., 2023; Sukri et al., 2021). Certain microbes such as fungi secrete both ligninolytic and hydrolytic enzymes allowing simultaneous degradation of cellulose, hemicellulose, and lignin (Daniel et al., 1989).

In the degradation of lignocellulosic waste, white rot fungi (WRF) such as *P. chrysosporium* have been widely used due to their ability to secrete ligninolytic enzymes such as laccase, pyranose, peroxidases (i.e., lignin peroxidase and manganese

peroxidase), and versatile peroxidase (VP) (Abdel-Hamid et al., 2013). In the early years, most studies on WRF focused on their ability to degrade lignin using H_2O_2-dependent (i.e., peroxidases) enzymes (Tien & Kirk, 1984). However, another study also reported that WRF such as *Pycnoporus cinnabarinus* have comparable lignin degradation to that of *P. chrysosporium* even though there is no peroxidases secreted, indicate a crucial role of laccase in lignin degradation (Eggert et al., 1997).

Even though MFC has the potential for generating energy, its low energy yield (output/cost) limits its application on a larger scale. The use of living microbes in electrochemical systems necessitates additional measures to sustain the microbes and their optimum growth, which in turn further increases its existing expensive cost. In order to obtain optimal energy output, MFC was supplied with buffer solution such as bicarbonate buffer, potassium dihydrogen phosphate, and citrate to maintain a desirable pH which usually is applicable for MFC with electricity-generating bacteria (Elakkiya & Matheswaran, 2013; Fan et al., 2007b; Igboamalu et al., 2019). Although utilizing buffer can result in a significant power increase with less cost, it is non-biodegradable and when released into the environments it causes eutrophication (Fan et al., 2007b; Wang et al., 2018). For example, MFCs have been almost exclusively studied for treatment and product recovery from wastewater. However, this application requires a continuous air aeration to supply oxygen for ORR (Malik et al., 2023).

Aside from that, expensive MFC components also leads to low energy yield. The catalytic air electrode and cell membrane account for 85% of total cost (Rozendal et al., 2008). ORR has a slow reaction rate, thus catalyst such as Pt-based catalyst is necessary to enhance the ORR in MFC. Although other types of catalyst such as metal-based, carbon-based, and biological catalyst have been widely studied as a substitute to Pt-based catalyst, the cost of the air electrode is still high due to its unique features.

A single MFC is practically unusable due to its low operating voltage (Koffi & Okabe, 2020). Most low-power electronic devices require an operating voltage in the range of 2 to 5 V. Stacking of MFCs to increase the energy output possesses different challenges. To solve this problem, most researchers opted for power management unit (PMU) to boost the voltage and prevent voltage reversal. Capacitors, DC/DC converter, and mechanical switch are among the components used in PMU. Despite its ability to

improve MFC performance, operation of PMU requires an additional power supply. Outsourcing an external power supply will further decrease its energy yield while self-regulated by the MFC stack will consume about 20% to 50% of the power generated by MFC stack (Yang et al., 2019).

In summary, MFC energy yields is still low and far from providing reasonably priced and energy-balanced operation. The outstanding issues remain to be the expensive system components and the dependencies on auxiliary systems such as the air-purging and power management unit. Therefore, the challenge is to construct an MFC with simple design features and less expensive components, yet capable to produce high output. Further, the system must be self-sustaining to remove as much control features as possible. To-date, the microbial zinc/air cell employing the white rot fungi (i.e., *Phanerochaete chrysosporium*) has demonstrated promising prospects as a low-cost, self-sustaining MFC with high energy output (Sukri et al, 2021). This work shall continue to adopt the same system and focusses on the following:

- Reducing the system cost by offering a cheaper air cathode that can operate under submerged condition without the aid of electrolyte aeration.
- Introducing a novel MFC stack that mitigates the issues of parasitic current and current reversal.
- Utilizing the microbial zinc/air cell as a lignocellulosic waste degrading cell.

1.2 PROBLEM STATEMENT

Microbial fuel cells (MFC) have been dubbed as one of the possible renewable energies that can replace energy from fossil fuels. However, the living microbes biocatalytic reactions are complex and occur under controlled surroundings. Therefore, auxiliary systems are required to maintain the MFC operation under optimum conditions. As such, among others, air purging is needed to increase the dissolved oxygen content, anolyte/catholyte replenishment is needed to prolong the MFC service duration, and a power management unit is needed to increase its low voltage and to stabilize the fluctuating output. Each of these auxiliary systems requires an external power source.

In terms of MFC design and construction, its essential components are very expensive. For a typical air-cathode based MFC, the air cathode and membrane separator contributed ~85% of the total capital cost (Rozendal et al., 2008). Consequently, the auxiliary systems and MFC components costs become the high-order denominator determining the MFC energy gain yields (i.e., output/cost).

On the other hand, increasing the MFC power output necessitates the stacking configurations. Even though stacking may improve the MFC performance, issues such as high internal resistance, parasitic current, voltage reversal, and current reversal need to be addressed. While control electronics could overcome those issues, introducing additional control features would forfeit the benefit of output gains and further diminish the inherently low energy yields of MFC.

1.3 RESEARCH PHILOSOPHY

A self-sustaining MFC is the key element in enhancing its low energy yields and paving the way for its practical applications. In achieving MFC operational sustainability, the following factors must be considered:

- A robust microbe with high tolerance to changing surroundings to minimize the need for auxiliary systems.
- A slow degrading organic substrate to avoid frequent replenishment
- A simple cell design to minimize the cost and yet producing high energy output.
- An innovative cell configuration to avoid the need for external control electronics in stack design.

The present work is devoted towards developing a self-sustaining MFC capable of generating high energy output.

1.4 RESEARCH OBJECTIVES

The following is a summary of the research's objectives:

i. To mitigate the occurrence of parasitic current and current reversal in a parallel-stack configuration using an open-parallel unit cell configuration.

ii. To design an easy-to-fabricate, non-catalytic, submerged air electrode for microbial fuel cells from compressed layers of carbon felt, carbon fibre sheet and nickel mesh.

iii. To investigate viability of microbial zinc/air cell as a lignin-rich agrowaste decomposing cell.

1.5 RESEARCH METHODOLOGY

This work adopted a hybrid MFC by pairing a zinc anode with an air electrode in a membraneless, single enclosure filled with fungal microbes of *P. chrysosporium,* fed with lignin-rich EFB. In essence, the hybrid electrochemical system is a microbial zinc/air cell. The cell is left to operate in uncontrolled, ambient surroundings. The ability of an MFC to operate in uncontrolled ambient surroundings is a pre-requisite in enhancing the energy yields of bioelectrochemical systems.

For most practical applications, multiple MFC units have to be configured in serial-stack, parallel-stack or a combination of both, in order to obtain higher operating voltage and current, and extended operation duration. Parallel-stack configuration offers the benefits of enhanced capacity and higher limiting current. However, this configuration induces parasitic current due to the differences and fluctuations in individual cell potential, and consequently a current reversal may also occur. Thus, the first part of this work introduced a novel configuration to overcome those issues, i.e., an open-parallel unit cell configuration. In open-parallel unit cell configuration all individual MFC units are both hydraulically and electrically connected.

The air cathode is an essential component in an air cathode MFC and accounts for nearly 45% of the overall capital costs of the entire system (Rozendal et al., 2008).

An air cathode MFC is commonly accompanied by an air purging or aeration component to ensure sufficient oxygen content to the air cathode. The air cathode is expensive due to its unique design features and the catalytic material content. Therefore, the second part of this work focused on the design and fabrication of a low-cost carbon-based air cathode for submerged applications. It is considered low cost due to the absence of catalytic material in the air cathode. Besides, the air cathode fabrication does not require any specific treatment such as high temperature and pressure calendaring. Air electrodes were fabricated from carbon felt, carbon fiber sheet, and nickel mesh as air entrapper, conductive layer, and current collector respectively.

At present, the main interest is to utilize MFCs in converting waste into non-polluting, benign by-products while generating electrical current. Concerted efforts have been directed almost exclusively towards wastewater treatment (Ahn & Logan, 2010; Venkata Mohan et al., 2008; Wu et al., 2016). As such, in the final part of this work, the viability of microbial zinc/air cell as a lignin-rich agrowaste decomposing cell was studied.

1.6 SCOPE OF RESEARCH

To achieve the stated objectives, the present work is divided into three parts:

i. A novel MFC stack configuration - Design and characterization of open-parallel unit cell configuration.

   A parallel-stack microbial zinc/air power unit was constructed from three-unit cells. All anodes and cathodes were respectively connected in a parallel configuration but all three-unit cells shared a common electrolyte. The parallel-stack power unit were analyzed under parallel and open-parallel unit cell configurations. The open circuit voltage (OCV), polarization and power profiles, and discharge capacity were tested using a Neware BTS 4000 battery tester. The occurrence of parasitic current was monitored using UT804 multimeter equipped with data acquisition software.

ii. A low-cost air-cathode MFC - Design, fabrication, and characterization of carbon-based submerged air cathode.

The air cathode comprised of layered structure of carbon felt, carbon fibre sheet, and nickel. All the components were cut into the desired sizes and wedged between the two cylindrical PVC tubes. The aim was to fabricate a low-cost and easy-to-fabricate air cathode. The fabricated air cathode was then tested in the zinc/air MFC. The efficacy of the air cathode was evaluated directly from its galvanostatic discharge capacity at 1 mA using the Neware BTS 4000 battery tester and compared against a commercial air cathode. The surface morphologies of the carbon felt, carbon fiber sheets, and commercial air electrode were observed using a scanning electron microscope (SEM), and the hydrophobic contact angle of the carbon felt was analysed using ImageJ image processing software.

iii. Waste degradation using MFC – Viability of microbial zinc/air cell as a lignocellulosic waste degrading cell.

The degradation of lignocellulosic EFB was evaluated under the influence MFC discharge current. Lignin content was analysed using two methods, the thermogravimetric analysis method, and the chemical method (i.e., acid-chlorite method). The findings were further supported by the Scanning Electron Microscopy (SEM) observations.

1.7 THESIS ORGANIZATION

Chapter 1 of the thesis provides an overview of the work which includes problem statement, research philosophy, objectives, research methodology, and scope of research.

Chapter 2 presents a brief review on MFC working principle, electron transfer mechanism, MFC's design, scaling up of MFC system, fabrication of air electrode, and lignin degradation.

Chapter 3 introduces a novel MFC stack configuration i.e., an open-parallel unit cell configuration. This novel configuration improves the MFC stack output and mitigates the occurrence of parasitic current and current reversal.

Chapter 4 reports the design, fabrication, and characterization of a low-cost carbon-based submerged air cathode. It is designed as an easy-to-fabricate air cathode. The performance is compared against a commercial E4 air cathode.

Chapter 5 focusses on the evaluation of microbial zinc/air cell as a waste degrading cell. The degradation of lignocellulosic EFB waste was studied as a function varying cell discharge current.

Chapter 6 summarizes the contribution of this work towards producing a self-sustaining MFC with high energy yields.

Finally, **Chapter 7** concludes the findings of this research and propose for the future work directions.

CHAPTER TWO

LITERATURE REVIEW

2.1 INTRODUCTION

Biofuel cells (BFC) are a device that converts chemical energy into electrical energy through electrochemical reactions relying on the enzyme-based catalyst in the form of isolated proteins or whole microorganisms to assist the reactions either for oxidation or reduction. While conventional fuel cells such as direct methanol fuel cells (DMFC) utilized metal-based catalysts on both the anode and cathode (Manoharan et al., 2019). BFC can be split into two primary categories, specifically, enzymatic fuel cells (EFC) and microbial fuel cells (MFC).

Compared to other fuel cells, biofuel cell has mild control parameters (20-40 °C and near neutral pH) and the fuel used is versatile but it has several downsides such as low energy yields (low output/high cost) and required several control parameters (Bullen et al., 2006; Sukri et al., 2021; Yang, Fu, et al., 2019). High operation cost mostly comes from the cost of components (i.e., the cost of membranes up to 60% of the total cost) and catalysts (i.e., Pt-catalyst contributed 50% of total cost) (Ramirez-Nava et al., 2021; Saha et al., 2013). This cost can be reduced by finding an alternative with fewer control features and a low-cost design that have a good performance. For example, instead of using a double-chamber fuel cell, a single-chamber fuel cell was used with electrodes and membranes that are less expensive, as well as minimizing catalyst content (Liu et al., 2004). Table 2.1 show a list of prices of components that are commonly used for BFC.

Aside from mild control parameters, BFC can operate with various substrates from a simple substrate (e.g., glucose, acetate) to complex substrates (e.g., lignocellulosic material, wastewater, acetaminophen). Previous study shows that BFC with a mixed culture of fungi and bacteria is able to remove acetaminophen (APAP) and 4-aminophenol (PAP) while generating energy (Shabani et al., 2021). Several studies show the effectiveness of BFC for wastewater treatment, for example, swine wastewater

and alcohol distiller wastewater was treated using a BFC system and were able to remove chemical oxygen demand (COD) up to 83.8% and 80-90% respectively (Huang et al., 2011; Zhuang et al., 2012). Aside from that, membrane-less BFC powered with sludge supplemented with lignocellulosic waste (i.e., banana peel, corn, bran, and POME) show the highest COD removal efficiency of 49.10% from sludge + banana peel and recorded maximum power of 0.152 mW (Mohd Zaini Makhtar & Tajarudin, 2020). Lignocellulosic waste acts as carbon, hydrogen, and sulphur sources, which act as an electron donor BFC system.

Table 2.1 Cost of components for biofuel cell (BFC)

Component	Cost	Reference
Nafion® 117 membrane	2229 $/m^2	(Hernández-Flores et al., 2019)
Platinum catalyst	185 $/g	(Fuel Cell Store, 2022)
Pt-based cathode	612.99 $/m^2	(Rozendal et al., 2008)
Laccase (from *Trametes versicolor*)	165.56 $/g	(Sigma-Aldrich, 2022)

2.2 MICROBIAL FUEL CELL (MFC) WORKING PRINCIPLE

Microbial fuel cell (MFC) is a technology that utilizes electrons from the biochemical reactions catalysed by microbes for electricity generation. In MFC, the microbes break down the substrate by secreting extracellular enzymes. During the oxidation of organic matter at the anode by microorganism, electrons, protons, and metabolized matter were produced. The electrons and protons produced simultaneously transferred to the anode. Electrons were first transferred to the anode directly or using mediators and flow to the cathode through an external circuit, while protons were transferred to the cathode through the membrane. At cathode, an electron acceptor such as oxygen and ferricyanide was then reduced into water.

With ferricyanide as electron acceptor, no catalyst are required due to ferricyanide good reaction kinetics (Lawson et al., 2020). On the other hand, although oxygen is an ideal electron acceptor for MFC due to its abundance and high redox potential, it still requires a catalyst since it has sluggish oxygen reduction reaction (ORR) which lead to potential loss (Yuan et al., 2016). ORR follows two different pathways: four-electron pathway and two-electron pathway. These two pathways differ in terms of the product of interest, where four-electron pathway produced water molecules, while the two-electron pathway produced hydrogen peroxide molecules.

$$O_2 + 4H^+ + 4e^- \rightarrow 2H_2O \quad \text{[Four-electron pathway]} \quad (2.1)$$

$$2O_2 + 4H^+ + 4e^- \rightarrow 2H_2O_2 \quad \text{[Two-electron pathway]} \quad (2.2)$$

To accelerate the sluggish kinetics of ORR, for example in two-electron pathway, catalyst such as platinum (Pt), metal oxides (i.e., manganese oxide, nickel cobalt oxides and cobalt oxides), carbon-based catalyst (i.e., activated carbon), and biological catalyst (i.e., whole microbial cells, organelles of living cells and isolated enzymes) was used (Choi et al., 2019; Fu et al., 2019; Mahmoud et al., 2020; Watson et al., 2013).

However due to the high cost of Pt-based catalyst and complex preparation for other types of catalyst, researcher have shifted to biological catalyst especially whole microbial cells because it can be used as it is and enzyme isolation and purification are not needed (Reinhard et al., 2020). A well-known example of whole microbial cell used in MFC are *Phanerochaete chrysosporium* and *Galactomyces reessii*. Both *P. chrysosporium* and *G. reessii* able to secrete extracellular laccase, which able to transfer electrons from the cathode to oxygen (Li et al., 2018; Sukri et al., 2021). Laccase or 'multi-copper' oxidases play a crucial role in transferring electrons generated from oxidation of phenolic compound to oxygen (Blanford et al., 2008; Gupta et al., 2004).

2.3 MFC ELECTRON TRANSFER MECHANISM

Theoretically, microbes in an anodic chamber will act as biocatalysts for the oxidation of organic or inorganic substrates and generating electrons. The electrons generated was

then transferred from the inside of the cell to the anode surface either by direct electron transfer mechanism (DET) or mediated electron transfer mechanism (MET).

DET mechanism usually applicable when exoelectrogen were in direct interaction with anode. Direct interactions between exoelectrogen and anode can be either via membrane-bound cytochrome for short-range electron transfer or via electrically conductive pili for long range electron transfer (see Figure 2.1). DET via membrane-bound cytochrome requires the cell membrane and its cytochrome which act as an electron carrier to directly in contact with the anode. An example of exoelectrogen with ability of DET are *Methylococcus capsulatus* (Bath), *Shewanella putrefaciens*, and *Rhodoferax ferrireducens* (Hasan et al., 2012; Tanaka et al., 2018). Certain microorganisms such as *Geobacter sulfurrenducens* and *Shewanella oneidensis* MR-1 however can evolve to transfer electrons in a long-range using electrically conductive pili which are connected to the membrane-bound cytochrome (Gorby et al., 2006; Holmes et al., 2016). However, for microorganisms with DET mechanism, its electron transfer rate was too low due to active site locations which are deep into the protein, therefore leading to the low current generation (Umar et al., 2020).

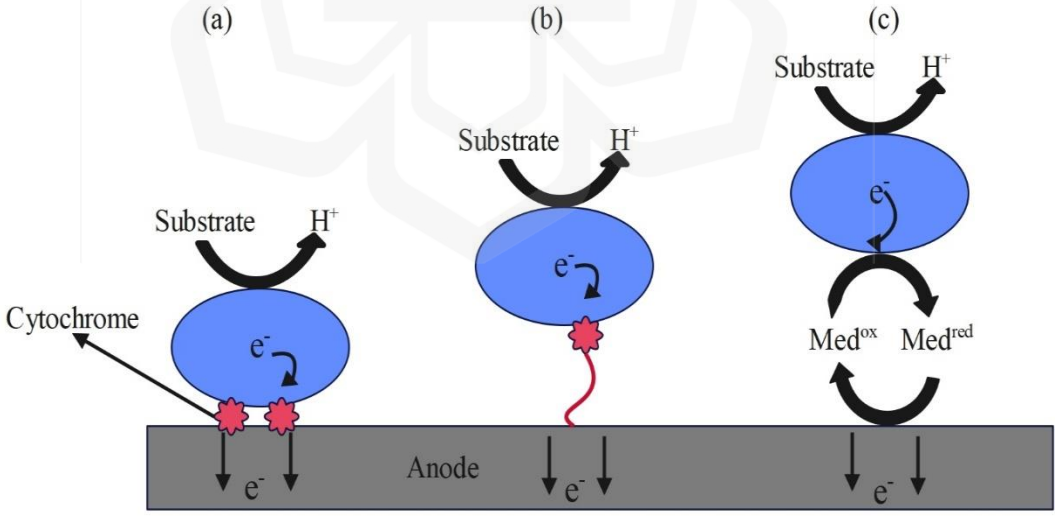

Figure 2.1 Anodic electron transfer mechanism via (a) membrane-bound cytochrome (b) electronically conductive pili (c) mediator

Moving on now to consider indirect electron transfer by exoelectrogen using mediators (see Figure 2.2). There are two types of mediators, endogenous redox mediators where mediators are generated by microorganisms, and exogenous redox mediators or artificial mediators which are used by microorganisms that are unable to transport electrons. Microorganisms such as *Pseudomonas aeruginosa, S. oneidensis, G. sulfurreducens,* and, *Clostridium butyricum* can secrete mediators by itself such as pyocyanine and 2-amino-3-carboxy-1,4-naphthoquinone (Ali et al., 2018; Zhou et al., 2014). Although these microorganisms used mediators for electron transfer, it is considered as "direct electrochemistry" since the mediators are secreted by the exoelectrogen instead of using artificial mediators (Zou et al., 2017). While, microorganisms such as *Escherichia coli*, *Pseudomonas sp*., *Proteus,* and *Bacillus* are unable to transfer electrons directly to the electrode, thus artificial mediators such as humic acid, thionine, methylene blue, neutral red, and neutral blue are used to facilitate electron transfer (Tiwari et al., 2021; Zhou et al., 2014). Even though the addition of artificial mediators may increase the electron transfer rate, at high concentrations it may be toxic to the microorganism and lead to a decrease in MFC performance (Sayed et al., 2012).

Turning now to cathodic electron transfer which had same electron transfer mechanism as anodic electron transfer (i.e., DET and MET), except cathode act as electron donor instead of electron acceptor. Same as anodic electron transfer mechanism, electron can be transferred from cathode to the cell either via membrane-bound cytochrome or via electrically conductive pili or using mediators. Example of microbes that can uptake electron from cathode via cytochromes, pili, or shuttle compounds for reduction reaction are *G. sulfurreducens* and *Desulfovibrio* spp., and *P. chrysosporium* (Croese et al., 2011; Strycharz et al., 2011; Sukri et al., 2021).

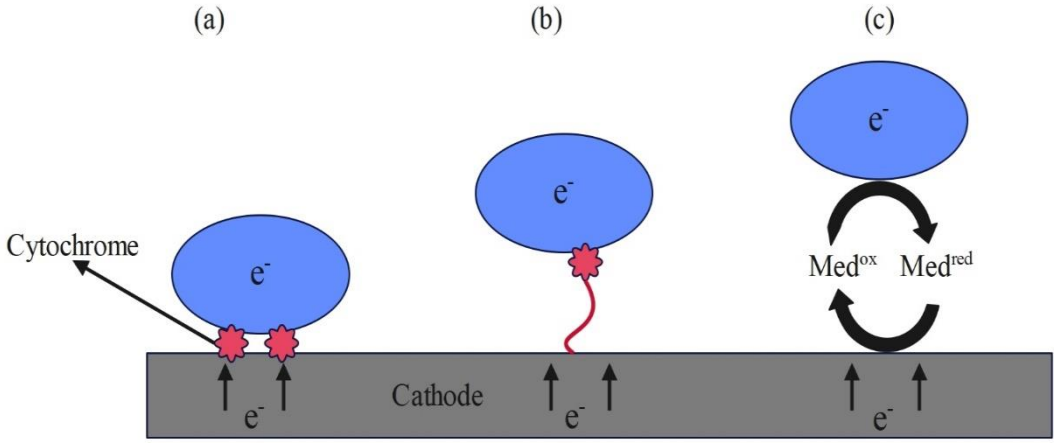

Figure 2.2 Cathodic electron transfer mechanism via (a) membrane-bound cytochrome (b) electronically conductive pili (c) mediator

2.4 DESIGN OF MFCs

Even though MFC technology has been used for various application such as biosensor, wastewater treatment system, and power generation systems, much of it has only been used in lab settings due to the low energy output. The performance of MFC depends on its volume, electrode spacing, oxygen supply, membrane area, and reactor design. Even though improving MFC components is one of the essential elements to obtain high output, reactor configuration such as single-chamber MFC (Figure 2.3a) and double chamber MFC (Figure 2.3b) has a huge impact on MFC's performance when scaled up. Table 2.2 shows how the performance is affected by the MFC configuration.

Aside from reactor configuration, Table 2.2 also show that type of substrates also greatly influences MFC performance. MFC with simple substrates such as acetate, glucose, and sucrose have a better performance compared to MFC with complex substrate such as wastewater, palm oil mill effluent (POME), and lignocellulosic biomass. It is because simple substrates are easier to degrade to produce higher power output.

Table 2.2 MFC performance relative to configuration

Types	Anode	Cathode	Substrate	Electron acceptor	Max power (mW/m^2)	Ref
Single chamber	Carbon cloth	Carbon cloth	Glucose	Oxygen	401	(Sharma & Li, 2010)
Single chamber	Carbon paper	Carbon paper	Acetate	Oxygen	661	(Liu et al., 2005)
Single chamber	Graphite rod	Carbon cloth	Groundwater	Oxygen	48.26	(Liu et al., 2018)
Single chamber	Carbon cloth	Carbon cloth	Domestic wastewater	Oxygen	80	(Fan et al., 2007a)
Double chamber	Graphite rod	Graphite rod	Acetate	Oxygen	114	(Ullah & Zeshan, 2020)
Double chamber	Carbon cloth	Carbon cloth	Glucose	-	136	(Ali et al., 2017)
Double chamber	Carbon paper	Carbon paper with Pt	Swine wastewater	Oxygen	45	(Min et al., 2005)
Double chamber	PACF	PACF	POME	-	45	(Baranitharan et al., 2013)

Note. Palm oil mill effluent (POME); Polyacrylonitrile carbon felt (PACF)

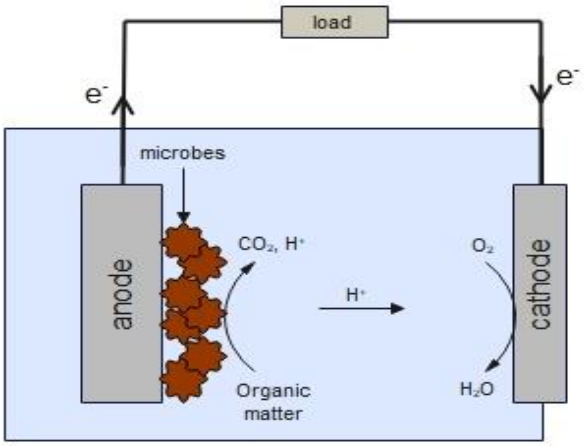

(a)

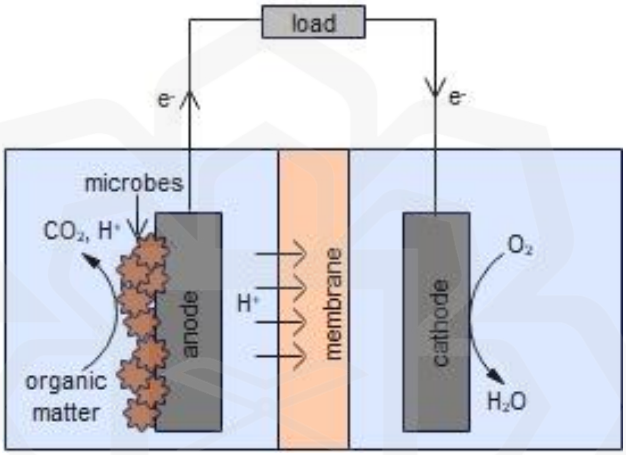

(b)

Figure 2.3 Schematic of the basic components of (a) single-chamber MFC (b) double-chamber MFC

2.4.1 Double Chamber Microbial Fuel Cell

Double chamber MFC is the most common type of MFC configuration with two compartments for anolyte and catholyte each separated by a proton exchange membrane (PEM). Usually, microorganisms are inoculated inside anolyte compartments for substrate oxidation. Compared to single-chamber MFC, double-chamber MFC can generate a higher output voltage, power density, and volumetric density. However, maintenance cost and operation complexity also increase since it requires several chambers with the addition of PEM to separate the anode and cathode chambers.

Aside from the high cost, the usage of PEM is also associated with several issues such as oxygen transfer to an anaerobic anode chamber, high internal and membrane resistance, change in pH, and membrane fouling (Rahimnejad et al., 2014). One study by Behera et al. reported that there is a decrease in pH after a few days of operation due to H^+ accumulation which led to low power density (Behera et al., 2018).

Another researcher attempted to evaluate the influence of membrane used on internal resistance, and it was shown that thinner membrane has higher power density. However, a thin membrane led to an increase in internal current and fuel crossover which contribute to the concentration loss at high current density (Atifi et al., 2014; Lefebvre et al., 2011). One more problem associated with the utilization of PEM is oxygen crossover into an anaerobic anode chamber. At the cathode, oxygen was used as an electron acceptor and reduced to water. Nevertheless, over an extended period, oxygen can permeate into cathode chamber, causing aerobic respiration (Rahimnejad et al., 2014). Eventually, this results in the MFC system experiencing low coulombic efficiency.

Besides that, during extended operation of MFC, the performance might deteriorate caused by the accumulation on the membrane originating from the formation of biofilm. A dense biofilm due to the accumulation of microbes gradually causes a decrease in mass and charge transfer. In earlier research regarding the impact of fouling on membranes on the performance of MFC, researchers have discovered that following six months of operation, the output of MFCs experienced a drastic drop owing to the membrane's biofouling. The power generation decreased by 37% less than the initial value (Flimban et al., 2020). Numerous attempts have been done at preventing the formation of biofouling. These include treating using hydrogen peroxide and sulphuric acid, applying polydopamine coating, and adding layers of AgNP and polydopamine (Ghasemi et al., 2013; Kim et al., 2014; Park et al., 2021).

However, it is not cost-effective as replacing it with any other membrane alternatives or completely remove it, as PEM cost approximately 38% of MFC's total cost. Thus, several cheaper alternatives with comparable effectivity to Nafion 117 membranes such as ultrafiltration membranes, J-cloth, and Zirfon membranes can be used (Tang et al., 2010). Previous research by Tang et al. has shown that Nafion (1.4 x

10^{-4} cm/s) has a lower oxygen mass transfer coefficient than microfiltration membrane (5.9×10^{-4} cm/s) indicating higher diffusion of oxygen with a similar value of internal resistance and maximum power densities with the value of 267 Ω (0.872 W/m^2), and 263 Ω (0.831 W/m^2) respectively, suggesting microfiltration was as effective as Nafion 117 membrane in terms of its electrochemical properties (Tang et al., 2010). Another alternative is by using single chamber MFC which will be discussed in the next topic.

2.4.2 Single Chamber Microbial Fuel Cell

Membrane-less MFC or single chamber MFC configuration is a single-compartment MFC with a cathode directly in contact with air. It is simple and with low maintenance due to the lack of membrane. The advantages of single-chamber MFC are no aeration is required, small volume, does not require chemical regeneration of catholyte and produces higher power density (Chatterjee et al., 2018; Fan et al., 2007a). However, several challenges need to be overcome such as low coulombic efficiency (CE) caused by oxygen diffusion into anodic chamber, limitation on electrode distance, and catalyst on the cathode of oxygen reduction reaction (ORR) (Chatterjee et al., 2018; Fan et al., 2007a).

The coulombic efficiency of single-chamber MFC ranges from 9-12% which is lower compared to double-chamber MFC (40-90%) (Cheng et al., 2006a). One of the reasons CE for the single-chamber is lower is because the oxygen which supposedly acts as an electron acceptor at the cathode diffused into the anode and lead to aerobic respiration where organic matter was used as a fuel instead of using it for electricity generation (Li et al., 2013; Saravanan & Karthikeyan, 2018). To overcome this downside, previous studies demonstrate that making a few improvements to the design such as modifying the thickness of the diffusion layer on the cathode by coating it with PTFE up to 8 layers can improve CE from 19.1% to 32% (Cheng et al., 2006a).

Regarding electrode spacing, the study presented thus far supports the idea that as the distance between two electrodes is reduced, the internal resistance also reduced thus increased power production, for instances the power density increases from 7.4 mW/m^2 to 10.9 mW/m^2 when electrode spacing was reduced from 28 cm to 24 cm

(Ghangrekar & Shinde, 2007). Data reported by Liu et al., also show an improvement in power generation from 720 mW/m^2 to 1210 mW/m^2 when electrode spacing was reduced from 4 to 2 cm (Liu et al., 2005). However, another report shows that, when electrode spacing was reduced from 2 cm to 1 cm, it shows a decrease in power generation (i.e., 811 mW/m^2 to 423 mW/m^2) even though its internal resistance decrease (i.e., 35 Ω to 16 Ω) (Cheng et al., 2006b), indicating the optimum electrode spacing is 2 cm. The possible explanation for this occurrence is due to a decrease in microbes' activity on the anode which is explained by the decrease in the open circuit potentials of the anode and also due to the short-circuit which is a potential occurrence when electrodes are placed too close (Cheng et al., 2006b; Liu et al., 2005).

Last but not least, ORR is a rate-limiting step, thus catalysts have an important role in assisting in the reduction of oxygen. The most common catalyst that has been used is a metal-based catalyst (e.g., Pt). Even though a Pt-based catalyst is known as an efficient ORR catalyst, it has several downsides such as high cost, scarcity, poor durability, and a high tendency for poisoning (Choi et al., 2019; Merino-Jimenez et al., 2016). To overcome this, several alternatives have been studied and proven qualified as a substitute for Pt-based catalysts such as metal oxides (e.g., manganese oxides), carbon-based catalysts (e.g., activated carbon), and biological catalysts (e.g., laccase) (Fu et al., 2019; Gellett et al., 2010; Watson et al., 2013).

2.5 SCALING UP MICROBIAL FUEL CELLS (MFC) SYSTEM

There are several methods of scaling up such as increase reactor volume, modifying electrode, applying power management unit (PMU), and stacking. Typically, stacking multiple individual cells in a series or parallel connection have been used for scaling up as it can improve energy output efficiently compared to other methods. Other method such as increasing reactor volume may lead to a decline in power density due to volumetric ohmic unless there is an increase in effective surface area of electrode.

In the case of modifying electrode, for example increasing cathode surface area does not ensure a linear increase in current generation due to the ohmic loss and mass

transport loss (Jiang et al., 2010). While, applying power management system (PMU) is useful for preventing voltage reversal in stacked MFC, however installing a PMU will reduce power conversion efficiency since PMU consumes between 20% to 50% of power generated by MFC (Nguyen et al., 2019; Yang et al., 2019).

Thus, the most suitable method for scaling up is stacking. Contrary to increasing the MFC's size, stacking multiple small-size MFC is more viable considering that stacking can minimize volumetric ohmic resistance, reduces electrode spacing and increase surface-volume ratio, therefore produce higher power density (Clauwaert et al., 2008; Mateo et al., 2018). Stacking in series and parallel produce higher voltage and current respectively, thus this method can satisfy the requirement to powered up any devices.

2.5.1 Serial Configuration and Open-Serial Configuration

In serial configuration, the output voltage is the total voltage of individual MFC unit stacked with output current is the average current of individual MFC unit stacked. Hassan et al., used three individual MFC with voltage of 0.736 V, 0.727 V, and 0.735 V and stack in series, produced open circuit voltage (OCV) of 2.17 V and closed circuit voltage (CCV) of 0.644 when connected with external load of 1000 Ω which indicated an increase in voltage output for both open circuit voltage (OCV) and closed circuit voltage (CCV) with value of 2.17 V and 0.644 respectively (Hassan et al., 2014).

However, several issues have been associated with stacking in serial configuration. Thus far, several studies have reported occurrence of contact voltage losses, erratic operation, and voltage reversal when multiple MFC were stacked in serial configuration (Zhong et al., 2010). Li et al., reported at current of 7 mA, voltage of serially-stack MFC dropped from 3.2 to 1.7 due to the voltage reversal (Li et al., 2017). Similarly, a research by Gurung and Oh demonstrated that 3 unit cells connected serial configuration show a voltage reversal at MFC-1 after operated for 70 h (Gurung & Oh, 2012). Voltage reversal in both cases may attributed to substrate depletion and discrepancy of the individual MFC performance.

Connecting multiple unit cells in series with hydraulically fluid connected (open-serial configuration) further complicate the MFC operation. In series configuration, the formation of internal parasitic cell is unavoidable. The formation of internal parasitic cell between cathode-1 and anode-2 which connected electronically and hydraulically (see Figure 2.4) lead to voltage loss. Voltage loss was caused by parasitic current which generated when electrons from anode-2 flow to the cathode-1 through external wire.

Zhuang and Zhou (2009) reported that, the OCV value of two cells connected in series configuration with common electrolyte decrease from 1.31 V to 0.96 V which caused by parasitic current generated from parasitic cell measured 3.19 mA. A study by Oliot et al., (2017) also show that series configuration with common electrolyte (0.7 mW at 0.21 V) have smaller maximum power output by 41 % compared to theoretical value (1.7 mW at 0.47) which is also caused by parasitic current. Another report demonstrate that aside from voltage loss, the formation of internal parasitic cell also may reduce both coulombic efficiency and current produced caused by current loss (Ghadge & Ghangrekar, 2015).

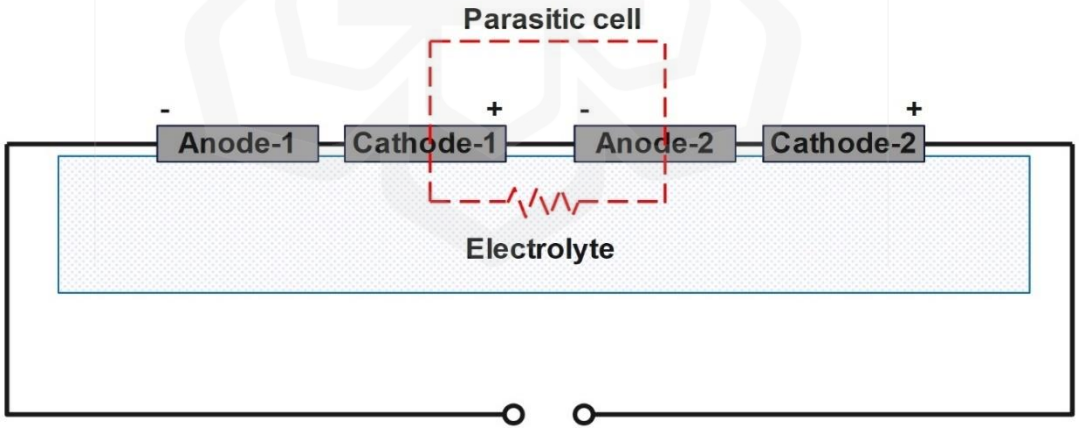

Figure 2.4 Illustration of formation of parasitic cell in the serial configuration

2.5.2 Parallel Configuration and Open-Parallel Configuration

Connecting multiple cells in parallel configuration will generate higher current output which is the cumulative current value of individual cells with the voltage output is average voltage for the individual cells. In contrary to serial configuration, parallel configuration yield lower internal resistance with a stable operation and higher current output with minimal energy losses (Gurung & Oh, 2012; Wang & Han, 2009). This is evident in the case of operation of 5 stack cell in serial and parallel configuration which operated for 45 cycles to examine the stack stability. The overall result shows that parallel cell configuration has a stable operating voltage and instantaneous power densities compared to serial cell configuration (Whiddon et al., 2019). Another advantage of parallel configuration over serial configuration is failure of a single cell will not influence the performance the rest of the cells (Pandit et al., 2020).

However, in parallel configuration the formation of parasitic current also possible to formed, not by the formation of parasitic cell but due to the difference in potential value of each cell. Theoretically, parallel configuration should have a uniform potential for each of an individual cell. However, in MFC system it is almost impossible to maintain similar voltage throughout operation due to the difference in microbial activity in each cell, thus resulting in formation of parasitic current (i.e., non-Faradaic current).

Aside from difference in microbial activity, other factors that may influenced the potential of each cells are passive air diffusion to the cathode, passive air supply to the catholyte, and non-mixing conditions (An, Kim, et al., 2015; An, Sim, et al., 2015). All three factors related to the oxygen exchange between liquid(electrolyte)-air(oxygen)-solid (catalyst/current collector) interface at which the ORR takes place.

In parallel cell configuration with a different potential value, cell with higher potential value (MFC-1) supplied electrical energy to the cell with lower potential value (MFC-2). This resulted in energy loss even though it is not as significant as energy loss caused serial cell configuration (An, Sim, et al., 2015). Electrical current out of MFC-1 is called Faradaic current while current flow into MFC-2 or charging current is called as non-Faradaic current or parasitic current. Parasitic current in parallel cell can be

calculated based on Kirchhoff's second law which stated that sum of source voltages equals the amount of voltage drop in a loop:

$$iR_{int1} + iR_{int2} = V_1 - V_2 \rightarrow i = (V_1 - V_2)/(R_{int1} + R_{int2}) \quad (2.3)$$

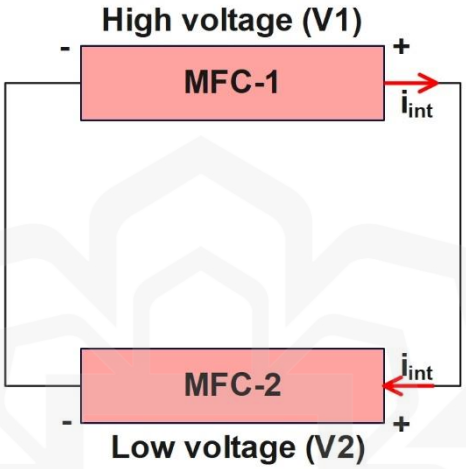

Figure 2.5 A conceptual diagram of non-Faradaic current flow in open circuit mode

Another issue related to parallel cell configuration is current reversal during closed circuit mode. Usually, current reversal happened when the cell operated at high external resistance. A study by Wu et. al., show that there is a current reversal when five MFC modules connected in parallel when operated at high external current (>100 Ω) (Wu et al., 2016). This author also suggest that the differences between OCV also influence the occurrence of current reversal since it only occurred in MFC module with low OCV where current reversal increase with an increase in difference between OCVs (Wu et al., 2016). The presence of current reversal during closed circuit mode will reduces the overall efficiency of the MFC.

To improve the overall efficiency of the MFC, the cells can be connected in parallel with a common electrolyte. Similar to bipolar configuration in parallel connection, this configuration can balance the voltages of individual cells (An et al.,

2014). Once the voltage of individual cell is more balance, the difference between voltage value will reduce hence reduce parasitic current and current reversal value.

2.6 FABRICATION OF AIR ELECTRODE

Electrodes play an important role in the performance of MFC. Factors such as conductivity, corrosion resistance, hardness, current loss, form and size need to be carefully thought about when fabricating the electrodes especially for air-cathode. Air-cathode is an air breathing cathode where it enables the oxygen to diffuse into the electrode and convert it into OH^- (Tomboc et al., 2020). Theoretically, air-cathode consist of three main parts which are conductive current collector, catalyst layer, and gas diffusion layer (GDL) (see Figure 2.6).

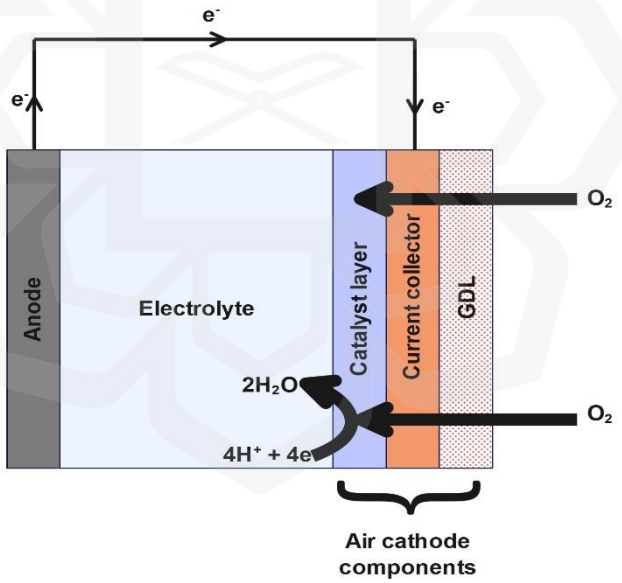

Figure 2.6 Components of air cathode

2.6.1 Catalyst layer

Usually, air electrode was fabricated from carbon-based material due to its low cost and high conductivity. However, air-cathode fabricated from carbon-based material possess

a low catalytic activity. Its catalytic activity can be improved by incorporated catalyst onto gas diffusion layer forming catalyst layer (Sonawane et al., 2019). Catalyst layer is a layer where oxygen reduction reaction (ORR) takes place thus it is considered as limiting factor (Choi et al., 2019).

Good catalyst layer typically allow maximum triple-phase contacts where oxygen, electrons, and protons are all present at the same time (Wei Yang, Li, et al., 2019). The active sites of catalyst layer should be exposed to the reactants, hence it surface should be hydrophilic (Tomboc et al., 2020). Two of the most common deposition method for catalyst layer is by spraying the catalyst onto carbon support or by embedded it within carbon/PTFE matrix (Sonawane et al., 2019).

Pt-based catalyst is widely used to assist due to its high catalytic activity and fast kinetics. However, it is not suitable for large scale operation due to its high cost, limited availability, and low stability limit (Choi et al., 2019; Tomboc et al., 2020). Other alternatives such metal oxides (e.g., cobalt oxides and manganese oxides) and activated carbon also have been widely research but it has limited success, thus it is ruled out for large scale application (Khilari et al., 2014).

Biological catalyst including isolated enzymes, whole microbial cell and living cell organelles also one of the widely used alternatives for Pt-based catalyst due it cost, mild reaction conditions and environmentally friendly. Among the three types of biological catalyst, isolated enzymes can achieve high current and power densities, but it has low efficiency at anode and cathode (Gellett et al., 2010). Another downside of isolated enzymes is it deteriorated with time; thus, it is not suitable for long term operation. While, both whole microbial cell and living organelles have higher conversion rate of chemical energy into electrical energy despites its low volumetric catalytic activity (Gellett et al., 2010).

Example of whole microbial cell and living organelles are white rot fungi (WRF), *Sphingobacterium sp*., *Acinetobacter sp*., and *Ltothrix discophora sp*. (Khilari & Pradhan, 2018; Sukri et al., 2021). A notable example of whole microbial cell used as a biological catalyst is WRF *P. chrysosporium* which secrete laccase. Laccase is an oxidoreductase that belongs to the copper-containing enzyme family and demonstrates

a specific affinity for oxygen as its electron acceptor (Gupta et al., 2004). Laccase combine the electron reduction of oxygen (i.e., dissolved oxygen or atmospheric oxygen) into two molecules of water with the oxidation of substrates such as phenols, arylamines, anilines, thiols, and lignin (Dashtban et al., 2010).

2.6.2 Gas Diffusion Layer (GDL)

Gas diffusion layer (GDL) is a layer where oxygen diffusion between electrolyte and oxygen takes place and also to minimize electrolyte flooding (Tomboc et al., 2020; Wulin Yang et al., 2015). Properties such as porosity, gas permeability and electronic resistivity have a significant influence on cathode's performance (Shu et al., 2013). Porous structure of GDL typically made of carbon-based material and coated with a hydrophobic layer. A well-known hydrophobic coating for GDL includes polytetrafluoroethylene (PTFE), poly(vinylidene fluoride) (PVDF), and poly(dimethylsiloxane) (PDMS) (Ungan & Bayrakçeken Yurtcan, 2019; Wulin Yang et al., 2014).

It is necessary to ensure both inner side and outer side of GDL have an appropriate hydrophobicity and porosity since it influences MFC performance. For example, inner side of GDL with full hydrophobicity will limit proton supply to the ORR reaction site, while outer side with less hydrophobicity will cause electrolyte flooding. On the other hand, an increase in porosity of outer side of GDL will improve oxygen penetration of oxygen from air through GDL until catalyst layer. An author analyzed influence of GDL porosities of 40%, 60% and 80%, the data showed that at it has better distribution of oxygen mass fraction at high GDL porosity (Amadane et al., 2019).

In conclusion, to ensure an efficient gas diffusion and less electrolyte flooding, GDL should have smaller pore and slightly hydrophobic inner side to improve mass transport, and larger pores and highly hydrophobic outer side to capture oxygen (Cheng et al., 2006a; Moosavi et al., 2017; Tomboc et al., 2020). Aside from that, GDL should have high resistant against rapid oxidation and strong alkaline electrolyte for long term operation (Tomboc et al., 2020).

2.6.3 Conductive Layer

Conductive base layer can usually place either in between GDL and catalyst layer or incorporated with GDL which act as an electron carrier to the catalyst layer for ORR (Yang et al., 2019). Good conductive layer should have high conductivity, good mechanical strength, and good mechanical stability. Usually, conductive layer used carbon-based material due to its good electrochemical and chemical stability (Janicek et al., 2015). A classic example of carbon-based conductive layer are carbon cloth and carbon paper (Cheng et al., 2006a; Sonawane et al., 2019).

However, compared to metal-based material such as stainless steel, nickel mesh, and nickel foam, carbon-based material possesses lower electrical conductivity as shown in previous study, where it test on conductivity of stainless steel, carbon cloth, and carbon felt with stainless steel possess highest conductivity and carbon felt has lowest conductivity (Merino-Jimenez et al., 2016). Thus, in order to achieve a good cathode conductivity, carbon-based and metal-based material can be incorporated together where metal-based material act as structural support and current collector, for example, nickel-coated carbon fiber where it has better performance compared to carbon cloth and carbon fiber (Luo & He, 2016).

2.6.4 Cathode Configuration

Air-cathode is a limiting factor in MFC performance. Hence, it is important to modify the air-cathode either by improving its catalyst layer or GDL. Aside from these two, cathode configuration also has an influence on MFC performance. Generally, when choosing an air cathode, one of the factors that need to be considered is its surface area. A large surface area can improve oxygen diffusion into the cathode and provide more active sites for oxygen reduction reaction (ORR) thus improving MFC performance. Previous studies on varying cathode surface areas from 24 cm^2 to 96 cm^2 show that there is an increase in power density from 24 W/m^3 to 78 W/m^3 (Cheng & Logan, 2011). Another study compared two types of commercial electrodes (i.e., H 23 and MGL 190) in terms of discharge capacities with MGL 190 (0.037 mAh cm^{-2}) delivering higher discharge capacity compared to H 23 (0.024 mAh cm^{-2}) (Ha et al., 2020). In both cases,

it is caused by an increase in cathode-specific surface area. A high cathode-specific surface area can provide more active sites for ORR and allow efficient oxygen diffusion.

In terms of design, cathodes with packed and brush structures have been identified as two ideal configurations for achieving high surface area. However, these two configurations have their downside. Packed cathodes are usually less porous compared to brush cathodes; as a result, it is more susceptible to clogging. While brush-cathode with clumping fibres may reduce effective surface area (Wei et al., 2011).

Another cathode configuration that has the potential to improve MFC performance is the cylindrical cathode. Like packed and brush cathode, the cylindrical cathode has a high surface area, thus it allows for efficient oxygen diffusion and offers more active sites for ORR. Aside from that, this configuration may easily improve the surface area-to-volume ratio, reduce electrode spacing, and easy to scale up (Li et al., 2023). This is proven by previous study where power output of cylindrical cathode (46 W/m^3) is higher than flat cathode (23 W/m^3) even though both cathode have same cathode working area of 7 cm^2 and this is due to the high surface area-to-volume ratio and small electrode spacing (Li et al., 2023).

One of the easiest ways of scaling up cylindrical cathode is by stacking. Even so, stacking should be done in miniaturized concept since for cylindrical/tubular reactor operate more efficient in smaller size (Logan et al., 2015). A previous research show that by stacking multiple MFC units in cascade configuration (i.e., 12 cascades with 4 MFC units in each cascade) able to generate average power per unit of 53.8 μW (Preen et al., 2019). Another report shows that, miniaturized cylindrical ceramic-based MFC can be stack in modular stack configuration and able to generate power output up to 245 mW with 560 units MFC stack (Gajda et al., 2018).

2.7 APPLICATION OF MFC

MFCs have multiple applications, including energy production, wastewater treatment, bioremediation, and biosensors.

2.7.1 Wastewater treatment

Wastewater such as brewery wastewater, domestic wastewater, industrial wastewater, and food processing wastewater were some of the most studied substrates for microbial fuel cells. It is estimated that the cost of conservative wastewater treatment technologies was 3% of the global electricity demand, with effluent disposal which accounts for 50% of the total cost of wastewater treatments (Nawaz et al., 2022). The energy production from the MFC system might have been low, but it was still able to effectively degrade organic matter and reduce COD levels with less energy consumption and lower costs by eliminating effluent disposal. COD removal for most wastewater treated with MFC falls under the range of 80% except for petrochemical wastewater due to the existence of phenolic lignin which requires selected microbes to degrade it.

Wastewater falls under the category of complex substrates. Unlike simple substrates which provide an immediate source for product output, certain complex substrates may require additional steps before using it as a substrate. For example, autoclaving diluted wastewater to kill anaerobic bacteria and sonification increased the power density of MFC from 96 to 110 mW/m^2 (Min et al., 2005). Aside from its complexity, wastewater was considered an ideal substitute for simple substrate due to its high chemical oxygen demand (COD) (i.e., high organic matter) which is beneficial for microbial growth and mass transport. As an example, a double chamber MFC with an increase in initial COD concentration from 500 to 10000 mg/L shows an increase in microbial growth and an increase in power density from 15.3 to 50.7 mW/m^2 (Rahmani et al., 2022). However, it is only applicable for certain ranges which was demonstrated by a previous report where power output increased from 0.18 to 1.04 W/m^3 with an increase of COD concentration from 100 to 850 mg/L and showed no change when COD concentration was higher than 850 mg/L (Jiang & Li, 2009). Another study also shows a decrease in power output from 80.64 to 5.12 W/m^3 when COD concentration was increased from 6000 to 17143 mg/L (López Velarde Santos et al., 2017). This is because factors such as pH and biofilm thickness may limit the performance of MFC, not just substrate concentration. In addition, the saturated substrate can also hinder the oxidation mechanism, which eventually affects the MFC performance.

Table 2.3 Different types of wastewaters used in microbial fuel cell (MFC)

Type of wastewater	COD removal (%)	Power density	References
Petrochemical wastewater	40	0.75 W/m^3	(Sarmin et al., 2020)
Brewery wastewater	87	5.1 W/m^3	(Feng et al., 2008)
Swine wastewater	86	110 mW/m^2	(Min et al., 2005)
Fish market wastewater	77	3.81 W/m^3	(Bhowmick et al., 2020)
Mustard tuber wastewater	85	6.6 W/m^3	(Guo et al., 2013)
Paper recycling wastewater	76	501 mW/m^2	(Huang & Logan, 2008)
Chocolate industry wastewater	90	22.9 W/m^3	(Noori & Najafpour Darzi, 2016)

In wastewater treatment using MFC, instead of pure culture, mixed cultures of bacteria from the wastewater were used as a biocatalyst to improve the COD removal efficiency. For wastewater treatment, a mixed culture is ideal due to its flexibility in operating conditions and substrate usage, which is ideal for wastewater. A mixed culture can be obtained from various sources, with wastewater and activated sludge being the most common. For example, thermophilic MFC used anaerobic digestion sludge from the wastewater treatment as the inoculum for the MFC with distillery wastewater as substrate and able to generate power density and current density up to 1.0 W/m^2 and 2.3 A/m^2 (Ha et al., 2012). A research study was conducted to analyze the impact of various industrial wastewater types such as bakery, brewery, paper, and dairy on the MFC's performance and microbial composition. The results of the study revealed that each type of wastewater has a distinct bacterial community and can produce a maximum current density of 125 mA/m^2 for paper wastewater, 25 mA/m^2 for dairy wastewater, and 10 mA/m^2 for both brewery and bakery wastewater. (Velasquez-Orta et al., 2011).

2.7.2 Biosensor

Aside from wastewater treatment, MFC can also be utilized as a biosensor due to its self-sustainability without the need for signal transducer devices or specialized chemicals. MFCs have been used for in situ monitoring for several parameters such as substrate concentration, microbial respiration rate, toxic pollutants such as Cd and Pb, and BOD and COD sensors.

Prior research utilized microbial fuel cells (MFC) to monitor in-situ microbial respiration and analyte concentration. This was achieved by using *Geobacter sulfurreducens* as an external electron acceptor. In the MFC system, microorganisms respire by transferring electrons to the anode, which results in the production of electrical current. The in-situ microbial respiration was analyzed based on the electrical current generated in the MFC system (Tront et al., 2008). The analyte concentration was also analyzed based on the current generated (Tront et al., 2008).

Another study reported that MFC can monitor toxic pollutants including organophosphorus compounds, PCBs, Pb, and Hg by measuring the generated current. A decrease in current indicates the presence of toxic pollutants (Kim et al., 2007). Similarly, another research also successfully used MFC as a biosensor for the detection of heavy metals (Pb^{2+} and Cd^{2+}), avermectins, and tetracyclines based on the change of output voltage (Yi et al., 2019).

2.7.3 Degradation of Lignocellulosic Biomass

Lignocellulosic waste is usually disposed of by burning or natural decomposition. However, disposal by burning may cause greenhouse gas emissions, while natural decomposition takes a long time due to the high lignin content. Instead of disposing of it, lignocellulosic waste can be used as an energy source using methods such as cofiring, direct combustion, gasification, and pyrolysis (Singh et al., 2009). Aside from these methods, MFC systems also have been used for lignocellulosic waste degradation since they can generate energy and degrade lignocellulosic waste simultaneously using microorganisms.

Lignocellulosic biomass consists of lignin (5% - 35%), cellulose (9% - 80%), and hemicellulose (10% - 50%) where all three components consist of hydroxyl groups (Xu & Li, 2017). Lignin is a hydrocarbon polymer that contains both aliphatic and aromatic components which give a rigid and hard protective layer for cellulose and hemicellulose (Christopher et al., 2014). Lignin is formed by random cross-linking of *p*-coumaryl, coniferyl, and sinapyl alcohol (see Figure 2.8) (Calvo-Flores, 2020).

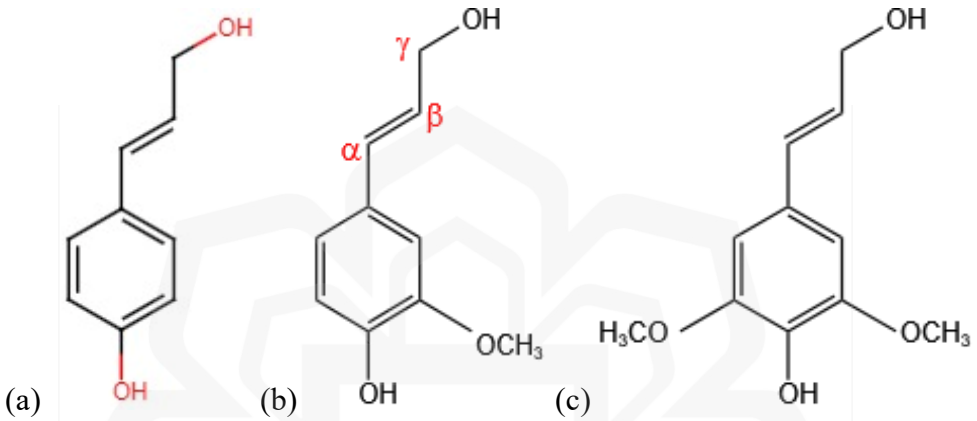

Figure 2.7 Three basic monolignol constituents of lignin; (a) *p*-coumaryl, (b) coniferyl, and (c) sinapyl alcohol

Cellulose is a homopolymer of glucose which is linked by β-1-4 linkages. It consists of microfibrils or bundles of polysaccharides that are grouped in fibrils (Brigham, 2018). While, hemicellulose is made up of pentoses (xylanes), alternating units of mannose, and glucose or galactose (Brunner, 2014). Among the three components of lignocellulosic biomass, lignin becomes a major hurdle during degradation due to the phenylpropane units with an aromatic backbone (Abdullah & Sulaiman, 2013).

White rot fungi (e.g., *P. chrysosporium*) are one the most efficient lignin degraders due to their ability to secrete ligninolytic enzymes, for instance, laccase, peroxidases (e.g., lignin peroxidase (LiP), manganese peroxidase (MnP), and versatile peroxidase (VP)), and H_2O_2-producing enzymes (Kirk & Farrell, 1987). Both phenolic and non-phenolic lignin can be oxidized by WRF with laccase-oxidized phenolic lignin and peroxidases oxidize non-phenolic lignin. Peroxidases are H_2O_2-dependent

enzymes, thus to facilitate lignin degradation H_2O_2 from external sources or oxidases (i.e., glucose-1-oxidase and glucose-2-oxidase) was used (Cho et al., 2001; Schoemaker & Leisola, 1990).

2.7.3.1 Lignin Degradation by Laccase

The main function of laccase in lignin degradation is to catalyse the oxidation of phenolic hydroxyl groups to form free phenoxy radicals. Lignin degradation by laccase involves Cα-oxidation, Cα-Cβ cleavage, and aryl-alkyl cleavage of β-1 and β-0-4 dimers. Figure 2.8 shows a degradation mechanism of the β-O-4 lignin model. Syringylglycerol-β-guaiacyl ether was cleaved into glyceraldehyde-2-guaiacyl ether and 2,6-dimethoxyhydroquinone by aryl-alkyl cleavage, and into α-carbonyl dimer by Cα-oxidation. α-carbonyl was further cleaved into syringic acid and guaiacol via Cα-Cβ cleavage. Higuchi stated that phenoxy radical was used as an intermediate for side chain cleavage (Higuchi, 2004).

Similarly, β-1 lignin model compound (I) was degraded via Cα-Cβ cleavage, aryl-alkyl cleavage, and Cα-oxidation to produce II-VII (see Figure 2.10). Before proceeding with aryl-alkyl cleavage and Cα-oxidation, a cation intermediate from the disproportionation of phenoxy radical was formed. The Cα proton from the cation intermediate was then initiated Cα-oxidation producing product II. While, products V, VI, and VII were formed via aryl-alkyl cleavage where water molecules attack the cation intermediate from disproportionation of phenoxy radical. Instead of disproportionation, phenoxy radicals went through Cα-Cβ cleavage forming radicals and quinone methide. The radicals was react with reacted with molecular oxygen forming IV, while III comes from quinone methide (Kawai et al., 1988).

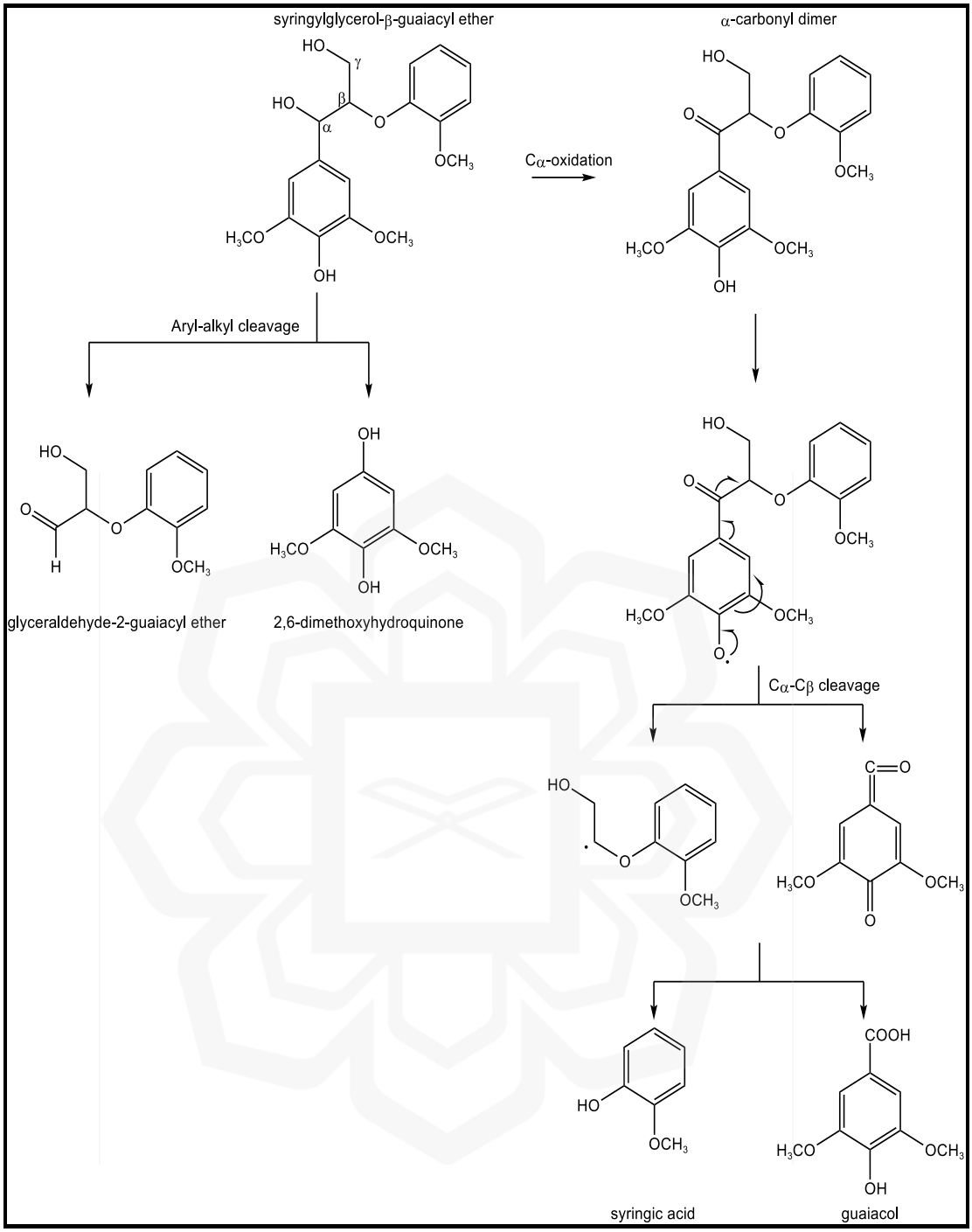

Figure 2.8 Degradation mechanism of phenolic β-O-4 lignin model

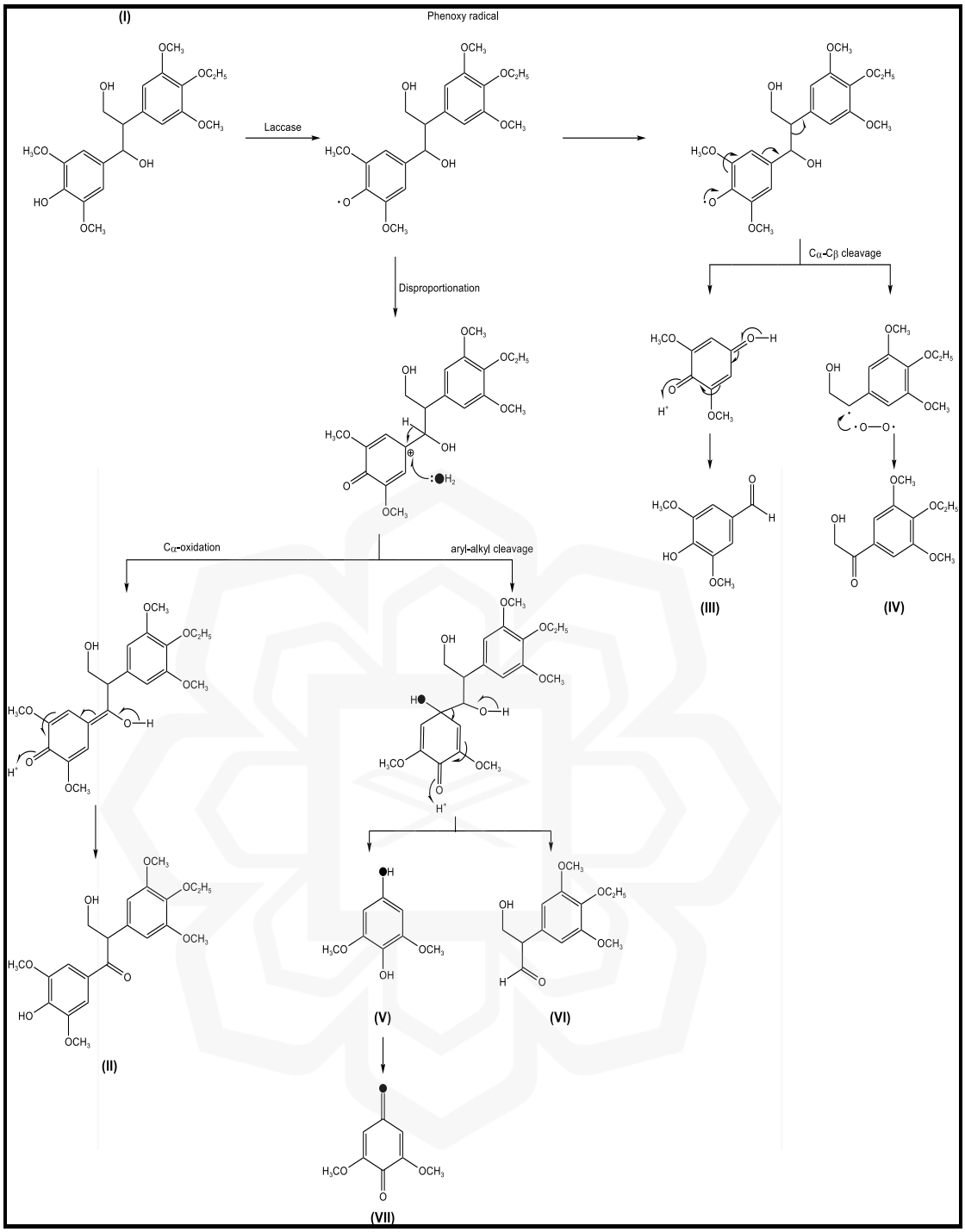

Figure 2.9 Degradation mechanism of phenolic β-1 lignin model **(I)** 1-(3,5-dimethoxy-4-hydroxyphenyl)-2-(3,5-dimethoxy-4-ethoxyphenyl) propane-1,3-diol **(II)** 1-(3,5-dimethoxy-4-hydroxyphenyl)-2-(3,5-dimethoxy-4-ethoxyphenyl)-3-hydroxypropanone **(III)** syringaldehyde **(IV)** 1-(3,5-dimethoxy-4-ethoxyphenyl)-2-hydroxyethanone **(V)** 1-(3,5-dimethoxy-4-ethoxyphenyl-3-hydroxypropanal) **(VI)** 2,6-dimethoxy-*p*-hydroquinone (VII) 2,6-dimethoxy-*p*-benzoquinone

2.8 SUMMARY

Biofuel cell (BFC) has a great potential as an alternative renewable energy. However due to its low energy yield which caused by low output and high cost, it is only suitable for small devices and not suitable for large devices. To reduce the cost while maintaining the output, the BFC need a simple design with less control parameters. One of the methods for increasing BFC's output is by stacking either in parallel or series. However, both parallel and series stacking may result in energy loss due to parasitic cell and parasitic current, respectively. Therefore, it is important to design a new stacking configuration that can minimize the energy loss caused by parasitic cell and parasitic current. Aside from generating electricity, the BFC system can also be used for wastewater treatment, act as a biosensor for COD, BOD, and toxic substance, and can degrade lignocellulosic waste simultaneously during electricity generation.

CHAPTER THREE

A NOVELMFC STACK CONFIGURATION – AN OPEN-PARALLEL UNIT-CELL CONFIGURATION

3.1 INTRODUCTION

MFC stacking is required to enhance its inherently low energy output and limiting current. Compared to the chemical fuel cell, MFC power output is three orders of magnitude lower; thus, it is unsuitable for commercialization (Gurung & Oh, 2012). Stacking can be done either in parallel or series configuration. Even though stacking may improve MFC performance, issues such as high internal resistance, parasitic current, voltage reversal, and current reversal may arise in MFC with a large number of cells which eventually lead to significant energy losses. The main setback of a series configuration is the total power lost should any unit cell in the series arrangement malfunction. Next, a series configuration results in the accumulation of the internal resistance of each individual unit cell and thus induces high energy loss. Finally, a series configuration is susceptible to voltage reversal due to the fuel starvation (Fischer et al., 2018).

To avoid those issues, more attention has been focused on the parallel configuration. Theoretically, a parallel cell's total voltage is the average voltage of the total cells, while its current is the total current of all cells. Further, in a parallel configuration, the total internal resistance of all cells is smaller than the smallest internal resistance among the individual unit cells. Consequently, a parallel stack MFC possesses an increase in total current whilst keeping the same voltage value and with reduced total internal resistance. This will produce an MFC stack with a larger discharge current density and an enhanced discharge duration (Wu et al., 2006; Ghadge & Ghangrekar, 2015).

Ideally, each cell in a parallel configuration should have the same voltage. However, since MFC reaction mechanisms involve microorganisms, the voltage value will fluctuate throughout its operation. The voltage imbalance, unfortunately, will

induce parasitic current. Current will flow from the cell with a higher voltage towards the cell with a lower voltage until all cells have uniform voltage. This current flow is called reverse current and this phenomenon causes energy losses even when the MFC stack is in an open circuit state to the external load (Oliot et al., 2017). Installing control electronics seems to be the solution now. However, the control electronics itself must be externally powered and this will only reduce the MFC energy yield.

This work introduced an open-parallel MFC stack configuration. The individual unit cells are connected in parallel configurations, but all cells share a common electrolyte. Since they share a common electrolyte as one unit cell, there will be no voltage differences between individual unit cells. As a result, the performance of the MFC stack is enhanced while the occurrence of parasitic current is mitigated.

3.2 EXPERIMENTAL DESIGN

3.2.1 The MFC Unit Cell

The cell simply comprised two electrodes (zinc anode and air cathode) inserted into a membraneless, single chamber, cylindrical jar, which was filled with 250 mL of electrolyte, 5 g of the dried specimen of *P. chrysosporium*, and 2 g of EFB as the organic substrate (see Figure 3.1). The electrolyte comprised 24 g/L potato dextrose broth (PDB).

The zinc anode (99% purity) was a 250-μm-thick foil cut into a 3 cm x 3 cm size. The air cathode used was a commercial E4/E4A EFL (Electric Fuel Ltd.) air electrode strip (300 μm thick) cut into the same size of 3 cm x 3 cm. E4 air electrode comprises laminated structures of fibrous carbon sandwiched against a nickel mesh which acts as a current collector and a gas-permeable hydrophobic layer from Teflon.

In the MFC, the fungal microbes were left to be freely suspended in the electrolyte. They eventually grew and attached to the EFB at the bottom of the cell enclosure (refer to Figure 3.1). The electrolyte was not buffered, and no additives, such as electron transfer mediator, microbe's growth enhancer, or special nutrients, were

added into the electrolyte. The MFC was left to operate in the uncontrolled ambient surroundings.

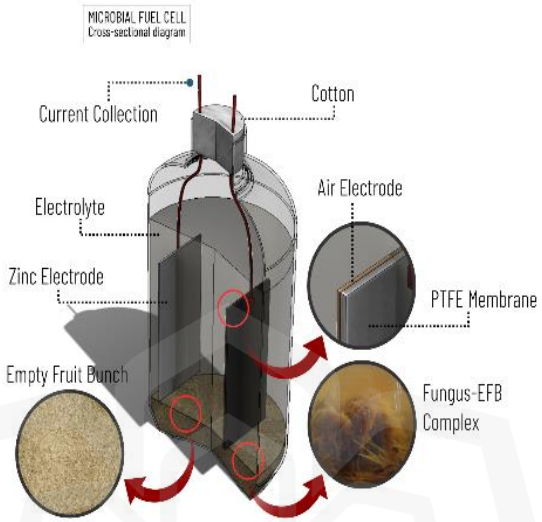

Figure 3.1 Schematic illustration of single biofuel cell

3.2.2 Microbes and Organic Substrates

A white rot fungus strain, *Phanerochaete chrysosporium* was used as an organic waste-degrading and source of cathodic catalyst. *P. chrysosporium* secrete several ligninolytic enzymes such as lignin peroxidase (LiP), manganese peroxidase (MnP), and laccase. Among the three enzymes secreted, laccase plays a crucial role in MFC operation due to its ability to reduce O_2 to H_2O. *P. chrysosporium* was first cultivated in a potato dextrose agar (PDA) for 6 days and was then transferred into potato dextrose broth (PDB) for re-cultivation for 14 days. The specimens were then filtered out from PDB and dried until its moisture content was less than 15%.

Empty fruit bunch (EFB) was manually shredded into small sizes of around 0.5 cm. Shredded EFB was then soaked in distilled water for 24 hours, rinsed, and dried under UV light.

3.2.3 MFC Operation Principle

When an air cathode is supplied a lignin-rich EFBs, the *P. chrysosporium*-derived fungal microbes will secrete ligninolytic enzymes that predominantly contain laccase, which has a specific affinity for O_2 molecules as its electron acceptor. Therefore, while the fungal microbes degrade the lignocellulosic wall, the laccase will catalyse the reduction of molecular O_2.

$$O_2 + 4H^+ + 4e^- \xrightarrow[laccase]{} 2H_2O \quad (3.1)$$

As such, a bio-catalysed electrochemical MFC can be produced by pairing a zinc anode with an air cathode in a medium that is rich with *P. chrysosporium* hyphae.

3.2.4 MFC Stack with Open-Parallel Configuration

The MFC stack comprised of three-unit cells (referred as mini cells) as described in Section 3.2.1 housed in a rectangular compartment filled with the same PDB electrolyte. The fungal microbes and the EFB substrate were localized in the respective mini cells. The three mini cells were connected in parallel configuration i.e., all anodes were connected to a single point and likewise for all cathodes. When the electrolyte level in the rectangular compartment was lower than the mini cell height, the MFC stack possessed the normal parallel configuration (refer to Figure 3.2a). But when the electrolyte level in the rectangular compartment is higher that the mini cell height, all unit cells were then hydrodynamically connected forming the open-parallel configuration (refer to Figure 3.2b). From an electrical point of view, both parallel and open-parallel configurations are connected in parallel, but the open-parallel unit cell configuration was considered as one single cell since all electrodes shared the same electrolyte.

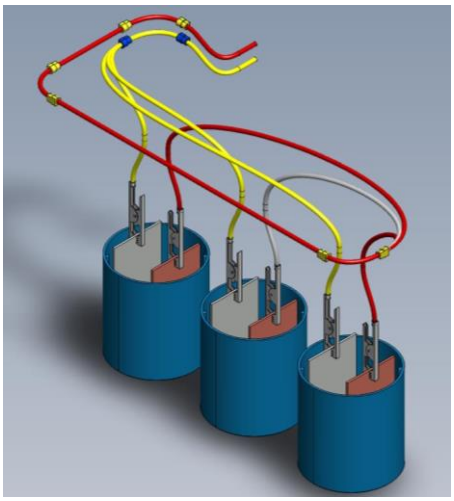

(a)

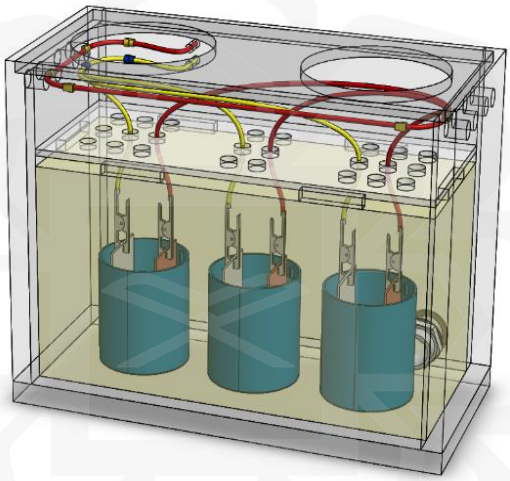

(b)

Figure 3.2 Schematic illustration of fungal biofuel cell: (a) parallel cell and (b) open-parallel configuration

3.2.5 MFC Characterisation

MFC was characterised based on its open circuit voltage (OCV), polarisation profile, power density profile, and discharge profile at constant resistance of 1000 Ω using Neware Battery Tester (BTS 4000, Neware, Shenzhen, China). OCV was measured in two cycles with each cycle consisting of the OCV measurement of open-parallel configuration and then the parallel configuration for 12 hours each. Current produced by each mini cell was measured throughout the OCV and discharge states by connecting

a multimeter equipped with a data acquisition system (UT 804, UNI-T, Guang Dong, China).

3.3 RESULTS AND DISCUSSION

To better understand the energy loss in a parallel configuration and the benefit of an open-parallel configuration, the three mini cells that formed the MFC stack (cell-1, cell-2, and cell-3) were first independently characterized by measuring its OCV, polarisation and power profiles. As anticipated, each mini cells registered different profiles. The OCV stabilized at around 1.27 V, 1.32 V, and 1.31 V for cell-1, cell-2, and cell-3 respectively (see Figure 3.3). The polarisation profiles suggested that the polarisation losses mainly come from the ohmic loss region and mass transfer region with small activation loss. From the ohmic loss region, the internal resistance of each mini cell was estimated as 274 Ω (Cell-1), 294 Ω (Cell-2), and 291 Ω (Cell-3) respectively (see Figure 3.4). The corresponding power profiles are also shown in Figure 3.4. Cell-1 possessed the best profile i.e., maximum power of 1.54 mW at 2.5 mA which tallies with its lowest internal resistance. Besides, it shows a more distinct profile as compared to Cell-2 although the OCVs of both cells seem identical.

The microbial zinc/air cell comprised of fungal microbes which are left to be freely suspended and finally attached to the EFB at the bottom of cell enclosure. The fungal colony density in the vicinity of air cathode will definitely varies among mini cells. This in turn will affect the heterogeneity of passive air diffusion to the cathode and heterogeneity in local concentrations of hydroxyl ions on the cathode (An, Kim, et al., 2015; Popat et al., 2012). The variation and fluctuation in MFC unit cell voltage is therefore unavoidable regardless of the type of microbes employed.

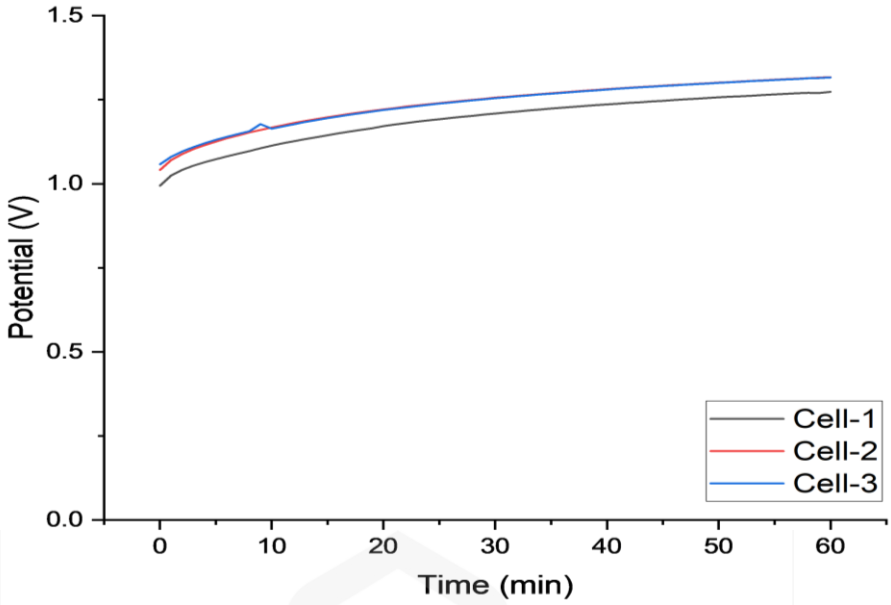

Figure 3.3 Open circuit voltage (OCV) profiles of cell-1, cell-2, and cell-3

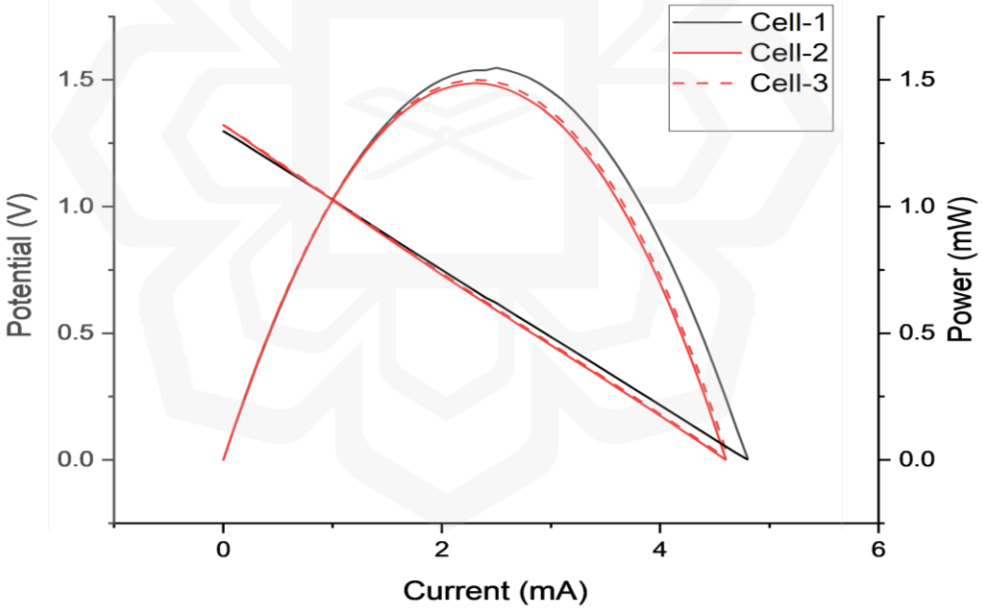

Figure 3.4 Polarisation and power profiles of Cell-1, Cell-2, and Cell-3

Energy loss in parallel configuration is negligible on a small scale, however, it will increase with the increase in the number of stacks with non-uniform voltage of individual mini cell or stack. Let's consider a parallel stack that comprises of three mini cells as constructed in the present work. According to Kirchhoff's law, the voltage around a loop equals the sum of voltage drops (V) in a loop for any closed network.

Since the parallel stack consists of three-unit cells, there will be two closed loops (see Figure 3.5). Assume that each mini cells possesses a unique internal resistance (r) and dissimilar emf (E). So, considering both Kirchhoff's current law (KCL) and Kirchhoff's voltage law (KVL) in an open circuit state, the following relations could be derived:

In the presence of parasitic current i, the voltage drop V across the mini cell can be obtained from

$$E = i(r + R) \rightarrow E = V + ir \rightarrow V = E - ir \quad (3.2)$$

Using KCL:

$$i_1 + i_2 + i_3 = 0 \quad (3.3)$$

KCL indicates that for $i_n \neq 0$ $(i = 1,2,3)$, at least one of the parasitic currents will flow towards the mini cell i.e., negative current (since the sum $\sum i_n = 0$)

Using KVL:

Loop 1: $V_1 - V_2 = 0 \rightarrow E_1 - i_1 r_1 - E_2 + i_2 r_2 = 0$ (3.4)

Loop 2: $V_2 - V_3 = 0 \rightarrow E_2 - i_2 r_2 - E_3 + i_3 r_3 = 0$ (3.5)

Solving for i_1, i_2, and i_3 :

$$i_1 = [(E_1 - E_2)r_3 + (E_1 - E_3)r_2]/(r_2 r_3 + r_1 r_2 + r_1 r_3) \quad (3.6)$$

$$i_2 = \frac{E_2 - E_1 + i_1 r_1}{r_2} \quad (3.7)$$

$$i_3 = -(i_1 + i_2) \quad (3.8)$$

where i_n denotes current (A) in the loop, r_n denotes internal resistance (Ω), E_n denotes electromotive force (emf) (V), and V_n denotes potential difference across the cell (V) with n=1,2,3.

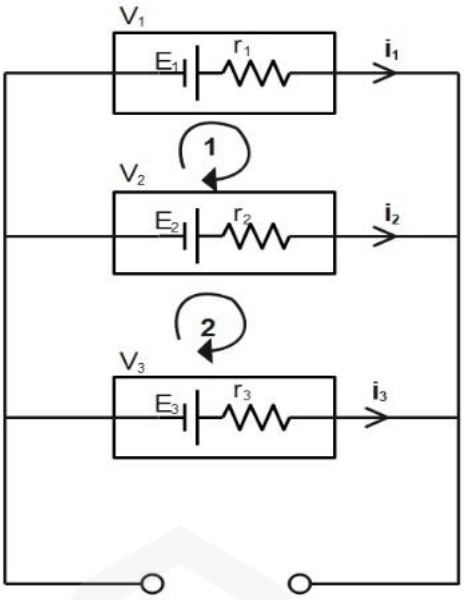

Figure 3.5 Parallel circuit configuration with voltage drop

Substituting the values of E_n and r_n $(i = 1,2,3)$ obtained from each mini cells constructed gives the following values of parasitic currents:

Table 3.1 Calculated parasitic current of mini cells

Mini cell	Emf, E (V)	Internal resistance, r (Ω)	Parasitic current, i (μA)	Power loss (during open circuit state) (μW)
Cell-1	1.27	274	-107.0	3.1
Cell-2	1.32	294	70.3	1.5
Cell-3	1.31	291	71.1	1.5

Take note there will be a total power loss of 6 μW from the parallel stack during the open circuit state which is 144 μWh/day even without connecting to the external load. Therefore, the higher the number of mini cells per stack, the higher the parasitic energy loss during a passive state. The next observation is pertaining Cell-1. Cell-1 possessed the best power profile and the lowest internal resistance. However, when

combined in a parallel configuration, Cell-1 was susceptible to the reversed parasitic current flow that would eventually degrade the cell performance. Even the parasitic energy loss is the highest across Cell-1. These are among the problems associated with parallel stack configuration.

The parallel MFC stack was then filled up with PDB electrolyte until all mini cells were totally submerged. Multiple mini cells sharing a common electrolyte is considered as one single cell. Hence, this arrangement is called an open-parallel unit cell configuration. This arrangement will immediately balance the individual voltage differences and as such ceases the occurrence of parasitic current. The effectiveness of open-parallel configuration in reducing energy loss can be seen in the power profile, V-I profile (see Figure 3.6). The open-parallel configuration possessed better polarization profile and hence better power output profile. The limiting current was more or less the same at around 6.2 mA but the maximum power was increased by 10% from 3.75 mW to 4.13 mW. In a parallel configuration, the total internal resistance (r_T) will be reduced according to:

$$\frac{1}{r_T} = \frac{1}{r_1} + \frac{1}{r_2} + \frac{1}{r_3} \tag{3.9}$$

Using the values in Table 3.1, the total internal resistance is expected to be reduced to 95 Ω. The slope of the ohmic region from the polarization profile (V-I) of the parallel stack MFC gave a value of around 92 Ω which was in good agreement with the expected value. Interestingly, the polarisation loss (ohmic region) of the parallel configuration was further reduced from 92 Ω to 82 Ω as all mini cells shared a common electrolyte (open-parallel configuration), a reduction of 11%.

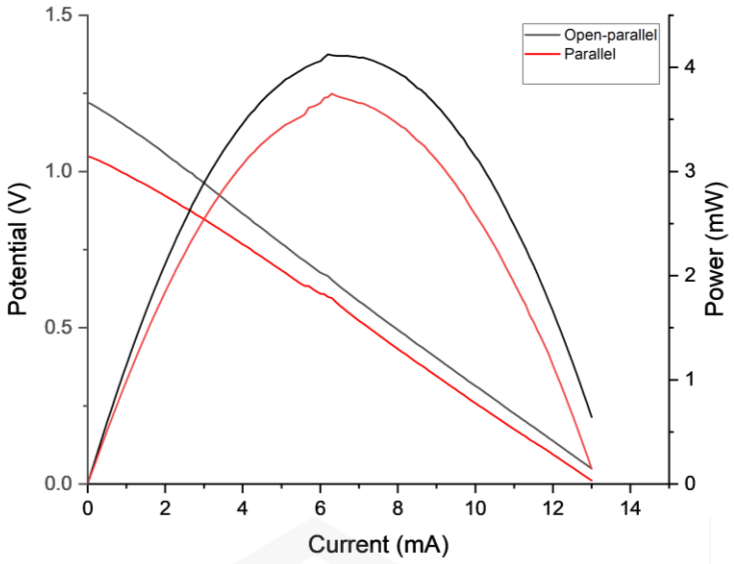

Figure 3.6 Polarisation and power profile of parallel configuration and open-parallel configuration

The OCV profile (see Figure 3.7) further demonstrates the advantage of open-parallel configuration. The transformation between open-parallel and parallel configurations were performed by simply draining and filling up the electrolyte of the MFC stack. Once all mini cells were submerged under a common electrolyte, they became connected in an open-parallel configuration. Alternately, if the electrolyte was drained until all mini cells were not hydraulically connected (i.e., the electrolyte level is lower than the individual cell height), they formed the parallel configuration. Obviously, the parallel stack MFC suffered a substantial voltage loss due to the presence of parasitic current as compared to the open-parallel stack MFC, almost a 15% decrease from 1.45 V to 1.24 V. When the electrolyte was filled up again to form the open parallel configuration (2^{nd} cycle), the OCV increases to 1.38 V and likewise decreases to 1.14 V when the MFC was transformed again into the parallel configuration. The changes in the average OCV values during the 1^{st} and 2^{nd} cycles were attributed to the disruption of the living microbial colonies during the filling up and draining of the MFC electrolyte.

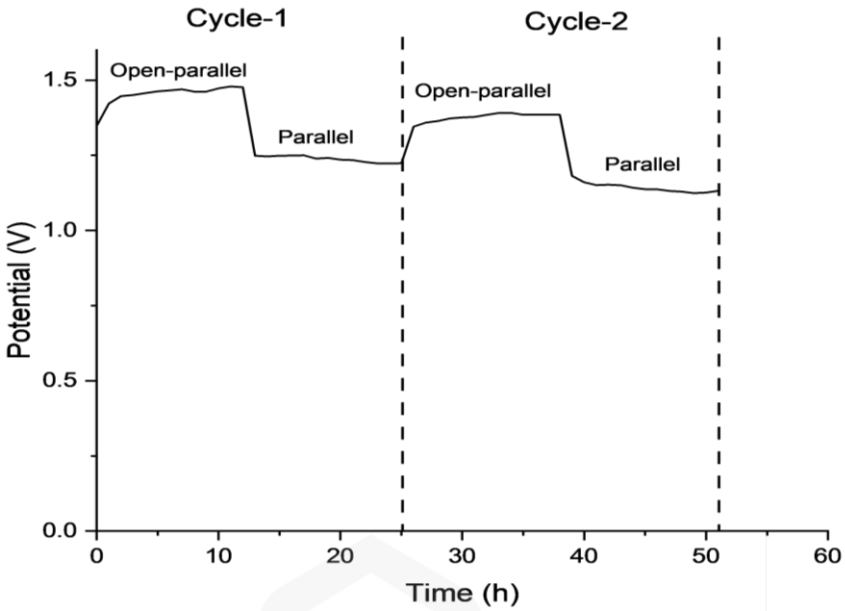

Figure 3.7 Open circuit voltage (OCV) of open-parallel configuration and parallel configuration

The presence of the parasitic current in the MFC stack during the OCV observation as it was transformed between open-parallel to parallel and vice versa was traced by digital multimeters (see Figure 3.8). In the 1st cycle during the open-parallel configuration, no parasitic current was observed, only fluctuations in the base reading (< 2 μA). When the connection between mini cells were transformed into parallel configuration, immediately parasitic currents (~ 110 μA) were detected in Cell-1 and Cell-3. These current ceased immediately as all mini cells were submerged in a common electrolyte in the 2nd cycle of open-parallel configuration. Further, as the mini cells connection was transformed again into parallel configuration, parasitic currents were detected from all mini cells. The variation in the parasitic current behaviour was attributed to the fluctuation in the mini cell voltage, changes in the internal resistance value and disruption of the microbial colonies during the transformation between open-parallel and parallel configurations.

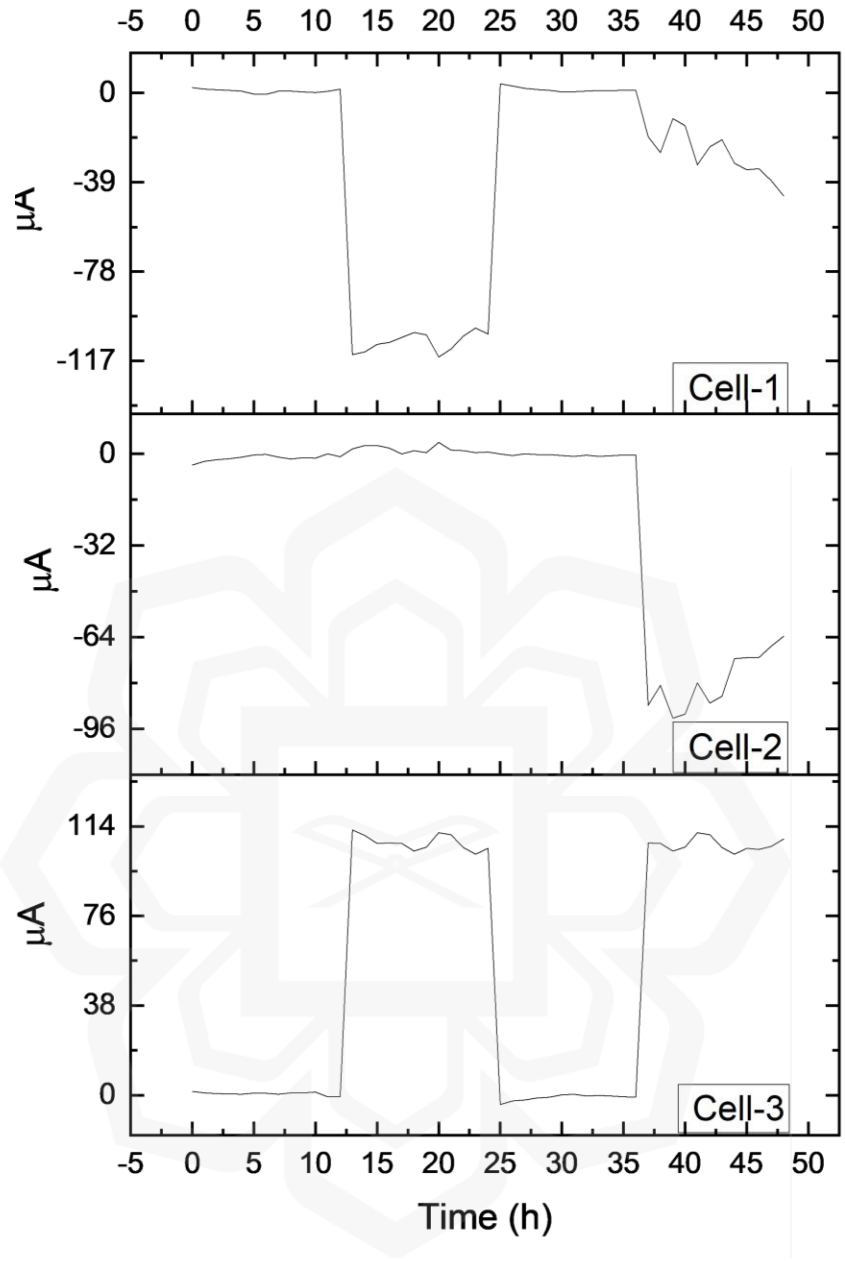

Figure 3.8 Parasitic current at Cell-1, Cell-2, and Cell-3 during open circuit voltage (OCV)

The MFC stack was then subjected to a discharge capacity test at a constant resistance of 1000 Ω. Figure 3.9 presents the discharge profiles for both the parallel and open-parallel configurations. The MFC with open-parallel configuration demonstrated a significant enhancement in the discharge capacity i.e., 3.4 times longer. The MFC with open-parallel configuration could operate continuously for 89 days as compared to 29

days for the MFC with parallel configuration. In terms of energy output, the MFC with open-parallel configuration produced a total output of 594 mWh as compared to 227 mWh for the MFC with parallel configuration i.e., 2.6 times larger.

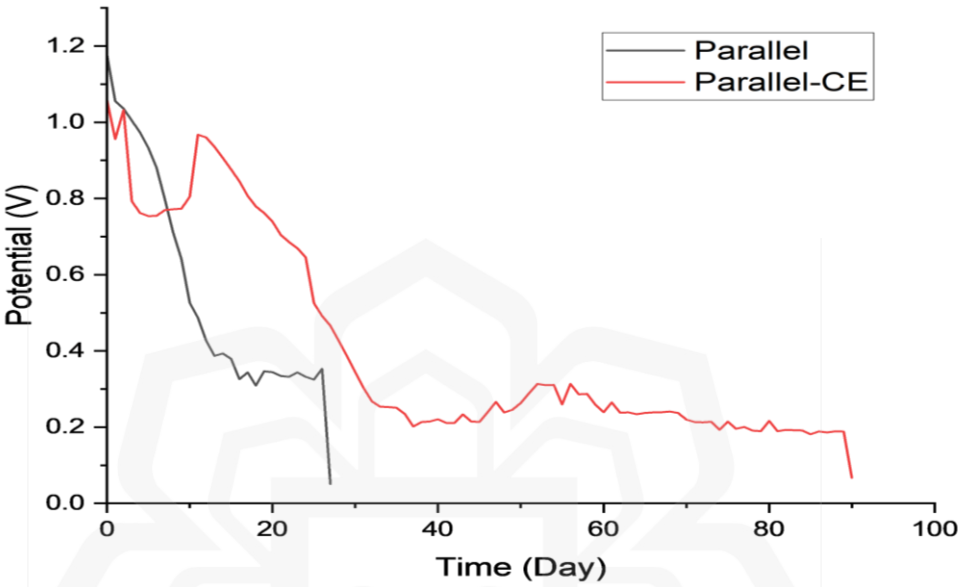

Figure 3.9 Discharge profile of the MFC with parallel and open-parallel unit-cell configurations at constant resistance of 1000 Ω

Table 3.2 shows the values of instantaneous discharge currents recorded at an interval of 24 hours. Discharge current was measured for Cell-1, Cell-2, Cell-3 and the external 1000 Ω resistor which represent the total output current. Fluctuations in the mini cell voltage will induce multi-loop current. For example, current generated by Cell-1 could pass through Cell-2, Cell-3 and the external 1000 Ω resistor, and the same goes for the other two mini cells. The direction and value of this multi-loop current is dynamically regulated by the variation in individual cell voltage and internal resistance. The discrepancy in the sum of current produced by all mini cells ($i_1 + i_2 + i_3$) and the total current measured through the 1000 Ω resistor (i_T) denotes the loss due to multiple current loops ($i_1 + i_2 + i_3 > i_T$).

Table 3.2 Current distribution in a parallel stack MFC during discharge at constant resistance of 1000 Ω

Time (Day)	i_1 (mA)	i_2 (mA)	i_3 (mA)	$i_1 + i_2 + i_3$ (mA)	i_T (mA)
0	0.33	0.27	0.54	1.14	1.19
1	0.36	0.32	0.36	1.04	0.99
2	0.35	0.32	0.34	1.01	0.97
3	0.34	0.31	0.33	0.98	0.94
4	0.33	0.3	0.32	0.95	0.92
5	0.32	0.28	0.31	0.91	0.87
6	0.3	0.28	0.28	0.86	0.81
7	0.27	0.26	0.25	0.78	0.74
8	0.25	0.24	0.17	0.66	0.66
9	-0.01	0.23	0.12	0.34	0.58
10	0.23	0.23	0.2	0.66	0.48
11	0.19	0.19	0.16	0.54	0.43
12	0.17	0.16	0.15	0.48	0.35
13	0.16	0.13	0.13	0.42	0.3
14	0.13	0.12	0.12	0.37	0.31
15	0.14	0.12	0.11	0.37	0.31
16	0.15	0.1	0.1	0.35	0.27
17	0.14	0.1	0.09	0.33	0.26
18	0.14	0.09	0.08	0.31	0.25
19	0.13	0.09	0.07	0.29	0.26
20	0.14	0.09	0.08	0.31	0.26
21	0.15	0.11	0.07	0.33	0.26
22	0.14	0.1	0.07	0.31	0.28
23	0.15	0.11	0.07	0.33	0.26
24	0.14	0.11	0.07	0.32	0.26
25	0.16	0.1	0.07	0.33	0.26
26	1.15	0.08	0.07	1.3	0.21

Figure 3.10 summarizes the current loss from the parallel stack MFC during the discharge duration. Negative values represent current loss i.e., $i_1 + i_2 + i_3 > i_T$. During the first nine days of the discharge, the current loss was rather consistent at around 5%. For the subsequent discharge duration, the current loss increased markedly and fluctuates around 25%. There were instances where $i_1 + i_2 + i_3 < i_T$ (day-0 and day-9). This is attributed to accumulation of charges across a cell during a reversed current flow. The accumulated charges will be discharged when the parallel stack MFC operating voltage is less than the OCV value of that particular cell (An, Sim, et al., 2015). Take note that Cell-1 was subjected to a reversed current flow (~ 110 µA) during the open circuit state, refer to Figure 3.8. Besides, data in Table 3.2 for Day-9 indicated that a reversed current flow of 10 µA was recorded at Cell-1. The difference was much higher in Day-9 despite the much lower reverse current is probably due to the much lower operating voltage at Day-9.

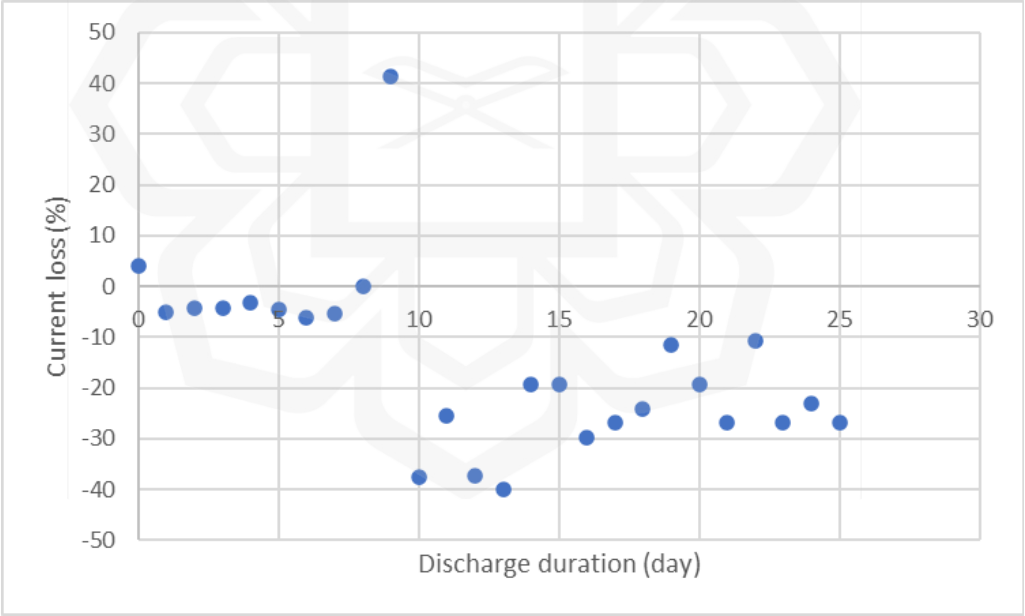

Figure 3.10 Current loss suffered by the parallel stack MFC during the discharge

3.4 SUMMARY

This work introduced a novel MFC stack configuration - an open-parallel configuration. In this configuration, all mini cells were connected in parallel but hydrodynamically connected in a common electrolyte. Using this approach, the MFC stack gains the advantages of a parallel configuration, namely, improved discharge duration and energy output by 3.4 times and 2.6 times respectively, while mitigating the parasitic energy loss that is associated with the parallel configuration. This passive approach does not require external control electronics and thus will enhance the energy yields of an MFC stack.

CHAPTER FOUR

AN EASY-TO-FABRICATE CARBON-BASED AIR CATHODE FOR MICROBIAL FUEL CELLS

4.1 INTRODUCTION

The second part of this work focusses on the design and fabrication of an effective for use in MFCs operating under submerged and unaerated conditions. The main purpose is to produce a carbon-based air cathode that relies solely on dissolved oxygen in the electrolyte so that air purging component could be eliminated. No catalytic material is incorporated into the air cathode. Further, the aim is also to develop an easy-to-fabricate air cathode that does not require any special treatment such as calendaring at high temperature or high pressure. Ultimately, these approaches shall reduce the cost of the air cathode which is the most expensive component in an air cathode MFC.

Carbon-based air cathodes; such as carbon felt, carbon cloth, carbon rods, and carbon fibre; are commonly used as they have a large surface area and good electrochemical properties (Reinhard et al., 2020). Catalysts are often used in an air cathode to increase its oxygen (O_2) affinity and decrease the activation energy required for the oxygen reduction reaction (ORR) to occur; which, in turn, increases the amount of energy discharged by the air cathode (Khilari et al., 2014). Although platinum-based air cathodes enable BFCs to discharge significantly higher density energy (Choi et al., 2019), they are very expensive. Cobalt oxides and manganese oxides-based air cathodes are some cheaper alternatives (Ahmed et al., 2012; Das et al., 2020).

An effective air cathode also requires a stable triple interface, which is the electrolyte (liquid), the O_2 (liquid), and the catalyst/current collector (solid) interface at which the ORR occurs. However, although this feature is unique to air cathodes, it is rarely discussed when reporting the performance of an air cathode. The airside of an air cathode is normally porous and coated with a semipermeable, hydrophobic membrane, such as Teflon™, while the electrolyte side is often dispersed with a catalyst and denser. This ensures a good balance between hydrophobicity and hydrophilicity in an air

cathode and, more crucially, prevents flooding, which occurs when an electrolyte accumulates in the porous airside of the air cathode and hinders the transportation of O_2 to the active sites of the catalyst or conductor (Gajda et al., 2014; Wang & Leung, 2017). Commercially available air cathodes are expensive due to the distinctive abovementioned features.

The proposed air cathode comprised layers of carbon felt and carbon fibre sheets fortified by a nickel mesh, without the use of a catalyst. All the components of the cathode were cut into the desired sizes and snugly assembled merely using the mechanical pressure of the cylindrical holders in the BFC. The proposed air cathode was tested in a microbial zinc-air MFC under a submerged condition. A submerged air cathode relies solely on the dissolved oxygen (DO) in the electrolyte, unlike an open-air air cathode. The DO concentration is merely one-third of the oxygen concentration in the ambient air. Therefore, in most MFC applications where a submerged air cathode is employed, the electrolyte is saturated with oxygen by bubbling air throughout the cell discharge operation. However, this approach will only decrease the existing low energy gain yields (output/cost) of MFCs.

Submerged aquatic plants rely on dissolved oxygen (DO) and dissolved inorganic carbon (DIC) for their respiration and photosynthesis (Pedersen et al., 2013). There are two major challenges for submerged aquatic plants as compared to those leaved plants exposed to atmospheric air, namely (i) significantly lower DO and DIC concentrations, and (ii) profound resistance of gas exchange under water (Pedersen et al., 2013). One of the special adaptation features or mechanisms for submerged aquatic plants is their hydrophobic leaves. A thin gas film forms on the surface of these leaves due to the hydrophobic nature of its surface. This gas film reduces the resistance to gas exchange which is caused the by diffusion boundary layer (DBL) (Verboven et al., 2014; Winkel et al., 2016). For a similar transport distance across a DBL and the same concentration gradient, the gas exchange under water is 10^4-fold slower than in air (Pedersen et al., 2013). Due to the large water-gas interfaces between DBL and thin gas film, more oxygen can be collected inside the thin gas film before diffusing into the stomata (Figure 4.1) (Verboven et al., 2014).

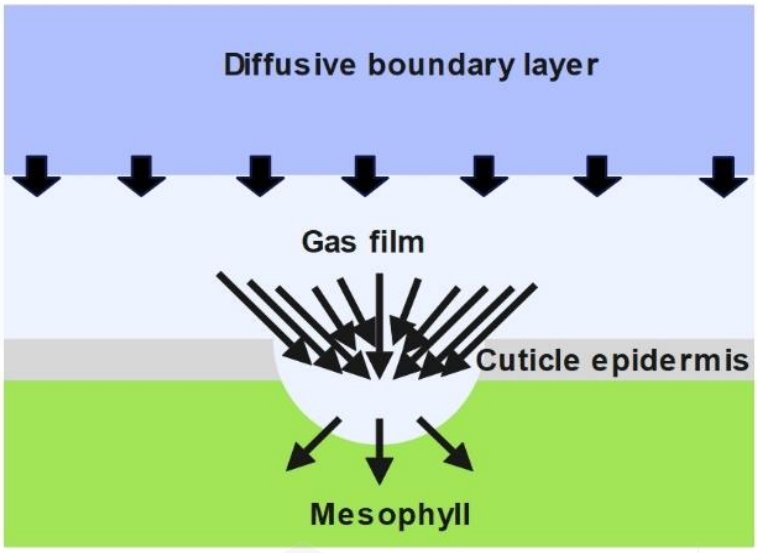

Figure 4.1 Schematic illustration of mechanism of O_2 diffusion to submerged leaves

Therefore, hydrophobicity must be considered when designing a totally submerged air cathode to ensure its effective functioning. The air cathode that this present study proposed comprised a nickel mesh, carbon felt, and carbon fibre sheets. The nickel mesh served as both structural support and the current collector for the external circuit, the sponge-like nature of the carbon felt served as an air trap while its intrinsic hydrophobicity enabled the formation of a gas film, and the carbon fibre sheets served as electron carriers for the ORR for the external circuit as it is compact, conductive, and has a large surface area.

4.2 EXPERIMENTAL DESIGN

4.2.1 Design Considerations and Fabrication of the Air Cathode

The holder of the air cathode comprised two polyvinyl chloride (PVC) tubes of different diameters (height = 45 mm, $\phi 1$ = 58 mm, $\phi 2$ = 50 mm) with a perforated inner insert. All the components of the cathode were cut into the desired sizes and wedged between the two cylindrical PVC tubes. This ensured that a uniform and uniaxial pressure was placed on the multiple layers of the air cathode, thereby, ensuring that the exact same properties were maintained for each test run. An inner insert ($\phi 2$) with a different

diameter could be used to apply a different uniaxial pressure. Figure 4.2a illustrates the overall arrangement of the cathode; which was carbon felt and 2-ply carbon sheets inserted between sheets of nickel mesh. As seen in Figure 4.2c, a bipolar configuration was later used to increase the surface area of the air cathode. For this configuration, two concentric cylindrical holders of differing diameters were used. The performance of the proposed air cathode was benchmarked against that of commercially available E4/E4A EFL air cathode strips that had been cut into identical 3 cm by 3 cm strips.

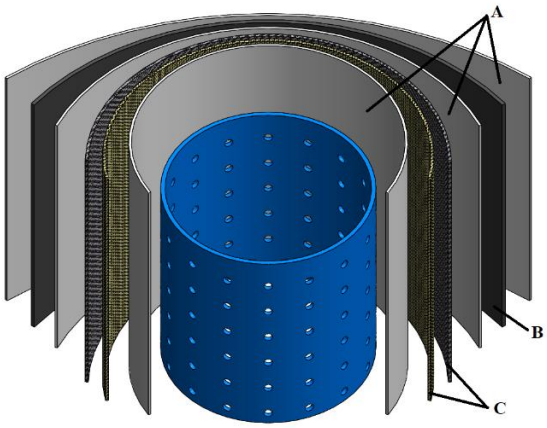

(a)

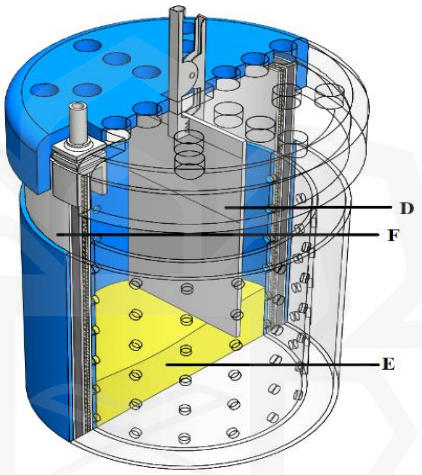

(b)

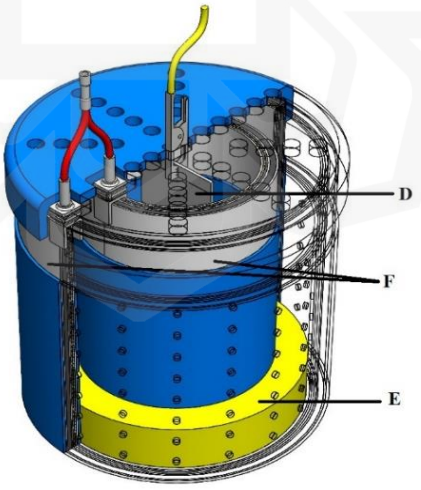

(c)

Figure 4.2 Schematic illustration of (a) air cathode components, (b) microbial zinc/air cell, and (c) microbial zinc/air cell employing double air cathode (bipolar design) Legend: A - Nickel mesh; B - Carbon felt; C - 2-ply Carbon fibre sheet; D - Zinc anode; E - Fungus cultivated EFB; F – Air cathode

4.2.2 Characterisation of the Structure of the Air Cathode

A JEOL® JSM-6700F field emission scanning electron microscope (FESEM; Tokyo, Japan) was used to observe the surface morphologies of the carbon felt and carbon fibre sheets of the proposed air cathode as well as the E4 air cathode. The ImageJ image processing programme was used to analyse the hydrophobic contact angle of the carbon felt.

4.2.3 Fabrication and Operating Principles of the Microbial Zinc-Air MFC

The membrane-less, single chamber cylindrical MFC was filled with 250-ml of 24 g/L unbuffered potato dextrose broth (PDB) electrolyte. The microbes were cultured from 5 g of dried *Phanerochaete chrysosporium* (*P. chrysosporium*) in an organic substrate of 2 g of oil palm-derived empty fruit bunches (EFBs). The fungus-cultivated EFBs resided at the bottom of the BFC enclosure. A 40 mm by 100 mm zinc anode strip was placed in the middle of the BFC enclosure. Further details can be referred to Section 3.2.

4.2.4 Electrochemical Analysis

A Neware® BTS 4000 battery tester (Shenzhen, China) was used to test the discharge capacity of the microbial zinc-air BFC containing the proposed air cathode under a constant current of 1 mA.

4.3 RESULTS AND DISCUSSION

The discharge capacity of the proposed air cathode at a constant current of 1 mA was used to gauge its performance (Figure 4.3). The microbial zinc-air BFC containing the proposed air cathode discharged an average operating voltage of 200 mV for 42 days. The total output energy, which was estimated based on the area under the discharge plot, was 211 mWh. The performance of the proposed air cathode was benchmarked against

that of a commercially available E4 air cathode. The E4 air cathode was able to discharge an average operating voltage of 280 mV for 53 days for a total output energy of 403 mWh. Obviously, being incorporated with manganese-based catalyst, E4 air electrode was able to discharge 2 times more energy than the proposed air cathode which is non-catalytic.

Enhancing the air cathode surface area has been identified as one of the most critical factors to increase the volumetric power density of an air cathode microbial fuel cell (MFC) (Cheng & Logan, 2011). It was reported that doubling the air cathode surface could increase the output by 62%. However, this option is very costly and not feasible for a catalytic-based air cathode. A bipolar configuration was then used to increase the surface area of the proposed non-catalytic air cathode, which significantly improved its discharge profile (Figure 4.3). More specifically, increasing the surface area of the proposed air cathode by 2.5 times enabled it to discharge more energy than the E4 air cathode for the first 31 days. Furthermore, although the enhanced proposed air cathode stopped discharging energy on Day 40, its total energy output was 396 mWh, which was only 1.7% lower than that of the E4 air cathode.

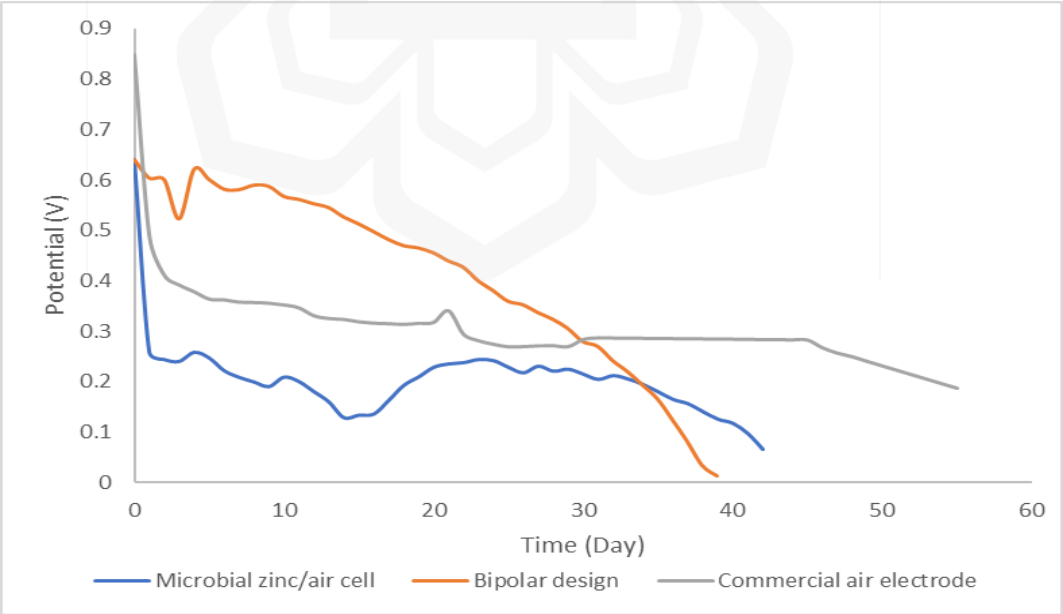

Figure 4.3 Evaluation of the air cathode from the cell discharge profile at 1 mA

Among the notable demonstrations of self-sustaining microbial fuel cell employing the air cathode is reported by Khaled et al., (2016). In a battery-mode (i.e., single supply of sodium acetate substrate, without replenishment) the MFC power stack was capable to operate a low-powered temperature sensor for 20 days. The power stack comprised of two MFCs and incorporated with a power management unit (PMU). The PMU comprised of a DC/DC converter, capacitors (to filter the fluctuations of the MFC output voltage) and a mechanical switch. Each MFC alternately powered the sensor in a 48-hour cycle. Their MFC was a single chamber 700-ml capacity, inoculated with industrial wastewater and fed with 0.7 g of sodium acetate. The anode was a stainless-steel mesh with projected area of 100 cm^2. The air cathode was a 120 cm^2 carbon cloth (30% Teflon treated, 0.5 mg/cm^2 platinum catalyst loading). The biofilm on the air cathode was developed separately. With a total platinum catalyst loading of 60 mg, the MFC registered a maximum power point about 1.1 mW/m^2 at around 3.5 mA and 0.9 V. Conversely, the microbial zinc/air cell employing the non-catalytic air cathode produced a maximum power point of 50 mW/m^2 at 4.2 mA and 0.3 V. The immediate consequence of a non-catalytic air cathode is the huge potential drop due to the high activation energy but compensated by its ability to sustain a higher current.

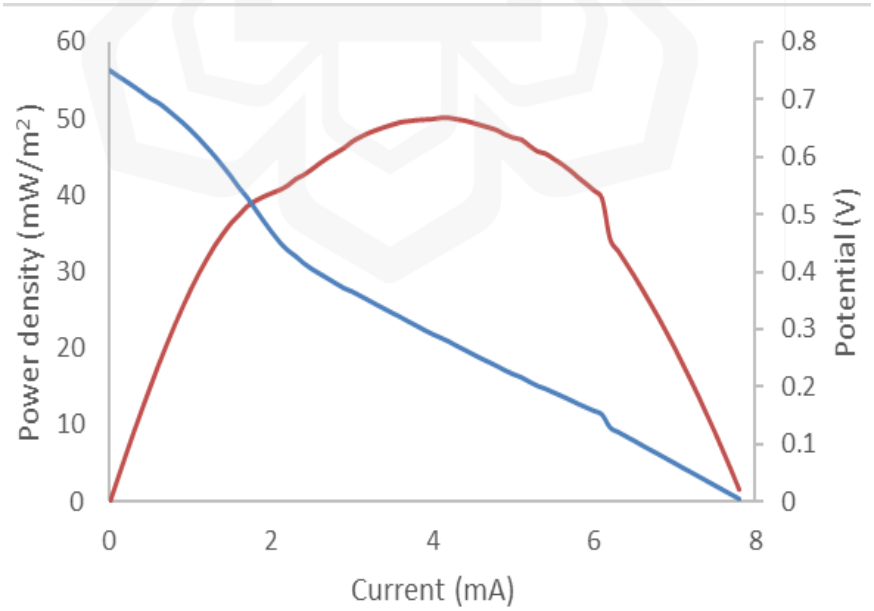

Figure 4.4 Power density profile of microbial zinc/air cell employing the proposed submerged air cathode

An air cathode, generally, comprises two components: a conductive base and a gas diffusion layer (GDL). If a catalyst is required, it is incorporated between these two components. The conductive base supplies the electrons that are required for the ORR to occur from the external circuit or anode, while the GDL is where O_2 diffusion occurs between the electrolyte and the active sites (Tomboc et al., 2020; Yang et al., 2015). As such, GDLs are designed to be hydrophobic to prevent the cathode from flooding (Tomboc et al., 2020). The GDL is normally called the "airside" while the conductive base is called the "waterside". The interface between the GDL and the conductive base is a triple interface; i.e., the electrolyte (liquid), the O_2 (liquid), and the catalyst/current collector (solid); at which the ORR occurs. Therefore, it is crucial to stabilise the triple interface to maintain the efficacy and functions of an air cathode.

Most metal-air cells contain an open-air air cathode, where one side is exposed to air. In a seawater aluminium/air cell, however, the air cathode is fully submerged in the liquid electrolyte. In such cases, the cell solely depends on the dissolved O_2 in the electrolyte liquid; which is available at significantly lower concentrations than the amount of O_2 in ambient air; to operate (Canadian Council of Ministers of the Environment, 1999). A hydrophobic GDL now performs another important function, which is to facilitate the exchange of O_2 between the cathode and the electrolyte at the gas-liquid interface (Arif et al., 2020; Pedersen et al., 2013). Air cathode BFCs often use submerged air cathodes (Chen et al., 2018; Saba et al., 2017). Although O_2 is bubbled throughout the operation of most cell configurations to increase the amount of dissolved O_2 available, a well-designed air cathode could further improve cell performance.

As the proposed air cathode functioned effectively, it supported the design estimations. The SEM results indicated that carbon felt contains loose and long carbon fibres that form a porous and spongy texture (Figure 4.5a), which enables it to entrap air. Figure 4.5b depicts the hydrophobic nature of carbon felt by placing a droplet of H_2O on it. Therefore, when the carbon felt is fully submerged in the electrolyte, its hydrophobicity should enhance its O_2 exchange with the electrolyte. Carbon fibre sheets were used as a conductive base to supply electrons from the external circuit for the ORR to occur. The SEM results indicated that carbon fibre sheets contain interwoven threads of carbon fibre bundles (Figure 4.5c). Carbon fibre sheets are widely used as a base in

cathodes as they are highly conductive and possess good chemical and electrochemical stability. Meanwhile, nickel mesh not only provides structural integrity in an air cathode but acts as a current collector.

When benchmarked against an E4 air cathode, the discharge duration and capacity of the microbial zinc-air BFC containing the proposed air cathode was shorter and 48% less, respectively, than that of the E4 air cathode. The E4 air cathode possesses two advantages. First, it is dispersed with a manganese-based catalyst within the air cathode structure. On the other hand, the proposed air cathode totally relied on the freely suspended biocatalyst excreted by the fungal microbes. Second, the electrolyte-side of the E4 electrode is dense in nature and prevented the penetration of fungal mycelia colonies. When the proposed air cathode was configured bipolarly which is a stack design, it discharged more energy than the E4 air cathode for the first 31 days. Its discharge duration, on the other hand, was still comparable to that of a single air cathode configuration.

SEM was used to examine the enhanced proposed air cathode once it had ceased operation. As seen in Figure 4.6a and Figure 4.6b, dense *P. chrysosporium* mycelia colonies had formed on the surfaces of both the carbon felt and carbon fibre sheets of the enhanced proposed air cathode. Conversely, as the surfaces of the carbon components of the E4 air cathode are dense, they prevent the penetration and proliferation of fungal mycelia colonies (Figure 4.6c). The airside of an E4 air cathode strip is encased in a Teflon™ membrane, which has comparable hydrophobicity to carbon felt. It is possible that the proliferation of fungal mycelia colonies between the carbon felt and carbon fibre sheet layers of the enhanced proposed air cathode prevented it from functioning effectively and sustaining the desired current output. Therefore, the carbon fibre sheets, or waterside, of BFCs that utilise fungal microbes must be protected or coated with a dense layer to prolong its service life. It is also noteworthy that, although the proposed air cathode does not contain any catalytic materials, its discharge performance could be tailored simply by increasing its surface area.

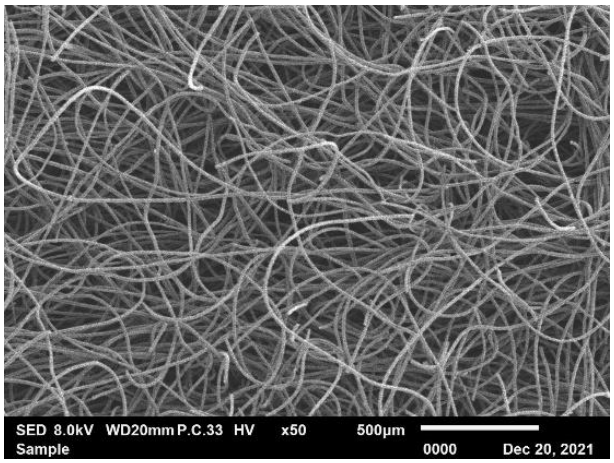

(a)

(b)

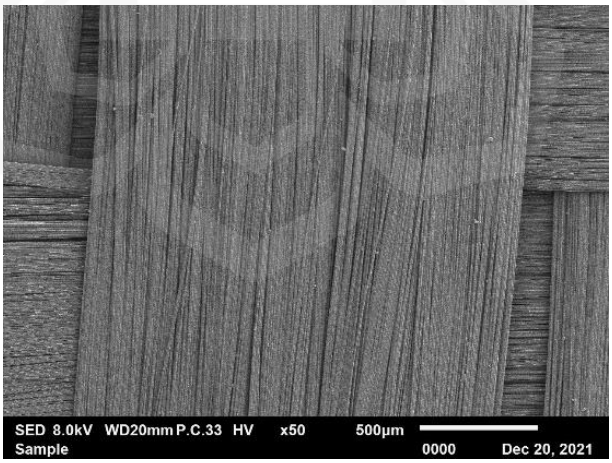

(c)

Figure 4.5 (a) SEM image of carbon felt depicting extended carbon fibre forming the spongy and porous matrix; (b) Digital image showing the hydrophobic nature of carbon felt; and (c) SEM image of carbon fibre forming compact structure

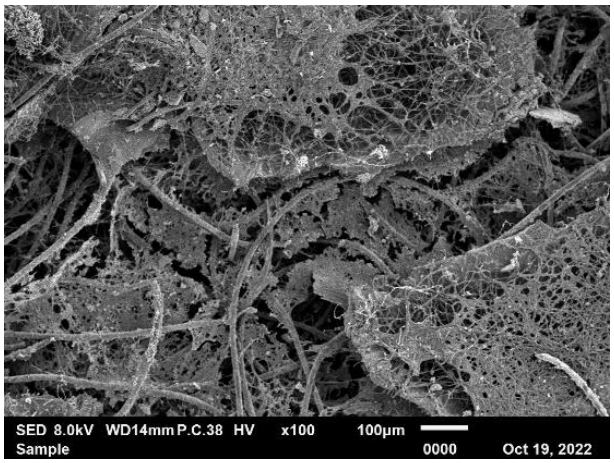

(a)

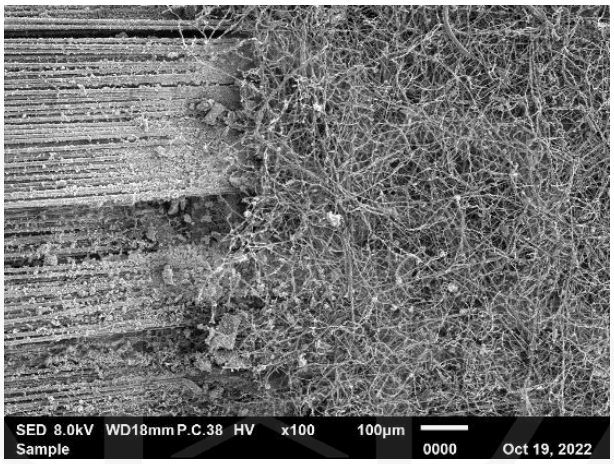

(b)

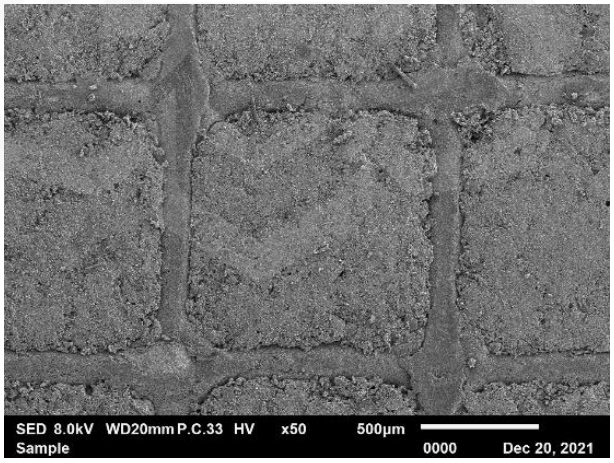

(c)

Figure 4.6 (a) SEM image depicting fungal colony growth on carbon felt; (b) SEM image depicting dense mycelia colony of *P. chrysosporium*; (c) SEM image of E4 air cathode depicting a compact structure of the waterside with no trace of fungal growth.

4.4 SUMMARY

A simple method to fabricate an effective, submerged carbon-based air cathode for use in MFCs has been developed. Commercially available carbon felt and carbon fibre sheets were, respectively, chosen as the GDL and conductive base of the proposed air cathode based on their as-purchased properties and used without any modifications. Therefore, the O_2-reducing performance and efficacy of the proposed air cathode could be further enhanced by pre-treating the carbon felt and carbon fibre sheet layers using multiple methods. The proposed air cathode was tested as a fully submerged air cathode in a microbial zinc-air MFC and found to be able to discharge a comparatively high constant current over a one-month period. Therefore, the proposed air cathode is a viable and effective to be employed under submerged condition, be it for non-air circulated or air circulated MFCs.

CHAPTER FIVE

VIABILITY OF MICROBIAL ZINC/AIR CELL AS LIGNOCELLULOSIC WASTE DEGRADING CELLL

5.1 INTRODUCTION

White rot fungi such as *Pleurotus ostreatus, Phanerochaete chrysosporium, Trametes versicolor, and Xylobolus frustulatum* has a unique ability to break down wood lignin (Eriksson et al., 1990; Shen et al., 2020). Lignin is a recalcitrant material that forms the protective structural matrix surrounding the hemicellulose and cellulose within the cell wall (Carrier et al., 2011; Christopher et al., 2014). Out of all the white-rot fungi, *P. chrysosporium* is the most commonly studied. Its fast growth rate, good ligninolytic properties, and ease of handling make it a preferable choice as compared to other fungi or bacteria species (Abdel-Hamid et al., 2013; Couto et al., 1998; Lee et al., 2014).

P. chrysosporium secrete ligninolytic enzymes such as laccase, and H_2O_2-dependent ligninase (i.e., lignin peroxidase, and manganese peroxidase) for lignin and other biopolymers degradation (Janusz et al., 2017). Among the ligninolytic enzymes, laccase is the most effective for lignin degradation. Laccase oxidizes both phenolic and non-phenolic substrate (Kiran et al., 2019). Oxidation of phenolic hydroxyl group is primarily catalysed by laccase and formed phenoxy radicals which leads to C_α-C_β cleavage, alkyl-aryl cleavage, and C_α oxidation (Bourbonnais et al., 1995). While, oxidation of non-phenolic by laccase may occur only if mediators, such as 2,2'-azinobis-(3-ethylbenzthiazoline-6-sulfonate) (ABTS) and 3-hydroxyanthranilic acid (HAA) are present (Wong, 2009).

Lignin is abundant in nature and represents a potential source of renewable chemicals and energy. However, its intrinsic mechanical and chemical resistance is the main challenge. *P. chrysosporium* has been widely researched for this purpose, given its ability to produce a more complete lignin-degrading enzyme complex than most other strains (Singh & Chen, 2008). Following the success of harvesting electricity from the microbial zinc/air cell employing *P. chrysosporium* fed with oil palm empty fruit

bunch (EFB), this work shall study the viability of microbial zinc/air cell as a lignocellulosic waste biodegrading cell.

EFB is one of the biomass solid wastes produced from the palm oil industries. EFB contributes 20-23% of the total solid waste produced (Rahayu et al., 2019). Other types of biomasses produced include oil palm kernel shell (OPKS), oil palm trunk (OPT), and oil palm fond (OPF). Most of the solid waste is burned or used as a mulching material and fertilizer (Rahayu et al., 2019). Although this disposal method is cost-effective, it can lead to greenhouse gas emissions and create homes for pests (Mohammad et al., 2020). Solid waste residues of palm oil are a carbon-rich material with a high amount of carbon of 43-51 wt% and fixed carbon of 30-39 wt% (Liew et al., 2018), therefore it is suitable for conversion into a value-added product such as biochar, synthetic fuel, biogas and biochemicals, and activated carbon.

EFB is a lignocellulosic biomass mainly composed of three main components which are cellulose (44.2%), hemicellulose (33.5%), and lignin (20.4%) (Rosli et al., 2017). Cellulose consists of glucose monosaccharide units that are linked by ether bonds, while hemicellulose consists of a branched polymer of five carbon saccharides (Abdullah & Sulaiman, 2013). Lignin is derived primarily from three lignin monomers; *p*-coumaryl, coniferyl, and sinapyl alcohol (Hatfield & Fukushima, 2005). Due to the bond heterogeneity, instead of hydrolytic enzymes, ligninolytic enzymes are required for the delignification, and basidiomycetes white rot fungi (WRF) (such as *P. chrysosporium*) have been proven to be most effective.

Under ligninolytic conditions (i.e., limited nitrogen), *P. chrysosporium* secretes laccase during secondary metabolism. Laccase is used for oxidation of lignin phenolic units to phenoxyl radicals. These radicals will lead to non-enzymatic lignin depolymerizing reactions through C_α oxidation, C_α-C_β cleavage, and aryl-alkyl cleavage (Sigoillot et al., 2012; Youn et al., 1995). Efficacy of laccase delignification can be characterized based on the substrate morphology and estimation of lignin content.

This work will assess the EFB degradation by *P. chrysosporium* under the influence of electric current. First, as a function discharge current from the electrochemical reactions of the microbial zinc/air cell fed with the fungus-cultivated

EFB. Second, as a function of external current passed through the enclosure containing the fungus-cultivated EFB.

5.2 EXPERIMENTAL DESIGN

5.2.1 Raw Material and Microorganisms

Empty fruit bunch (EFB) was collected from a palm oil plantation. The raw EFB was manually shredded and sieved into small sizes of around 0.5 cm (Figure 5.1a). It was then soaked for 24 hours, rinsed with distilled water, and dried under UV light.

(a) (b)

Figure 5.1 (a) Raw EFB (b) Soaked shredded in distilled water

The preparation of fungal microbes *Phanerochaete chrysosporium* and its cultivation on EFB were as described earlier in Section 3.2.

5.2.2 Preparation of Microbial Zinc/Air Cell

The cell was still the membrane-less, single chamber cylindrical MFC of 250-ml capacity filled with 24 g/L unbuffered potato dextrose broth (PDB) electrolyte. The zinc anode strip (30 mm x 30 mm) was paired with the commercial E4/E4A EFL air cathode

of the same dimension. The fungus-cultivated EFB was prepared from 5 g of dried *Phanerochaete chrysosporium* (*P. chrysosporium*), 2 g of oil palm-derived empty fruit bunches (EFBs) and incubated for six days.

5.2.3 Influence of Electric Current on EFB Degradation

The influence of electric current on EFB degradation was observed under two conditions:

(a) Self-powered MFC

The electric current was generated from the discharge current of the microbial zinc/air cell. The cell was discharged at constant current of 1 mA, 2 mA and 3 mA continuously for 30 days.

(b) Externally-applied current

The same microbial zinc/air cell was utilized but both electrodes were replaced with nickel mesh. External constant current passed was 1 mA, 2 mA and 3 mA continuously for 30 days.

For both conditions, the current was regulated using Neware Battery Tester (BTS 4000, NEWARE, Shenzhen, China). After 30 days of discharge, the EFB was retrieved, rinsed, and dried for characterization

5.2.4 EFB Degradation Characterisation

The state of EFB degradation was characterized according to its surface morphology, thermogravimetric analysis and acid-chlorite method.

Surface morphological changes were observed using scanning electron microscopy (SEM) (JSM-6700F, JEOL Ltd., Tokyo, Japan). Thermogravimetric analysis (TGA) (TGA4000, Perkin Elmer, Inc., Waltham, MA, USA) was carried out by heating approximately 30 mg of EFB from the temperature of 25℃ until 800℃ at a heating rate of 10℃/min under argon atmosphere at a flow rate of 50 ml/min. Lignin content was estimated from on mass loss curve.

Quantitative lignin content was determined from the acid-chlorite method. In this method (Yadav & Vivekanand, 2019), 0.15 g of EFB was first boiled twice with 75 ml of H_2O for 1 hour to remove the hot-water-soluble materials, dried at 60℃ for 15 hours and weighed (W_1). The samples were then treated with 30 ml of H_2O, 2 ml of 10% acetic acid and 0.6 g of sodium chlorite at 75℃ for 1 hour. Then, treated further with 10% acetic acid (2 ml) and 0.6 g of sodium chlorite at 75℃ for 2 hours. Finally, samples were rinsed with H_2O (five times), acetone (twice), and ether (once), then dried at 105℃ for 90 min and weighed (W_2). The quantity of lignin is then given by:

$$\% \text{ Lignin} = (W_1 - W_2)/0.15 \quad (5.1)$$

5.3 RESULTS AND DISCUSSION

Figure 5.2 depicts the scanning electron micrographs of EFB. EFB strands have a rigid and rough surface with craters and silica bodies attached to the surface (see Figure 5.2a). Silica bodies attached to the surface act as a protector from the penetrations of fungal hyphae into the cellulose and hemicellulose matrix. Once silica bodies were removed from the surface, it will be easier for the fungal hyphae to penetrate through for delignification. It is presumed that the EFB strand comprises of rod-shaped microfibrils that lumped together with cavities in the middle (see Figure 5.2b).

In the previous study, it was reported that upon exposure of EFB to *P. chrysosporium*, the outer protective lignin layer showed signs of degradation starting after twenty days and by the thirtieth day the cell walls were almost completely collapsed (Sukri et al., 2021). The present work now assessed the degradation rate of EFB in a microbial zinc/air cell fed with *P. chrysosporium* cultivated EFB. Vasileva et al. (2021) observed that phenol degradation by *Bradyrhizobium japonicum* was increased under the influence of an applied electric field. Since EFB consists of lignin with highly branched phenolic polymer, it would be interesting to observe the influence of applied electric field on lignin degradation as well. In this work, the electric field or electric current was self-generated from the e.m.f of the microbial zinc/air cell and also externally applied through the cell containing *P. chrysosporium* cultivated EFB. The

state of degradation and lignin content of EFB was evaluated after 30 days of exposure to the electric current.

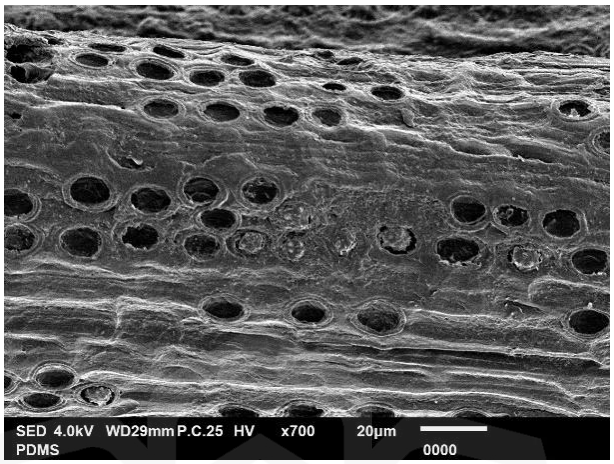

(a)

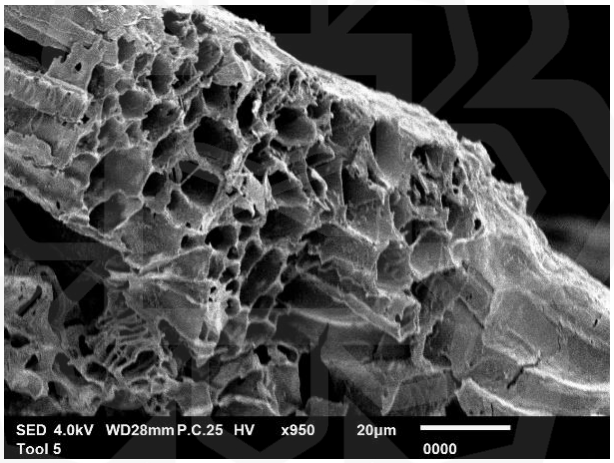

(b)

Figure 5.2 SEM images showing the EFB morphology before treatment (a) Longitudinal view (b) Cross-sectional view

As anticipated, the current generated had an influence on the EFB degradation. At constant discharge current of 1 mA (see Figure 5.3a), the outermost cell wall was almost completely degraded showing a pitted vessel and helical/matrix-like structure which is assumed to be the cellulose (Galiwango et al., 2018). With increasing discharge current of 2 mA, more pitted vessels were visible, exposing more matrix-like structure and allowing *P. chrysosporium* mycelium to penetrate through the innermost cell wall (see Figure 5.3b). Finally, at 3 mA discharge current, most of the outermost

cell wall, and the outermost matrix-like structure had almost completely collapsed showing the inner vessels and matrix-like structure.

To further validate the influence of discharge current on EFB degradation by *P. chrysosporium*, refer to the TGA profile in Figure 5.4. In the TGA profile, the composition of hemicellulose, cellulose, and lignin can be estimated based on the three distinct stages: dehydration (T< 273 ℃), rapid weight loss (273 ℃ < T < 433 ℃), and slow weight loss (T > 433 ℃). The first stage (T< 273 ℃) marks the gradual weight loss due to the release of moisture and light volatile matters from EFB. The second stage (273 ℃ < T < 433 ℃) is marked by the significant drop in weight loss. This corresponds to the removal of cellulose and hemicellulose from EFB. The last stage (T > 433 ℃) is marked by the long and stable weight loss which is corresponded to the lignin decomposition. The lignin content for fresh EFB was estimated around 35.6%.

Upon exposure to *P. chrysosporium* in the microbial zinc/air cell system under constant discharge current, the final lignin content after 30 days shows a strong influence of the discharge current. At 1 mA, the lignin content was around 34.9% (~2% decrease). Then, at 2 mA the lignin content was further decreased to 31.6% (~11% decrease). Finally, at 3 mA the lignin content was the lowest i.e., 25.3% (~29% decrease). Validation of the lignin content using the acid-chlorite shows the same trend, see Figure 5.5. However, determination of the lignin content using the acid-chlorite method gave lower lignin values and higher decrement in the lignin content as compared to the TGA method. Table 5.1 below compares the values obtained from both methods. The quantity of sample used for TGA was 30 mg while for acid-chlorite method the quantity used was 150 mg. Therefore, the data obtained from the acid-chlorite method provide stronger inferences. Besides, visual inspection and SEM observation suggest advanced EFB degradation state after 30 days of cell discharge. The cell could not sustain a higher discharge current than 3 mA.

Table 5.1 Percentage of lignin content as determined from TGA and acid-chlorite method as a function of microbial zinc-air cell discharge current

	Lignin Content (%) Upon 30-day Under Constant Discharge Current						
	Fresh EFB	1 mA	Decrement (%)	2 mA	Decrement (%)	3 mA	Decrement (%)
TGA	35.6	34.9	2	31.6	11	25.3	29
Acid-chlorite	28.4	24.2	15	20.3	29	17.9	37

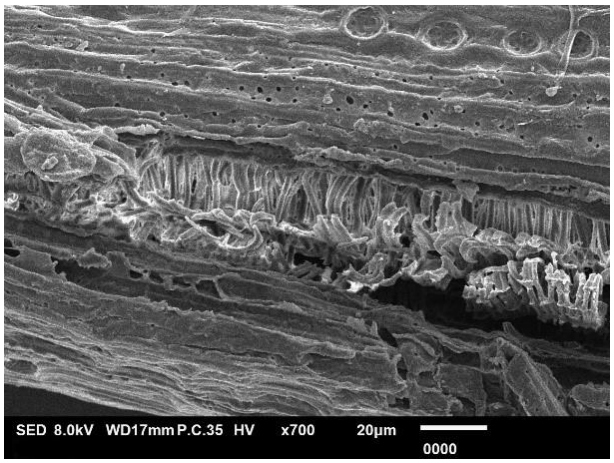

(a)

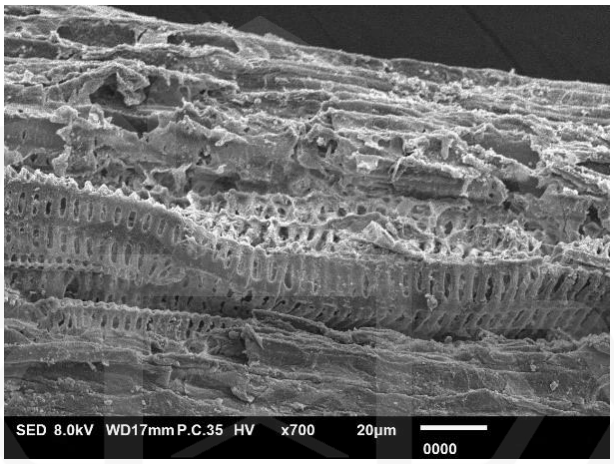

(b)

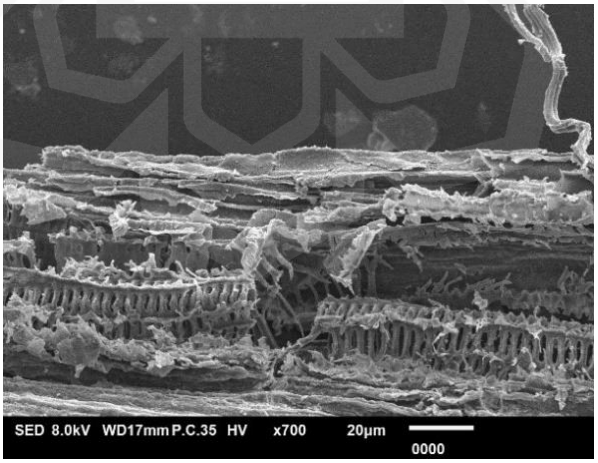

(c)

Figure 5.3 SEM images showing morphology of EFB when treated in self-powered microbial zinc/air cell at constant current discharged of (a) 1 mA (b) 2 mA and (c) 3 mA

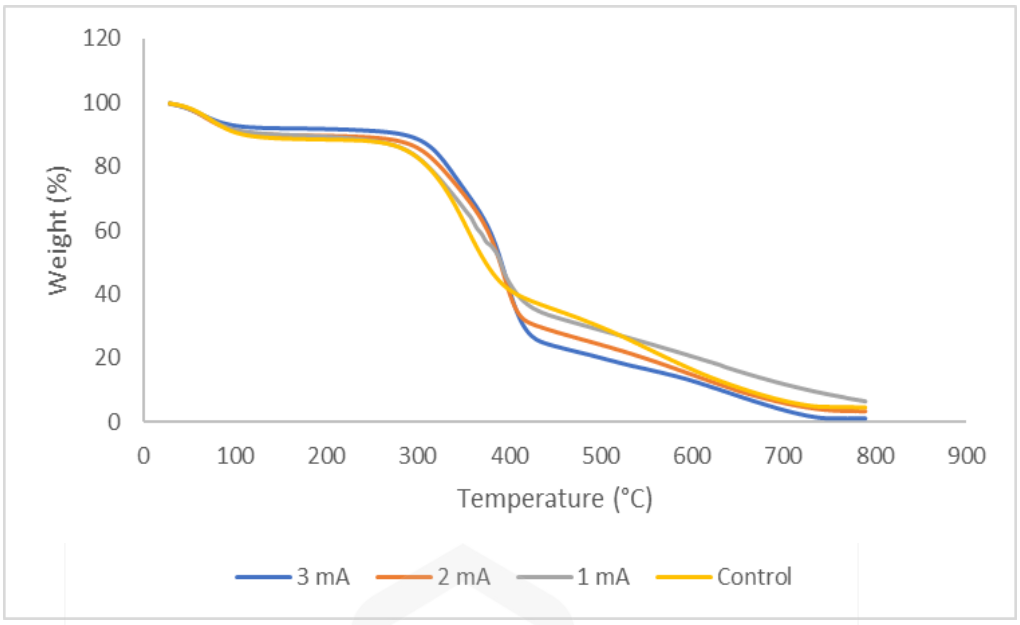

Figure 5.4 Thermogravimetric analysis of EFB when treated in self-powered MFC at constant current discharged of (a) 1 mA (b) 2 mA and (c) 3 mA

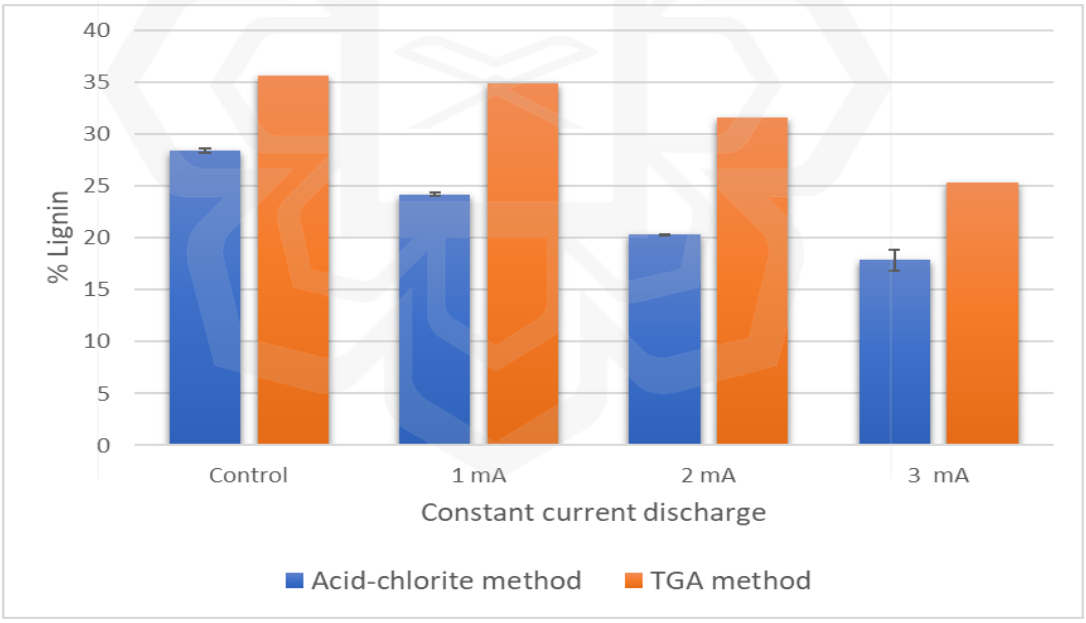

Figure 5.5 Percentage of EFB's lignin when treated in self-powered MFC at constant current discharged of (a) 1 mA (b) 2 mA and (c) 3 mA using acid-chlorite and TGA method

There was a report by Shen et al. (2020) on the effect of current stimulation on lignin degradation by *Trametes versicolor*. By utilizing the Electro-Fenton process, the study revealed an increase in lignin degradation from 25% to 85.4% when the current was increased from 0.05 A to 0.3 A. An Electro-Fenton process is an electrocatalytic reaction based on in situ generation of hydroxyl radicals. The huge amount of hydroxyl radicals produced was thought to promote the lignin degradation by LiP and MnP.

However, in this work, lignin degradation was promoted due to the increase in free electrons as higher current was drawn from the microbial zinc/air cell. As mentioned earlier, lignin degradation by laccase is initiated by oxidation of lignin phenolic units into phenoxyl free radicals and electrons. Free electrons are then transferred to the side chain leading to the bond cleavage. Thus, more free electrons from the oxidation of zinc will lead to more bond cleavage and finally resulted to an increase in lignin degradation. This approach is much cheaper than the Electro-Fenton process.

The presumption that the availability of free electrons promotes lignin degradation by *P. chrysosporium* was tested by applying external current to an enclosure containing the EFB cultivated with *P. chrysosporium*. Both zinc anode and air cathode were replaced by nickel mesh. An electric current was externally supplied to pass through the enclosure. Figure 5.6 shows the surface morphology of EFB upon exposure to *P. chrysosporium* under the influence of an external current. Almost similar observations were obtained when the *P. chrysosporium* cultivated EFB was under the influence of self-generated current. It started with the degradation of the outermost lignin layer showing a matrix-like structure (see Figure 5.6a). Once the external current was increased to 2 mA, the outermost matrix-like structure was exposed. As the applied current was increased up to 3 mA, most of the outermost matrix-like structure collapsed showing an inner matrix-like structure.

The estimated percentage mass loss of lignin from the TGA profiles (see Figure 5.7) also shows a decrease in lignin content with an increase of external current from 1 mA to 3 mA. However, at higher current the percentage of lignin loss did not continue to increase. At 5 mA and 6 mA, the lignin loss was roughly similar to that of 1 mA, refer to Figure 5.8. The highest percentage of lignin loss occurred when the external current

was 3 mA, (see Figure 5.8). Table 5.2 provides the estimated lignin content as determined from TGA and acid-chlorite methods. It is interesting to note that the EFB lignin content under the influence of external current was lower than that under the influence of cell discharge. It is thought that in the zinc/air cell, a quantity of charge participated in the electrochemical redox reactions, while the remaining was utilized in the fungal metabolic activities. On the other hand, when an external charge was applied in the absence of the anode-cathode couple, the entire charge was utilized in the fungal metabolic activities, thus contributing towards a higher lignin degradation

Table 5.2 Percentage of lignin content as determined from TGA and acid-chlorite method as a function of applied external current

		TGA	Acid-chlorite
Lignin Content (%) Upon 30-day Under Constant Discharge Current	Fresh EFB	35.6	28.4
	1 mA	22.9	22.8
	Decrement (%)	37	19
	2 mA	21.1	17.1
	Decrement (%)	42	40
	3 mA	18.8	7.5
	Decrement (%)	48	74
	5 mA	23.3	22.1
	Decrement (%)	36	22
	6 mA	20.2	22.2
	Decrement (%)	45	22

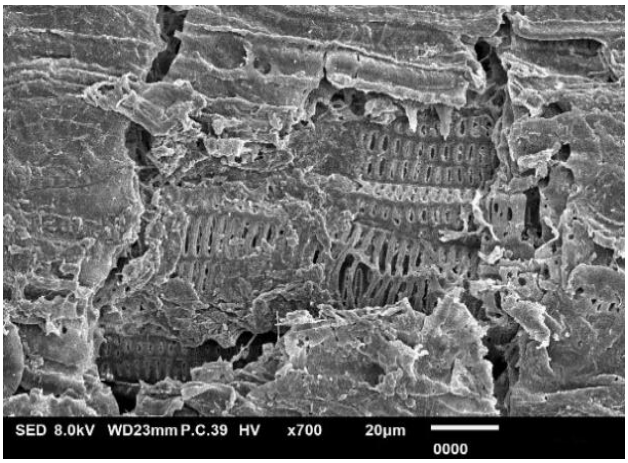

(a)

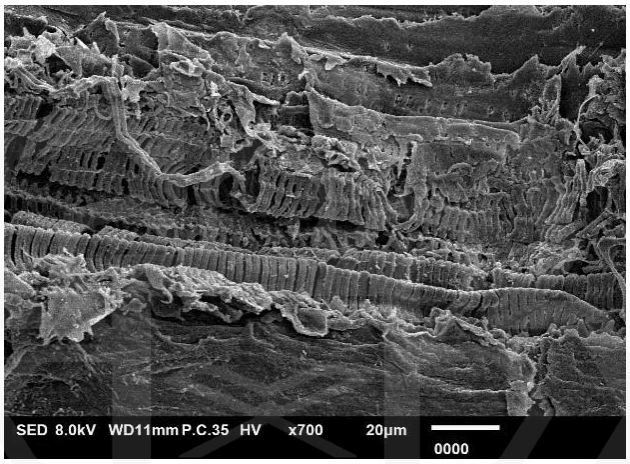

(b)

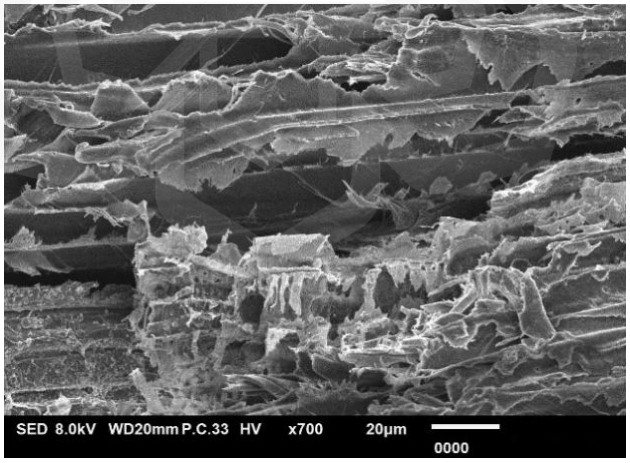

(c)

Figure 5.6 SEM images showing the morphology of EFB when treated in externally-powered MFC at a constant current of (a) 1 mA (b) 2 mA and (c) 3 mA

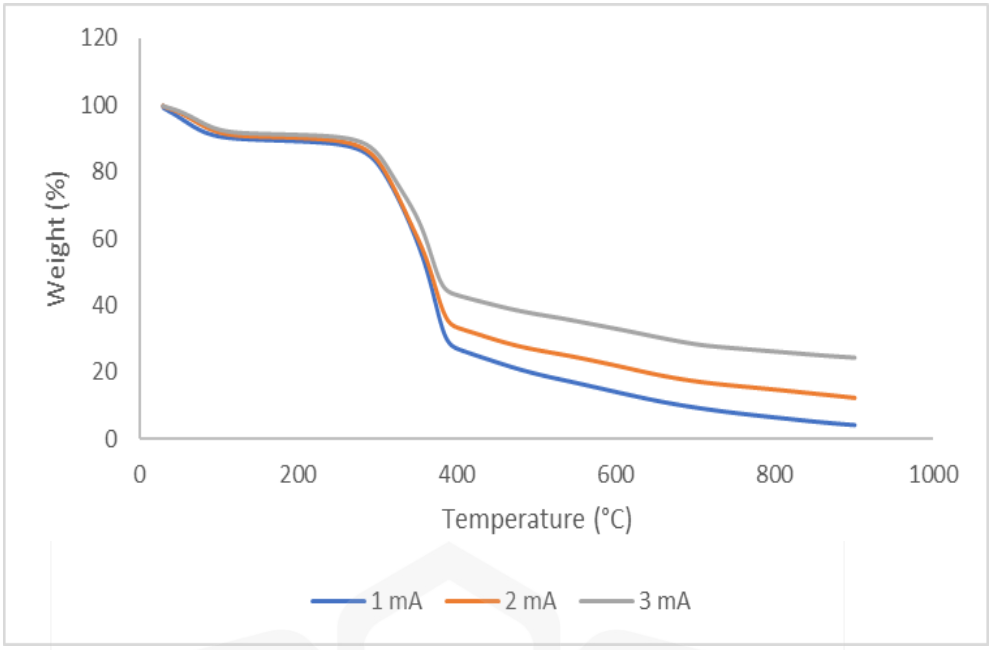

Figure 5.7 Thermogravimetric analysis of EFB when treated in externally-powered MFC at constant currents of 1 mA, 2 mA, and 3 mA

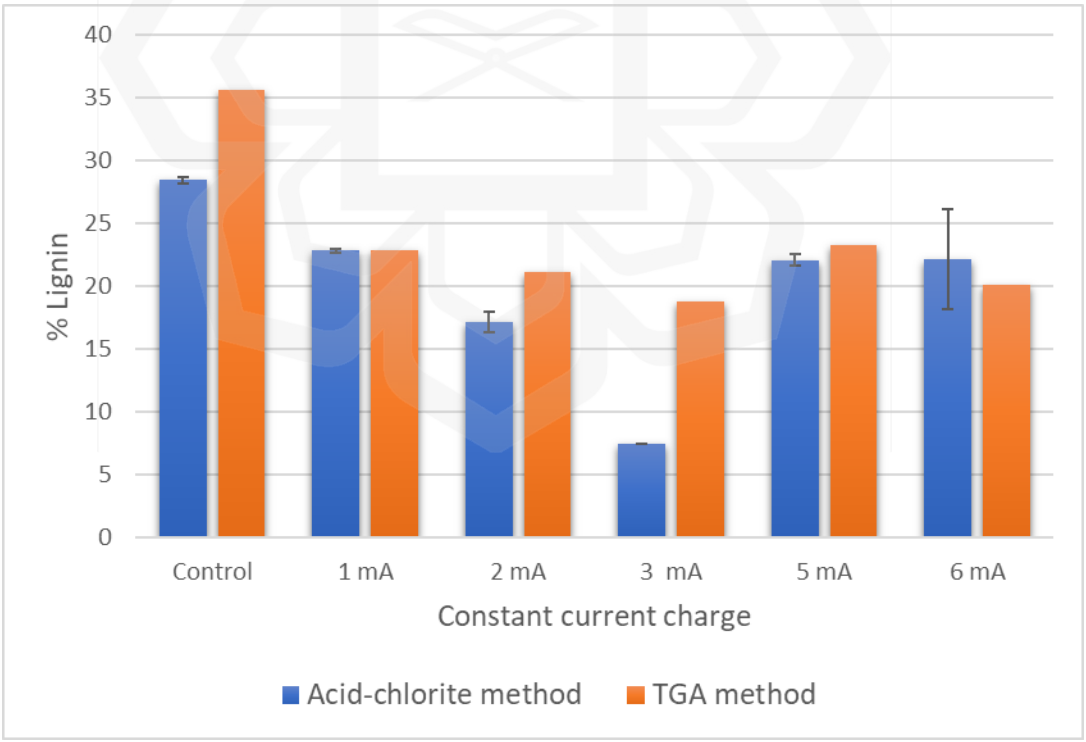

Figure 5.8 Percentage of lignin using acid-chlorite and TGA method when treated in externally-powered MFC at constant current of 1 mA, 2 mA, 3 mA, 5 mA and 6 mA

As the external current was beyond 3 mA, the free electrons supplied were no longer led to an increase in the lignin degradation. The are two possible scenarios. First, the excess charge supplied might have disrupted or inhibited the fungal metabolic activities and hence they were no longer at an optimum rate (Shen et al., 2020). Second, with increasing supply of free electrons, more reactive oxygen species will be generated which in turn will produce more phenoxyl free radicals. However, when too many phenoxyl free radicals are generated, they can react with other organic compounds such as cellulose and hemicellulose. A study by Brenelli et al. (2018) shows that in a laccase-mediated system, electrons from the delignification of lignin can be used as an activation for lytic polysaccharides monooxygenases (LPMOs) and ultimately enhanced the enzymatic hydrolysis of cellulose.

Figure 5.9 depicts the SEM micrographs of EFB under the influence of external current of 5 mA and 6 mA. At a first glance, they seemed to be at an advanced degradation stage which did not support the TGA and acid-chlorite lignin content data. Upon a careful observation, the inner vessels and matrix-like structure which correspond to cellulose and hemicellulose collapsed faster than the protective outermost structure i.e., the lignin layer. Therefore, most likely this was caused by the reaction of excess of phenoxyl free radicals.

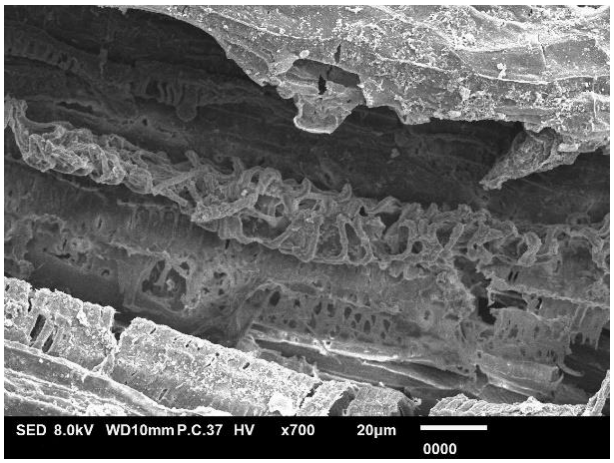

(a)

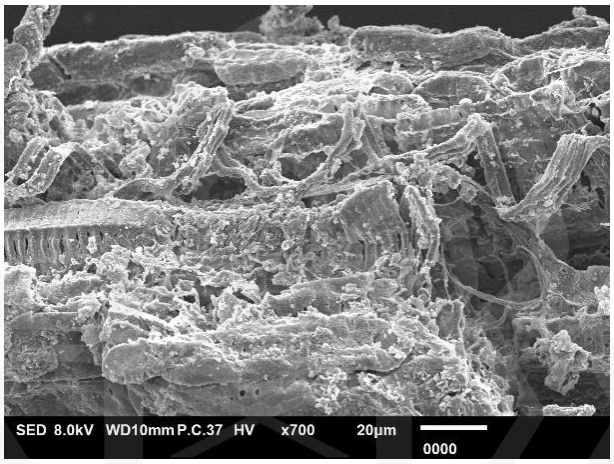

(b)

Figure 5.9 SEM images showing EFB degradation when treated in externally-powered MFC at a constant current of (a) 5 mA and (b) 6 mA

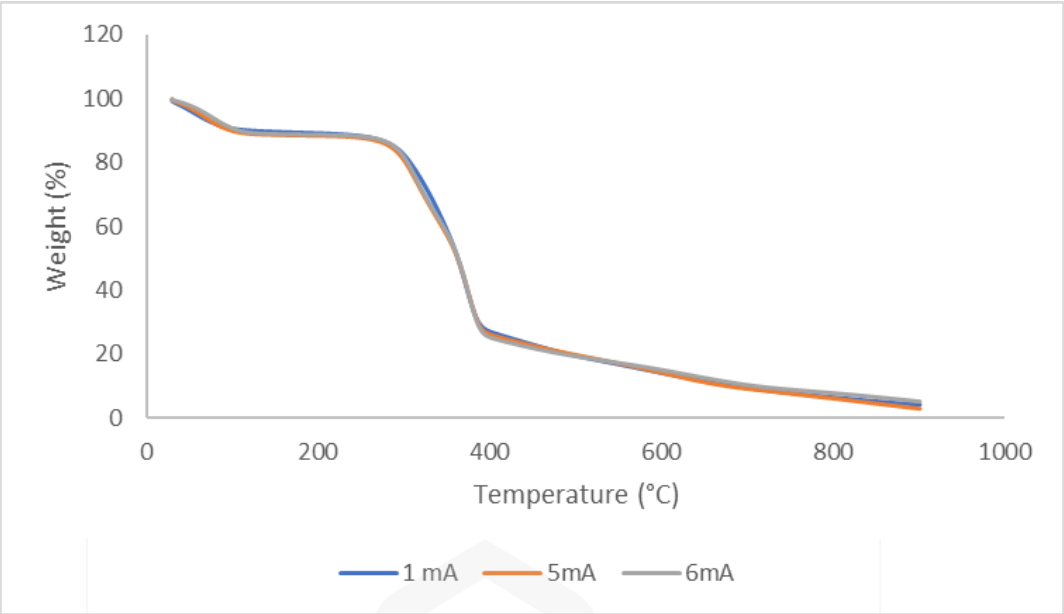

Figure 5.10 Thermogravimetric analysis of EFB when treated in externally-powered MFC at constant currents of 1 mA, 5 mA, and 6 mA

5.4 SUMMARY

This work has substantiated that lignin degradation could be enhanced by nearly 75% by merely supplying free electrons to *P. chrysosporium* cultivated EFB. The electron supply could be generated in situ by inserting redox couple electrodes. This approach is much cheaper than the electrocatalytic reactions of Electro-Fenton method. Therefore, the microbial zinc/air cell has the potential to be utilized as an agrowaste degrading cell.

CHAPTER SIX

DISCUSSION

Microbial fuel cell (MFC) technology is a potential source of alternative energy due to its ability to simultaneously generate electricity while treating waste such as wastewater and municipal solid waste landfill leachate (Damiano et al., 2014; Firdous et al., 2018). Recent developments in the MFC technology have pushed the maximum power density in the watt-range (Flimban et al., 2019; Liu et al., 2020). However, the energy gain yields i.e., the energy output-cost ratio remains far from the sustainability criteria (Li et al., 2014). MFC is comprised of living microbes fed with organic substrate. As such the system must be designed to sustain the living microbes and customized for their optimal metabolic activities so that maximum output could be harvested. As a result, MFC system designs are manifold, complex, and eventually become very costly.

The main pre-requisite to achieve sustainable criteria is that the MFC must be able to operate with a minimum control feature for an extended duration. Therefore, the living microbes employed must be robust and highly adaptive to changing environments. *Phanerochaete chrysosporium* white rot fungus has been extensively researched for bioremediation due to its ability to degrade a wide range of organic substrates. Shukri et al. (2021) first reported the use of *P. chrysosporium* in an air-cathode MFC fed with oil palm empty fruit bunch (EFB). The bioelectrochemical system could sustain a constant discharge current of 1 mA for 44 days continuously, and most importantly devoid of any control features. Even the electrolyte was not buffered. These results will pave the way towards achieving a sustainable MFC.

The next challenge in increasing the MFC energy gain yields is to reduce the MFC components' cost. Even without the control systems, the cell components are expensive. Catalytic electrodes and membrane separator account for more than 85% of the total cost. A single chamber, membraneless air-cathode MFC offer a much-simplified cell design while maintaining a high energy output (Cheng & Logan, 2011; Liu & Logan, 2004; Sukri et al., 2021). Sukri et al. (2021) further simplified the MFC design by introducing freely suspended fungal microbes in a single chamber,

membraneless cell filled with unbuffered electrolyte. *P. chrysosporium*'s network of filamentous hyphae provided the required medium for the bioelectrochemical system to sustain its charge transfer mechanisms between the air cathode and fungal microbes. In most MFCs, the electrolyte is buffered at a desirable pH to obtain optimal energy output (Elakkiya & Matheswaran, 2013; Fan et al., 2007b; Igboamalu et al., 2019). However, buffer solution is non-biodegradable and when released into the environments it causes eutrophication (Fan et al., 2007b; Wang et al., 2018). Therefore, the ability to do away with buffer electrolyte would contribute further towards sustainable and green energy system.

In order to utilize MFCs for practical applications, several units of MFCs must be configured in a stack configuration to obtain higher operating voltage, higher limiting current and longer service life (Jafary et al., 2013; T. Kim et al., 2017; Rusyn et al., 2021). A power management unit (PMU) is often incorporated in a battery stack configuration. However, PMU itself requires an external power supply. The more functions it serves, the higher the power demand. In one test study, a benthic MFC (BMFC) was used to power wireless temperature sensors and seafloor magnetometers (Arias-Thode et al., 2017). The BMFC stack was coupled to a DC-DC converter to boost its voltage and comprised of seven-stranded linear array of BMFC with a total length of 30 m. The BMFC stack could sustain its power for just 38 days. This example demonstrates that while it is technologically possible to enhance the MFC energy output to meet a specific demand, the huge increase in the system cost would eventually offset the energy gain.

This work introduced a novel MFC stack configuration. It is called an open-parallel unit-cell configuration. Parallel stack configuration offers higher limiting current, low internal resistance and longer service duration for the power module. However, it suffers from one major problem – parasitic current (An, Sim, et al., 2015). The fluctuations in the e.m.f. makes this problem even more prevalent in MFCs. Furthermore, with an increase in the number of individual cells, the possibility of parasitic current formation from each cell will increase, thus leading to more energy losses. The current solution is to incorporate control electronics. The use of an open-parallel unit-cell configuration eliminates the issue of parasitic current without the need for control electronics. In an open-parallel configuration, all individual cells were

connected in a parallel connection, but all cells shared a common electrolyte. Once all cells share a common electrolyte, the voltage variation of individual cells shall be equalized, hence mitigating the parasitic current problem. Figure 6.1 depicts the sudden drop in the parasitic current value as the MFC power module was transformed from parallel configuration and open-parallel configuration. Parasitic current occurs both during open circuit state and closed-circuit state. The elimination of parasitic current during MFC stack discharge also contributed towards enhancement of the energy output. In this work, the total energy output of the MFC stack employing the open-parallel unit-cell configuration was enhanced by 2.6 times.

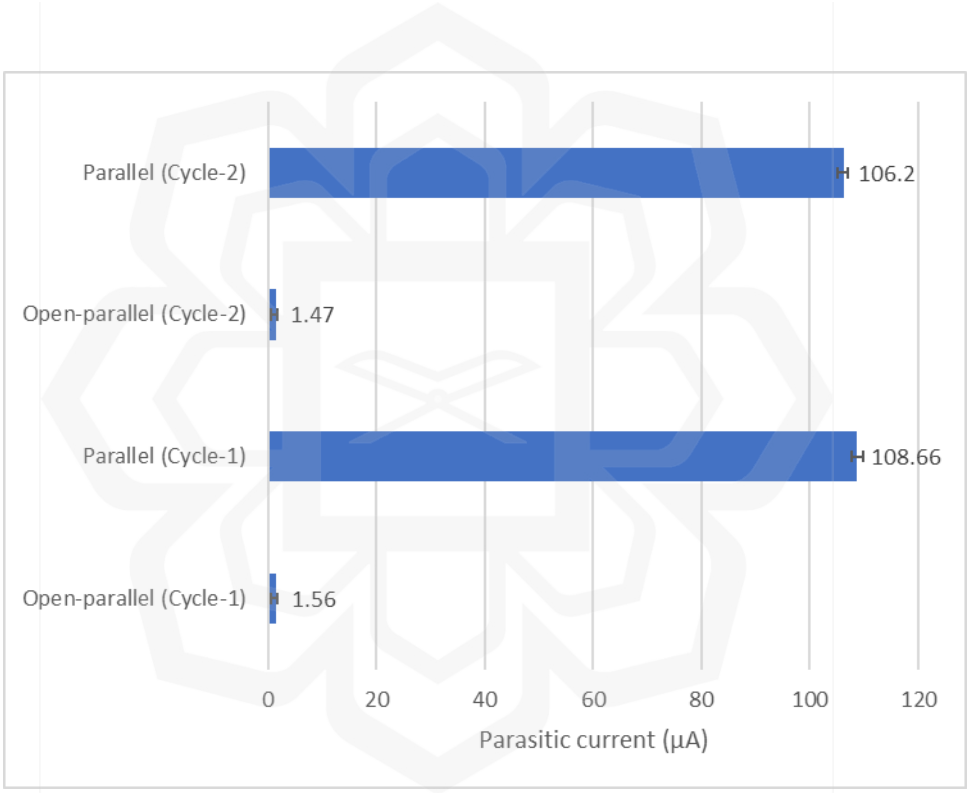

Figure 6.1 Average value of parasitic current in parallel and open-parallel cells for cycle-1 and cycle-2

Enhancing the MFC performance by connecting multiple electrodes (multipolar electrodes), especially the cathode, has been well reported. Increasing the cathode's surface area by multiplying the number of cathodes is more effective in improving power production than increasing the surface area of a single cathode (Bose et al., 2018; Jiang et al., 2010). In fact, increasing the surface area of a single cathode will reduce

the power density since the increment is not proportionate. Li et. al. (2008) reported a single chamber MFC with a bipolar air cathode could achieved up to 72 mW/m^2 with a low internal resistance of 75 Ω (Li et al., 2008). Shimoyama et al. (2008) reported a single unit MFC that comprised of combined multiple cassette electrodes (CE) was able to achieve a maximum power density of up to 899 mW/m^2 (Shimoyama et al., 2008). Therefore, what is the difference between an MFC unit with multipolar electrode and an MFC with open-parallel configuration since multiple unit cell sharing a common electrolyte is considered as one single cell? An open-parallel configuration is meant for MFC stacking configuration. The issue addressed in this work is that if a unit cell is to be replicated then the best configuration is the open-parallel configuration.

In a single chamber air-cathode MFC, the most expensive component is the air cathode. Therefore, this work designed and fabricated a non-catalytic air cathode for use in an air-cathode MFC. The commercial air cathode such as the E4 EFL is expensive due to its unique design features. The following considerations were taken into account for the proposed air cathode:

(i) Able to function under submerged conditions so that it relies on dissolved oxygen. This will eliminate the need for air aeration.

(ii) Does not require special process or treatment such as high temperature calendaring i.e., easy-to-fabricate concept and low cost.

(iii) No catalytic material was incorporated into the air cathode structure, reduced cost.

(iv) Fabricated from carbon-based components and readily available in the market.

All these considerations were taken to ensure minimal fabrication cost. For an effective functioning under submerged, non-aerated conditions, the 'airside' of the air cathode must be made hydrophobic. This approach imitates one of the adaptations of submerged aquatic plants. Under submerged conditions, the leaves have higher resistance to gas exchange which is caused by the diffusion boundary layer (DBL). The hydrophobic nature of the aquatic plant's leaves creates a thin gas film. The presence of the gas film will increase the interface between water and gas, thus facilitating the exchange between O_2 and water (Winkel et al., 2011, 2014).

The proposed air cathode was fabricated from layers of carbon felt and carbon fiber sheet, strengthened by nickel mesh. These components were assembled via mechanical press using custom made cylindrical cell holders. A microbial zinc/air cell employing the proposed air cathode was capable of sustaining a 1 mA discharge current for 42 days. Though the performance could not match to that of the commercial E4 air cathode, it must be pointed out that the commercial air cathode was incorporated with manganese-based catalyst. Besides, upon further investigation it was found that the carbon felt and carbon fibre sheet layers were penetrated and covered with dense mycelia colony of *P. chrysosporium* which were thought to disrupt the effective functioning of the air cathode beyond 42 days. The presence of thick biofilm may impede the transfer of H^+ and OH^- ions and also the diffusion of dissolved oxygen. These will lead to hindered ORR and increased internal resistance (Yang et al., 2009). As such, the waterside of the proposed air cathode must be made compact as the commercial air cathode to prevent such occurrences. In summary, the proposed air cathode has been demonstrated to be viable and effective to be used under submerged condition for both non-air circulated or air circulated electrolyte. Therefore, this work supported the conjecture that the hydrophobicity of the gas diffusion layer (GDL) must be taken into air cathode design considerations, especially under submerged applications.

In addition to stacking, other factors such as the size of electrode (in particular air cathode) and separation of electrode also influence MFC performance. Enlarging the cathode area by two or three times can lead to a 23.3% or 59.8% increase in maximum power output (Papillon et al., 2021). Numerous improvement ratios were reported (Cheng & Logan, 2011, Oh & Logan, 2006). However, the resulting energy gain yields is often neglected. In most cases, the increment in cost offsets the energy gains benefits. It is therefore crucial to minimize the cost of the air cathode for air-cathode MFCs. On the other hand, the size of reactors does not play a significant role in the performance of MFCs as exemplified in the work by Goto & Yoshida (2019). They studied the influence of reactor size (i.e., 1.5 L, 12 L, and 100 L) on MFC performance and concluded that the electrode separation was the determining factor that influence MFC's performance. Smaller electrode spacing led to better performance. The cylindrical air cathode configuration proposed in this work enabled the implementation of multipolar air cathode configuration with ease while minimizing the electrode distance.

Applications of MFC as an alternative energy source have been limited, thus far, to low-powered devices such as wireless sensors (Shantaram et al., 2005) and implantable medical devices (IMDs) (Dong et al., 2013). The contemporary interest is to utilise MFC in degrading waste and generating energy as its by-product. Agricultural wastewater such as palm oil mill effluent (POME), mustard tuber wastewater, brewery wastewater, and winery wastewater have been widely studied as a substrate for MFC systems (Guo et al., 2013; Jong et al., 2011; Kaewkannetra et al., 2011; Penteado et al., 2016). Aside from wastewater, agricultural residues such as wheat straw, corn stover, rice straw, and empty fruit bunches (EFB) waste also have been tested (Hassan et al., 2014; Mahmood et al., 2015; Zhang et al., 2013; Zhang et al., 2009).

Many types of bacteria or microbial consortia have been studied in an MFC system. However, when dealing with substrates that have high lignocellulosic content, white rot fungi (WRF) are the best candidate. WRF is capable of secreting various extracellular ligninolytic oxidative enzymes, including laccase, lignin peroxidase (LiP), and manganese peroxidase (MnP). This ligninolytic oxidative enzyme is well-known for its effectiveness in breaking down a variety of organic matter containing phenolic compounds and aromatic amines. Out of the three ligninolytic enzymes, laccase can utilize molecular oxygen to catalyse oxidation reactions of phenolic compounds. Therefore, laccase has been widely used as an oxygen reduction catalyst at the cathode of biofuel cells due to its ability to transfer electrons from the cathode to molecular oxygen.

In this work, lignin-rich EFB was used as a substrate for microbial zinc/air cell employing *P.chrysosporium*. *P. chrysosporium* is a type of WRF that is capable of effectively oxidizing lignin since it secretes all three ligninolytic enzymes (i.e., laccase, MnP, and LiP). As the microbial zinc/air cell generates electricity, it simultaneously degrades EFB. Therefore, this work proceeded to evaluate the efficacy of microbial zinc/air cell in degrading EFB. Besides, several reports have suggested that electrical stimulation influences phenolic compound degradation (Ailijiang et al., 2021, Shen et al., 2020, Vasileva et al., 2021). As such, the influence of electrical stimulation on EFB degradation was studied under self-generated and externally supplied conditions.

Figure 6.2 depicts the β-1 lignin model compound degradation by laccase. It begins with the oxidation of lignin's phenolic units, forming phenoxyl free radicals and electrons. The free electrons then initiate C_α-C_β cleavage, forming radicals and quinone methide. The radicals react with molecular oxygen, forming 1-(3,5-dimethoxy-4-ethoxyphenyl)-2-hydroxyethanone. Regardless of the lignin model compound, free electrons always serve essential roles. Therefore, the presence of free electron from external source would certainly influence lignin degradation as substantiated from this work. An increase in the current drawn from the microbial zinc/air cell enhanced the lignin degradation. As more electrons were generated from the oxidation of the zinc anode, more bond cleavage occurred, thus speeding up the lignin degradation. This was further verified from the externally supplied current. It was further observed that the lignin degradation was higher under externally supplied current. When the current was self-generated, some amount was utilized for the electrochemical reactions while all electrons from the externally supplied current were utilized for microbes' metabolic activities i.e., lignin degradation.

It is interesting to note that electric stimulus had a positive influence on lignin degradation only up to 3 mA. At 5 mA and 6 mA, the lignin degradation rates were decreased. Therefore, the free electrons supplied no longer contributed towards lignin degradation. There are two probable contributing factors. First, the electrical stimulus at 5 mA and 6 mA inhibited or disrupted microorganism activities, thus reducing delignification (Shen et al., 2020). Second, the excess free radicals caused a shift in the microbes' metabolic pathways (Brenelli et al., 2018). Therefore, these results suggest that by-products from waste degradation using an MFC could be customized by carefully selecting the appropriate electrical stimulus. For example, in one study the influence of electrical stimuli on the biodegradation of refractory phenolics (4-nitrophenol and 2,4-dinitrophenol) was examined in the forms of intermittent and continuous mode (Ailijiang et al., 2021). Both modes of electrical stimulus increased the removal of phenolic compounds, but interestingly, the intermittent mode of electrical stimulus resulted in higher degradation of phenolic compounds than the continuous mode. They attributed it to the increase in functional microbes under electrical stimulation, particularly in intermittent mode (Ailijiang et al., 2021).

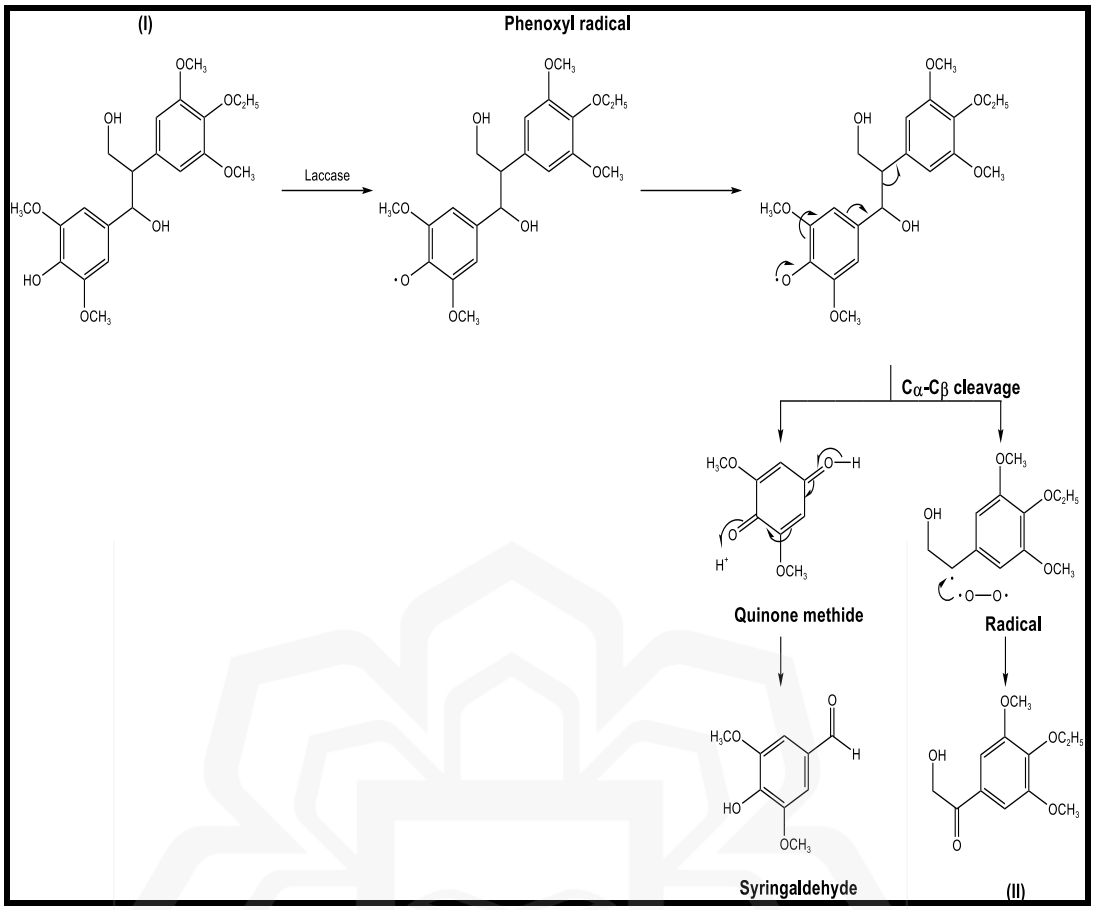

Figure 6.2: Mechanism of Cα-Cβ cleavage of β-1 lignin model initiated by free radical (I) 1-(3,5-dimethoxy-4-hydroxyphenyl)-2-(3,5-dimethoxy-4-ethoxyphenyl) propane-1,3-diol (II) 1-(3,5-dimethoxy-4-ethoxyphenyl)-2-hydroxyethanone (Kawai et al., 1988)

CHAPTER SEVEN

CONCLUSION AND RECOMMENDATION

7.1 CONCLUSION

This study aims to develop a sustainable, cost effective MFC that is capable to fulfil the output requirements for low-power applications. A microbial zinc/air cell employing fungal *Phanerochaete chrysosporium* fed with empty fruit bunch (EFB) has demonstrated promising results. An MFC inherently possesses low operating voltage and as such a single MFC is impractical. Therefore, several MFC units need to be stacked as a power module to increase the power output. MFC stacking suffers from several issues such as parasitic current, voltage reversal, and current reversal. Typically, the use of control electronics could address those issues. However, this will lead to an increase in cost, which eventually will reduce the energy gain yield. This work introduced a novel MFC stack configuration - an open-parallel unit-cell configuration. In this configuration, all unit cells are connected in parallel and share a common electrolyte. Using the open-parallel unit-cell configuration, the MFC stack gains the benefits of parallel configuration i.e., enhanced discharge capacity (3.4 times longer) and power output (2.6 times higher), while effectively eliminated the parasitic current. As no control electronics were involved, this passive approach would definitely enhance the energy gain yields of an MFC stack.

In an air-cathode MFC such as the present microbial zinc/air cell, air cathode is the most expensive component and in most cases is accompanied with an air purging system. Therefore, this work designed and fabricated a submerged, non-catalytic air cathode for use in an air-cathode MFC. The proposed air cathode comprised of commercially available carbon felt, carbon fibre sheet, and nickel mesh without any pre-treatment. Carbon felt with its hydrophobic nature served as a gas diffusion layer (GDL), carbon fibre sheet served as a conductive base, and nickel mesh served as a current collector. All components were assembled merely by mechanical press of the cell holders. The fabricated air cathode was capable to deliver a comparatively high constant current of 1 mA for 42 days under submerged condition. This proved that the

proposed air cathode is viable and effective to be employed under submerged conditions without the need for an air aeration. Besides, the cylindrical air cathode design enabled the assembly of multipolar electrodes with ease while minimizing the electrode separation.

Since the microbial zinc/air cell was fed with lignin rich EFB, this work evaluated the viability of the cell as a lignin-rich agrowaste decomposing cell. The degradation of lignocellulosic EFB was evaluated under the influence of MFC discharge current (i.e., self-powered MFC) and also under the influence of externally supplied current. The electric current, both self-generated and externally supplied, enhanced the lignin degradation. The lignin degradation was higher when the current was externally supplied. However, when the current was too high i.e., 5 mA in this work, the excess free electrons may inhibit or induce a change in the fungal metabolic activities and hence disrupted the lignin degradation rates.

In summary, this work has successfully increased the energy gain yields of an air-cathode MFC employing fungal microbes by introducing a novel stack configuration (i.e., open-parallel unit cell configuration), and proposing a cheaper submersible air cathode which could function effectively without any aeration. Finally, this work has demonstrated that the MFC could be utilized as an agrowaste degrading cell.

7.2 RECOMMENDATION

There are several improvements that can be made to improve the zinc/air MFC energy yield and lignin degradation such as:

i) The performance of the proposed air cathode can be further enhanced by pre-treating the carbon felt and carbon fiber sheet.

ii) The zinc anode can be replaced with metal wastes and thus the MFC totally operates based on wastes.

iii) Increase *Phanerochaete chrysosporium* concentration to enhance the optimum current and lignin degradation.

REFERENCES

Abdel-Hamid, A. M., Solbiati, J. O., & Cann, I. K. O. (2013). Insights into Lignin Degradation and its Potential Industrial Applications. *Advances in Applied Microbiology*, *82*, 1–28.

Abdullah, N., & Sulaiman, F. (2013). The properties of the washed empty fruit bunches of oil palm. *Journal of Physical Science*, *24*(2), 117–137.

Ahmed, J., Yuan, Y., Zhou, L., & Kim, S. (2012). Carbon supported cobalt oxide nanoparticles-iron phthalocyanine as alternative cathode catalyst for oxygen reduction in microbial fuel cells. *Journal of Power Sources*, *208*, 170–175.

Ahn, Y., & Logan, B. E. (2010). Effectiveness of domestic wastewater treatment using microbial fuel cells at ambient and mesophilic temperatures. *Bioresource Technology*, *101*(2), 469–475.

Ailijiang, N., Chang, J., Liang, P., Zhang, X., & Huang, X. (2021). Impact of electrical stimulation modes on the degradation of refractory phenolics and the analysis of microbial communities in an anaerobic-aerobic-coupled upflow bioelectrochemical reactor. *Bioresource Technology*, *320*, 124371.

Ali, J., Sohail, A., Wang, L., Haider, M. R., Mulk, S., & Pan, G. (2018). Electro-microbiology as a promising approach towards renewable energy and environmental sustainability. *Energies*, *11*(7), 1–30.

Ali, N., Anam, M., Yousaf, S., Maleeha, S., & Bangash, Z. (2017). Characterization of the electric current generation potential of the pseudomonas aeruginosa using glucose, fructose, and sucrose in double chamber microbial fuel cell. *Iranian Journal of Biotechnology*, *15*(4), 216–223.

Amadane, Y., Mounir, H., El Marjani, A., & Ettouhami, M. K. (2019). The Effect of Gas Diffusion Layer (GDL) Porosity Variation on Oxygen Distribution Along the PEM Fuel Cell. In *Advanced Intelligent Systems for Sustainable Development* (Vol. 7, pp. 286–293). Springer Berlin Heidelberg.

An, J., Kim, B., Chang, I. S., & Lee, H. S. (2015). Shift of voltage reversal in stacked microbial fuel cells. *Journal of Power Sources*, *278*, 534–539.

An, J., Kim, B., Jang, J. K., Lee, H. S., & Chang, I. S. (2014). New architecture for modulization of membraneless and single-chambered microbial fuel cell using a bipolar plate-electrode assembly (BEA). *Biosensors and Bioelectronics*, *59*, 28–34.

An, J., Sim, J., Feng, Y., & Lee, H. S. (2015). Understanding energy loss in parallelly connected microbial fuel cells: Non-Faradaic current. *Bioresource Technology*, *203*, 280–286.

Arias-Thode, Y. M., Hsu, L., Anderson, G., Babauta, J., Fransham, R., Obraztsova, A., Tukeman, G., & Chadwick, D. B. (2017). Demonstration of the SeptiStrand benthic microbial fuel cell powering a magnetometer for ship detection. *Journal of Power Sources*, *356*, 419–429.

Arif, M., Cheung, S. C. P., & Andrews, J. (2020). Influence of Hydrophobicity and Porosity of the Gas Diffusion Layer on Mass Transport Losses in PEM Fuel Cells: A Simulation Study Supported by Experiments. *Energy and Fuels*, *34*(10), 13010–13022.

Atifi, A., Mounir, H., & El Marjani, A. (2014). Effect of internal current, fuel crossover, and membrane thickness on a PEMFC performance. *Proceedings of 2014 International Renewable and Sustainable Energy Conference, IRSEC 2014*, *May*, 907–912.

Baranitharan, E., Khan, M. R., Prasad, D. M. R., & Salihon, J. Bin. (2013). Bioelectricity generation from palm oil mill effluent in microbial fuel cell using polacrylonitrile carbon felt as electrode. *Water, Air, and Soil Pollution*, *224*(5).

Behera, S. D., Kumari, U., Shankar, R., & Mondal, P. (2018). Performance analysis of a double-chambered microbial fuel cell employing a low-cost sulfonated polystyrene proton exchange membrane. *Ionics*, *24*(11), 3573–3590.

Bhowmick, G. D., Neethu, B., Ghangrekar, M. M., & Banerjee, R. (2020). Improved Performance of Microbial Fuel Cell by In Situ Methanogenesis Suppression While Treating Fish Market Wastewater. *Applied Biochemistry and Biotechnology*, *192*(3), 1060–1075.

Blanford, C. F., Carina, F. E., Heath, R. S., & Armstrong, F. A. (2008). Efficient electrocatalytic oxygen reduction by the “blue” copper oxidase, laccase, directly attached to chemically modified carbons. *Faraday Discussions*, *140*, 319–335.

Bose, D., Bose, A., Mitra, S., Jain, H., & Parashar, P. (2018). Analysis of sediment-microbial fuel cell power production in series and parallel configurations. *Nature Environment and Pollution Technology*, *17*(1), 311–314.

Bourbonnais, R., Paice, M. G., Reid, I. D., Lanthier, P., & Yaguchi, M. (1995). Lignin oxidation by laccase isozymes from Trametes versicolor and role of the mediator 2,2’-azinobis(3-ethylbenzthiazoline-6-sulfonate) in kraft lignin depolymerization. *Applied and Environmental Microbiology*, *61*(5), 1876–1880.

Brenelli, L., Squina, F. M., Felby, C., & Cannella, D. (2018). Laccase-derived lignin compounds boost cellulose oxidative enzymes AA9. *Biotechnology for Biofuels*, *11*(1), 1–12.

Brigham, C. (2018). Biopolymers: Biodegradable Alternatives to Traditional Plastics. *Green Chemistry: An Inclusive Approach*, 753–770.

Brunner, G. (2014). Processing of Biomass with Hydrothermal and Supercritical Water. *Supercritical Fluid Science and Technology*, *5*, 395–509.

Bullen, R. A., Arnot, T. C., Lakeman, J. B., & Walsh, F. C. (2006). Biofuel cells and their development. *Biosensors and Bioelectronics*, *21*(11), 2015–2045.

Calvo-Flores, F. G. (2020). Lignin: A Renewable Raw Material. *Encyclopedia of Renewable and Sustainable Materials*, 102–118.

Canadian Council of Ministers of the Environment. (1999). Canadian Water Quality Guidelines for the Protection of Aquatic Life - Dissolved Oxygen (Freshwater). In *Canadian environmental quality guidelines*.

Carrier, M., Loppinet-Serani, A., Denux, D., Lasnier, J. M., Ham-Pichavant, F., Cansell, F., & Aymonier, C. (2011). Thermogravimetric analysis as a new method to determine the lignocellulosic composition of biomass. *Biomass and Bioenergy*, *35*(1), 298–307.

Chatterjee, P., Ghangrekar, M. M., & Leech, D. (2018). A brief review on recent advances in air-cathode microbial fuel cells. *Environmental Engineering and Management Journal*, *17*(7), 1531–1544.

Chen, S., Patil, S. A., & Schröder, U. (2018). A high-performance rotating graphite fiber brush air-cathode for microbial fuel cells. *Applied Energy*, *211*(November 2017), 1089–1094.

Cheng, S., Liu, H., & Logan, B. E. (2006a). Increased performance of single-chamber microbial fuel cells using an improved cathode structure. *Electrochemistry Communications*, *8*(3), 489–494.

Cheng, S., Liu, H., & Logan, B. E. (2006b). Increased power generation in a continuous flow MFC with advective flow through the porous anode and reduced electrode spacing. *Environmental Science and Technology*, *40*(7), 2426–2432.

Cheng, S., & Logan, B. E. (2011). Increasing power generation for scaling up single-chamber air cathode microbial fuel cells. *Bioresource Technology*, *102*(6), 4468–4473.

Cho, N., Leonowicz, A., Rogalski, J., Wesenberg, D., Luterek, J., Hofrichter, M., Matuszewska, A., & Wilkolazka, A. (2001). Fungal laccase: properties and activity on lignin. *Journal of Basic Microbiology*, *41*(3-4), 185–227.

Choi, Y. J., Mohamed, H. O., Park, S. G., Al Mayyahi, R. B., Al-Dhaifallah, M., Rezk, H., Ren, X., Yu, H., & Chae, K. J. (2019). Electrophoretically fabricated nickel/nickel oxides as cost effective nanocatalysts for the oxygen reduction reaction in air-cathode microbial fuel cell. *International Journal of Hydrogen Energy*, *45*(10), 5960–5970.

Christopher, L. P., Yao, B., & Ji, Y. (2014). Lignin biodegradation with laccase-mediator systems. *Frontiers in Energy Research*, *2*(MAR), 1–13.

Clauwaert, P., Aelterman, P., Pham, T. H., De Schamphelaire, L., Carballa, M., Rabaey, K., & Verstraete, W. (2008). Minimizing losses in bio-electrochemical systems: The road to applications. *Applied Microbiology and Biotechnology*, *79*(6), 901–913.

Couto, S. R., Longo, M. A., Cameselle, C., & Sanromán, A. (1998). Influence of some inducers on activity of ligminolytic enzymes from corncob cultures of Phanerochaete chrysosporium in semi-solid-state conditions. *Progress in Biotechnology*, *15*(C), 703–708.

Croese, E., Pereira, M. A., Euverink, G. J. W., Stams, A. J. M., & Geelhoed, J. S. (2011). Analysis of the microbial community of the biocathode of a hydrogen-producing microbial electrolysis cell. *Applied Microbiology and Biotechnology*, *92*(5), 1083–1093.

Damiano, L., Jambeck, J. R., & Ringelberg, D. B. (2014). Municipal solid waste landfill leachate treatment and electricity production using microbial fuel cells. *Applied Biochemistry and Biotechnology*, *173*(2), 472–485.

Daniel, G., Nilsson, T., & Pettersson, B. (1989). Intra- and Extracellular Localization of Lignin Peroxidase during the Degradation of Solid Wood and Wood Fragments by Phanerochaete chrysosporium by Using Transmission Electron Microscopy and Immuno-Gold Labeling . *Applied and Environmental Microbiology*, *55*(4), 871–881.

Das, S., Chakraborty, I., Rajesh, P. P., & Ghangrekar, M. M. (2020). Performance Evaluation of Microbial Fuel Cell Operated with Pd or MnO 2 as Cathode Catalyst and Chaetoceros Pretreated Anodic Inoculum. *Journal of Hazardous, Toxic, and Radioactive Waste*, *24*(3), 1–7.

Dashtban, M., Schraft, H., Syed, T. A., & Qin, W. (2010). Fungal biodegradation and enzymatic modification of lignin. *International Journal of Biochemistry and Molecular Biology*, *1*(1), 36–50.

Dong, K., Jia, B., Yu, C., Dong, W., Du, F., & Liu, H. (2013). Microbial fuel cell as power supply for implantable medical devices: A novel configuration design for simulating colonic environment. *Biosensors and Bioelectronics*, *41*(1), 916–919.

Eggert, C., Temp, U., & Eriksson, K. E. L. (1997). Laccase is essential for lignin degradation by the white-rot fungus Pycnoporus cinnabarinus. *FEBS Letters*, *407*(1), 89–92.

Elakkiya, E., & Matheswaran, M. (2013). Comparison of anodic metabolisms in bioelectricity production during treatment of dairy wastewater in Microbial Fuel Cell. *Bioresource Technology*, *136*, 407–412.

Eriksson, K.-E. L., Robert A. Blanchette, & Ander, P. (1990). Microbial and enzymatic degradation of wood and wood components. In T. E. Timell (Ed.), *Springer Series in Wood Science*. Springer Berlin Heidelberg.

Fan, Y., Hu, H., & Liu, H. (2007a). Enhanced Coulombic efficiency and power density of air-cathode microbial fuel cells with an improved cell configuration. *Journal of Power Sources*, *171*(2), 348–354.

Fan, Y., Hu, H., & Liu, H. (2007b). Sustainable Power Generation in Microbial Fuel Cells Using Bicarbonate Buffer and Proton Transfer Mechanisms. *Environmental Science and Technology*, *41*(23), 8154–8158.

Feng, Y., Wang, X., Logan, B. E., & Lee, H. (2008). Brewery wastewater treatment using air-cathode microbial fuel cells. *Applied Microbiology and Biotechnology*, *78*(5), 873–880.

Firdous, S., Jin, W., Shahid, N., Bhatti, Z. A., Iqbal, A., Abbasi, U., Mahmood, Q., & Ali, A. (2018). The performance of microbial fuel cells treating vegetable oil industrial wastewater. *Environmental Technology and Innovation*, *10*, 143–151.

Fischer, F., Sugnaux, M., Savy, C., & Hugenin, G. (2018). Microbial fuel cell stack power to lithium battery stack: Pilot concept for scale up. *Applied Energy*, *230*(September), 1633–1644.

Flimban, S. G. A., Hassan, S. H. A., Rahman, M. M., & Oh, S. E. (2020). The effect of Nafion membrane fouling on the power generation of a microbial fuel cell. *International Journal of Hydrogen Energy*, *45*(25), 13643–13651.

Flimban, S. G. A., Ismail, I. M. I., Kim, T., & Oh, S. E. (2019). Overview of recent advancements in the microbial fuel cell from fundamentals to applications: Design, major elements, and scalability. *Energies*, *12*(17).

Fu, J., Liang, R., Liu, G., Yu, A., Bai, Z., Yang, L., & Chen, Z. (2019). Recent Progress in Electrically Rechargeable Zinc–Air Batteries. *Advanced Materials*, *31*(31), 1–13.

Gajda, I., Greenman, J., Melhuish, C., Santoro, C., Li, B., Cristiani, P., & Ieropoulos, I. (2014). Water formation at the cathode and sodium recovery using Microbial Fuel Cells (MFCs). *Sustainable Energy Technologies and Assessments*, *7*, 187–194.

Gajda, I., Stinchcombe, A., Merino-Jimenez, I., Pasternak, G., Sanchez-Herranz, D., Greenman, J., & Ieropoulos, I. A. (2018). Miniaturized ceramic-based microbial fuel cell for efficient power generation from urine and stack development. *Frontiers in Energy Research*, *6*(OCT), 1–9.

Galiwango, E., Rahman, N. S. A., Al-Marzouqi, A. H., Abu-Omar, M. M., & Khaleel, A. A. (2018). Klason Method: An Effective Method for Isolation of Lignin Fractions from Date Palm Biomass Waste. *Chemical and Process Engineering Research*, *57*(0), 46–58.

Gellett, W., Schumacher, J., Kesmez, M., Le, D., & Minteer, S. D. (2010). High Current Density Air-Breathing Laccase Biocathode. *Journal of The Electrochemical Society*, *157*(4), B557.

Ghadge, A. N., & Ghangrekar, M. M. (2015). Performance of low cost scalable air-cathode microbial fuel cell made from clayware separator using multiple electrodes. *Bioresource Technology*, *182*, 373–377.

Ghangrekar, M. M., & Shinde, V. B. (2007). Performance of membrane-less microbial fuel cell treating wastewater and effect of electrode distance and area on electricity production. *Bioresource Technology*, *98*(15), 2879–2885.

Ghasemi, M., Wan Daud, W. R., Ismail, M., Rahimnejad, M., Ismail, A. F., Leong, J. X., Miskan, M., & Ben Liew, K. (2013). Effect of pre-treatment and biofouling of proton exchange membrane on microbial fuel cell performance. *International Journal of Hydrogen Energy*, *38*(13), 5480–5484.

González-Ramírez, D., Muro-Urista, C., Arana-Cuenca, A., Téllez-Jurado, A., & González-Becerra, A. (2014). Enzyme production by immobilized Phanerochaete chrysosporium using airlift reactor. *Biologia*, *69*(11), 1464–1471.

Gorby, Y. A., Yanina, S., McLean, J. S., Rosso, K. M., Moyles, D., Dohnalkova, A., Beveridge, T. J., Chang, I. S., Kim, B. H., Kim, K. S., Culley, D. E., Reed, S. B., Romine, M. F., Saffarini, D. A., Hill, E. A., Shi, L., Elias, D. A., Kennedy, D. W., Pinchuk, G., … Fredrickson, J. K. (2006). Electrically conductive bacterial nanowires produced by Shewanella oneidensis strain MR-1 and other microorganisms. *Proceedings of the National Academy of Sciences of the United States of America*, *103*(30), 11358–11363.

Goto, Y., & Yoshida, N. (2019). Scaling up microbial fuel cells for treating swine wastewater. *Water (Switzerland)*, *11*(9).

Guo, F., Fu, G., Zhang, Z., & Zhang, C. (2013). Mustard tuber wastewater treatment and simultaneous electricity generation using microbial fuel cells. *Bioresource Technology*, *136*, 425–430.

Gupta, G., Rajendran, V., & Atanassov, P. (2004). Bioelectrocatalysis of oxygen reduction reaction by laccase on gold electrodes. *Electroanalysis*, *16*(13–14), 1182–1185.

Gurung, A., & Oh, S. E. (2012). The performance of serially and parallelly connected microbial fuel cells. *Energy Sources, Part A: Recovery, Utilization and Environmental Effects*, *34*(17), 1591–1598.

Ha, P. T., Lee, T. K., Rittmann, B. E., Park, J., & Chang, I. S. (2012). Treatment of alcohol distillery wastewater using a bacteroidetes-dominant thermophilic microbial fuel cell. *Environmental Science and Technology*, *46*(5), 3022–3030.

Ha, T. A., Pozo-Gonzalo, C., Nairn, K., MacFarlane, D. R., Forsyth, M., & Howlett, P. C. (2020). An investigation of commercial carbon air cathode structure in ionic liquid based sodium oxygen batteries. *Scientific Reports*, *10*(1), 1–10.

Hasan, K., Patil, S. A., Leech, D., Hägerhäll, C., & Gorton, L. (2012). Electrochemical communication between microbial cells and electrodes via osmium redox systems. *Biochemical Society Transactions*, *40*(6), 1330–1335.

Hassan, S. H. A., Gad El-Rab, S. M. F., Rahimnejad, M., Ghasemi, M., Joo, J. H., Sik-Ok, Y., Kim, I. S., & Oh, S. E. (2014). Electricity generation from rice straw using a microbial fuel cell. *International Journal of Hydrogen Energy*, *39*(17), 9490–9496.

Hatfield, R., & Fukushima, R. S. (2005). Can lignin be accurately measured? *Crop Science*, *45*(3), 832–839.

Hernández-Flores, G., Andrio, A., Compañ, V., Solorza-Feria, O., & Poggi-Varaldo, H. M. (2019). Synthesis and characterization of organic agar-based membranes for microbial fuel cells. *Journal of Power Sources*, *435*(April).

Higuchi, T. (2004). Microbial degradation of lignin: Role of lignin peroxidase, manganese peroxidase, and laccase. *Proceedings of the Japan Academy Series B: Physical and Biological Sciences*, *80*(5), 204–214.

Holmes, D. E., Dang, Y., Walker, D. J. F., & Lovley, D. R. (2016). The electrically conductive pili of Geobacter species are a recently evolved feature for extracellular electron transfer. *Microbial Genomics*, *2*(8), e000072.

Huang, J., Yang, P., Guo, Y., & Zhang, K. (2011). Electricity generation during wastewater treatment: An approach using an AFB-MFC for alcohol distillery wastewater. *Desalination*, *276*(1–3), 373–378.

Huang, L., & Logan, B. E. (2008). Electricity generation and treatment of paper recycling wastewater using a microbial fuel cell. *Applied Microbiology and Biotechnology*, *80*(2), 349–355.

Igboamalu, T. E., Bezuidenhout, N., Thomas Matsena, M., & Nkhalambayausi Chirwa, E. M. (2019). Microbial fuel cell power output and growth: Effect of pH on anaerobic microbe consortium. *Chemical Engineering Transactions*, *76*(2018), 1381–1386.

Jafary, T., Rahimnejad, M., Ghoreyshi, A. A., Najafpour, G., Hghparast, F., & Daud, W. R. W. (2013). Assessment of bioelectricity production in microbial fuel cells through series and parallel connections. *Energy Conversion and Management*, *75*, 256–262.

Janicek, A., Gao, N., Fan, Y., & Liu, H. (2015). High Performance Activated Carbon/Carbon Cloth Cathodes for Microbial Fuel Cells. *Fuel Cells*, *15*(6), 855–861.

Janusz, G., Pawlik, A., Sulej, J., Świderska-Burek, U., Jarosz-Wilkolazka, A., & Paszczyński, A. (2017). Lignin degradation: Microorganisms, enzymes involved, genomes analysis and evolution. *FEMS Microbiology Reviews*, *41*(6), 941–962.

Jiang, D., & Li, B. (2009). Granular activated carbon single-chamber microbial fuel cells (GAC-SCMFCs): A design suitable for large-scale wastewater treatment processes. *Biochemical Engineering Journal*, *47*(1–3), 31–37.

Jiang, D., Li, X., Raymond, D., Mooradain, J., & Li, B. (2010). Power recovery with multi-anode/cathode microbial fuel cells suitable for future large-scale applications. *International Journal of Hydrogen Energy*, *35*(16), 8683–8689.

Jong, B. C., Liew, P. W. Y., Juri, M. L., Kim, B. H., Mohd. Dzomir, A. Z., Leo, K. W., & Awang, M. R. (2011). Performance and microbial diversity of palm oil mill effluent microbial fuel cell. *Letters in Applied Microbiology*, *53*(6), 660–667.

Kaewkannetra, P., Chiwes, W., & Chiu, T. Y. (2011). Treatment of Brewery Wastewater and Production of Electricity through Microbial Fuel Cell Technology. *Fuel*, *90*(8), 2746–2750.

Kawai, S., Umezawa, T., & Higuchi, T. (1988). Degradation mechanisms of phenolic β-1 lignin substructure model compounds by laccase of Coriolus versicolor. *Archieves of Biochemistry and Biophysics*, *262*(1), 99–110.

Khaled, F., Ondel, O., & Allard, B. (2016). Microbial fuel cells as power supply of a low-power temperature sensor. *Journal of Power Sources*, *306*, 354–360.

Khilari, S., Pandit, S., Das, D., & Pradhan, D. (2014). Manganese cobaltite/polypyrrole nanocomposite-based air-cathode for sustainable power generation in the single-chambered microbial fuel cells. *Biosensors and Bioelectronics*, *54*, 534–540.

Khilari, S., & Pradhan, D. (2018). Role of cathode catalyst in microbial fuel cell. *Microbial Fuel Cell: A Bioelectrochemical System That Converts Waste to Watts*, 141–163.

Kim, K. Y., Yang, E., Lee, M. Y., Chae, K. J., Kim, C. M., & Kim, I. S. (2014). Polydopamine coating effects on ultrafiltration membrane to enhance power density and mitigate biofouling of ultrafiltration microbial fuel cells (UF-MFCs). *Water Research*, *54*, 62–68.

Kim, M., Sik Hyun, M., Gadd, G. M., & Joo Kim, H. (2007). A novel biomonitoring system using microbial fuel cells. *Journal of Environmental Monitoring*, *9*(12), 1323–1328.

Kim, T., Kang, S., Kim, H. W., Paek, Y., Sung, J. H., Kim, Y. H., & Jang, J. K. (2017). Assessment of organic removal in series- and parallel-connected microbial fuel cell stacks. *Biotechnology and Bioprocess Engineering*, *22*(6), 739–747.

Kiran, S., Huma, T., Jalal, F., Farooq, T., Hameed, A., Gulzar, T., Bashir, A., Rahmat, M., Rahmat, R., & Rafique, M. A. (2019). Lignin degrading system of Phanerochaete chrysosporium and its exploitation for degradation of synthetic dyes wastewater. *Polish Journal of Environmental Studies*, *28*(3), 1749–1757.

Kirk, T. K., & Farrell, R. L. (1987). Enzymatic "Combustion": The Mmicrobial Degradation of Lignin. In *Ann. Rev. Microbiol* (Vol. 41).

Koffi, N. J., & Okabe, S. (2020). High voltage generation from wastewater by microbial fuel cells equipped with a newly designed low voltage booster multiplier (LVBM). *Scientific Reports*, *10*(1), 1–9.

Lawson, K., Rossi, R., Regan, J. M., & Logan, B. E. (2020). Impact of cathodic electron acceptor on microbial fuel cell internal resistance. *Bioresource Technology*, *316*, 123919.

Lee, H., Jang, Y., Choi, Y. S., Kim, M. J., Lee, J., Lee, H., Hong, J. H., Lee, Y. M., Kim, G. H., & Kim, J. J. (2014). Biotechnological procedures to select white rot fungi for the degradation of PAHs. *Journal of Microbiological Methods*, *97*(1), 56–62.

Lefebvre, O., Shen, Y., Tan, Z., Uzabiaga, A., Chang, I. S., & Ng, H. Y. (2011). A comparison of membranes and enrichment strategies for microbial fuel cells. *Bioresource Technology*, *102*(10), 6291–6294.

Li, C., Zhang, L., Xu, M., Ding, L., Xu, K., Geng, J., & Ren, H. (2013). Influence of coulombic efficiency in air-cathode microbial fuel cell by temperature and baffle-microfiltration membrane barrier. *Asian Journal of Chemistry*, *25*(8), 4165–4170.

Li, D., Shi, Y., Wang, Z., Gao, F., Yang, L., Sun, Y., & Xiao, L. (2023). Characterising operational performance and oxygen crossover of the low-cost cylindrical cathode in microbial fuel cells. *Journal of Environmental Chemical Engineering*, *11*(2), 109462.

Li, J., Li, H., Fu, Q., Liao, Q., Zhu, X., Kobayashi, H., & Ye, D. (2017). Voltage reversal causes bioanode corrosion in microbial fuel cell stacks. *International Journal of Hydrogen Energy*, *42*(45), 27649–27656.

Li, W. W., Yu, H. Q., & He, Z. (2014). Towards sustainable wastewater treatment by using microbial fuel cells-centered technologies. *Energy and Environmental Science*, *7*(3), 911–924.

Li, X., Liu, G. G., Ma, F., Sun, S., Zhou, S., Ardhi, R. E. A., Lee, J. K., Yao, H., Fu, J., Liang, R., Liu, G. G., Yu, A., Bai, Z., Yang, L., Chen, Z., Chatterjee, P., Ghangrekar, M. M., Leech, D., Chaijak, P., … Feng, W. (2018). Enhancing electricity generation using a laccase-based microbial fuel cell with yeast Galactomyces reessii on the cathodes. *Electrochimica Acta*, *230*(8), 46–58.

Li, Z., Yao, L., Kong, L., & Liu, H. (2008). Electricity generation using a baffled microbial fuel cell convenient for stacking. *Bioresource Technology*, *99*(6), 1650–1655.

Liew, R. K., Nam, W. L., Chong, M. Y., Phang, X. Y., Su, M. H., Yek, P. N. Y., Ma, N. L., Cheng, C. K., Chong, C. T., & Lam, S. S. (2018). Oil palm waste: An abundant and promising feedstock for microwave pyrolysis conversion into good quality biochar with potential multi-applications. *Process Safety and Environmental Protection*, *115*, 57–69.

Liu, D., Chang, Q., Gao, Y., Huang, W., Sun, Z., Yan, M., & Guo, C. (2020). High performance of microbial fuel cell afforded by metallic tungsten carbide decorated carbon cloth anode. *Electrochimica Acta*, *330*, 135243.

Liu, H, Cheng, S., & Logan, B. E. (2005). Production of Electricity from Acetate or Butyrate Using a Single-Chamber Microbial Fuel Cell. *Environmental Science & Technology*, *39*(2), 658–662.

Liu, Hong, Cheng, S., & Logan, B. E. (2005). Power generation in fed-batch microbial fuel cells as a function of ionic strength, temperature, and reactor configuration. *Environmental Science and Technology*, *39*(14), 5488–5493.

Liu, Hong, & Logan, B. E. (2004). Electricity generation using an air-cathode single chamber microbial fuel cell in the presence and absence of a proton exchange membrane. *Environmental Science and Technology*, *38*(14), 4040–4046.

Liu, Hong, Ramnarayanan, R., & Logan, B. E. (2004). Production of Electricity during Wastewater Treatment Using a Single Chamber Microbial Fuel Cell. *Environmental Science and Technology*, *38*(7), 2281–2285.

Liu, S. H., Lai, C. Y., Ye, J. W., & Lin, C. W. (2018). Increasing removal of benzene from groundwater using stacked tubular air-cathode microbial fuel cells. *Journal of Cleaner Production*, *194*, 78–84.

Logan, B. E., Wallack, M. J., Kim, K. Y., He, W., Feng, Y., & Saikaly, P. E. (2015). Assessment of Microbial Fuel Cell Configurations and Power Densities. *Environmental Science and Technology Letters*, *2*(8), 206–214.

López Velarde Santos, M., Rodríguez Valadéz, F. J., Mora Solís, V., González Nava, C., Cornejo Martell, A. J., & Hensel, O. (2017). Performance of a microbial fuel cell operated with vinasses using different cod concentrations. *Revista Internacional de Contaminacion Ambiental*, *33*(3), 521–528.

Luo, S., & He, Z. (2016). Ni-Coated Carbon Fiber as an Alternative Cathode Electrode Material to Improve Cost Efficiency of Microbial Fuel Cells. *Electrochimica Acta*, *222*, 338–346.

Mahmood, N. A. N., Thong, L. K., Ibrahim, K. A., Chyan, J. B., & Ghazali, N. F. (2015). Power generation from pre-treated empty fruit bunch using single chamber microbial fuel cell. *Chemical Engineering Transactions*, *45*, 79–84.

Mahmoud, R. H., Samhan, F. A., Ibrahim, M. K., Ali, G. H., & Hassan, R. Y. A. (2020). Boosting the cathode function toward the oxygen reduction reaction in microbial fuel cell using nanostructured surface modification. *Electrochemical Science Advances*, *1*(1), 1–7.

Malik, S., Kishore, S., Dhasmana, A., Kumari, P., Mitra, T., Chaudhary, V., Kumari, R., Bora, J., Ranjan, A., Minkina, T., & Rajput, V. D. (2023). A Perspective Review on Microbial Fuel Cells in Treatment and Product Recovery from Wastewater. *Water*, *15*(2).

Manoharan, Y., Hosseini, S. E., Butler, B., & Alzhahrani, H. (2019). Hydrogen Fuel Cell Vehicles; Current Status and Future Prospect. *Applied Sciences (Switzerland)*.

Mateo, S., Cantone, A., Cañizares, P., Fernández-Morales, F. J., Scialdone, O., & Rodrigo, M. A. (2018). On the staking of miniaturized air-breathing microbial fuel cells. *Applied Energy*, *232*(September), 1–8.

Merino-Jimenez, I., Santoro, C., Rojas-Carbonell, S., Greenman, J., Ieropoulos, I., & Atanassov, P. (2016). Carbon-based air-breathing cathodes for microbial fuel cells. *Catalysts*, *6*(9), 1–13.

Min, B., Kim, J. R., Oh, S. E., Regan, J. M., & Logan, B. E. (2005). Electricity generation from swine wastewater using microbial fuel cells. *Water Research*, *39*(20), 4961–4968.

Mohammad, I. N., Ongkudon, C. M., & Misson, M. (2020). Physicochemical properties and lignin degradation of thermal-pretreated oil palm empty fruit bunch. *Energies*, *13*(22).

Mohd Zaini Makhtar, M., & Tajarudin, H. A. (2020). Electricity generation using membrane-less microbial fuel cell powered by sludge supplemented with lignocellulosic waste. *International Journal of Energy Research*, *44*(4), 3260–3265.

Moosavi, S. M., Niffeler, M., Gostick, J., & Haussener, S. (2017). Transport characteristics of saturated gas diffusion layers treated with hydrophobic coatings. *Chemical Engineering Science*, *176*, 503–514.

Nawaz, A., Haq, I. ul, Qaisar, K., Gunes, B., Raja, S. I., Mohyuddin, K., & Amin, H. (2022). Microbial fuel cells: Insight into simultaneous wastewater treatment and bioelectricity generation. *Process Safety and Environmental Protection*, *161*, 357–373.

Nguyen, C. L., Tartakovsky, B., & Woodward, L. (2019). Harvesting Energy from Multiple Microbial Fuel Cells with a High-Conversion Efficiency Power Management System. *ACS Omega*, *4*(21), 18978–18986.

Noori, P., & Najafpour Darzi, G. (2016). Enhanced power generation in annular single-chamber microbial fuel cell via optimization of electrode spacing using chocolate industry wastewater. *Biotechnology and Applied Biochemistry*, *63*(3), 427–434.

Oh, S. E., & Logan, B. E. (2006). Proton exchange membrane and electrode surface areas as factors that affect power generation in microbial fuel cells. *Applied Microbiology and Biotechnology*, *70*(2), 162–169.

Oliot, M., Etcheverry, L., Mosdale, R., & Bergel, A. (2017). Microbial fuel cells connected in series in a common electrolyte underperform: Understanding why and in what context such a set-up can be applied. *Electrochimica Acta*, *246*, 879–889.

Pandit, S., Savla, N., & Jung, S. P. (2020). Recent advancements in scaling up microbial fuel cells. In *Integrated Microbial Fuel Cells for Wastewater Treatment*. Elsevier Inc.

Pant, D., Van Bogaert, G., Diels, L., & Vanbroekhoven, K. (2010). A review of the substrates used in microbial fuel cells (MFCs) for sustainable energy production. *Bioresource Technology*, *101*(6), 1533–1543.

Papillon, J., Ondel, O., & Maire, É. (2021). Scale up of single-chamber microbial fuel cells with stainless steel 3D anode: Effect of electrode surface areas and electrode spacing. *Bioresource Technology Reports*, *13*.

Park, S. G., Rajesh, P. P., Hwang, M. H., Chu, K. H., Cho, S., & Chae, K. J. (2021). Long-term effects of anti-biofouling proton exchange membrane using silver nanoparticles and polydopamine on the performance of microbial electrolysis cells. *International Journal of Hydrogen Energy*, *46*(20), 11345–11356.

Pedersen, O., Colmer, T. D., & Sand-Jensen, K. (2013). Underwater photosynthesis of submerged plants - Recent advances and methods. *Frontiers in Plant Science*, *4*(MAY), 1–20.

Penteado, E. D., Fernandez-Marchante, C. M., Zaiat, M., Cañizares, P., Gonzalez, E. R., & Rodrigo, M. A. R. (2016). Energy recovery from winery wastewater using a dual chamber microbial fuel cell. *Journal of Chemical Technology and Biotechnology*, *91*(6), 1802–1808.

Popat, S. C., Ki, D., Rittmann, B. E., & Torres, C. I. (2012). Importance of OH- transport from cathodes in microbial fuel cells. *ChemSusChem*, *5*(6), 1071–1079.

Preen, R. J., You, J., Bull, L., & Ieropoulos, I. A. (2019). Design mining microbial fuel cell cascades. *Soft Computing*, *23*(13), 4673–4683.

Qi, J., Li, F., Jia, L., Zhang, X., Deng, S., Luo, B., Zhou, Y., Fan, M., & Xia, Y. (2023). Fungal Selectivity and Biodegradation Effects by White and Brown Rot Fungi for Wood Biomass Pretreatment. *Polymers*, *15*(8), 1–15.

Rahayu, D. E., Wirjodirdjo, B., & Hadi, W. (2019). Availability of empty fruit bunch as biomass feedstock for sustainability of bioenergy product (system dynamic approach). *AIP Conference Proceedings*, *2194*(December).

Rahimnejad, M., Bakeri, G., Ghasemi, M., & Zirepour, A. (2014). A review on the role of proton exchange membrane on the performance of microbial fuel cell. *Polymers for Advanced Technologies*, *25*(12), 1426–1432.

Rahmani, A. R., Navidjouy, N., Rahimnejad, M., Alizadeh, S., Samarghandi, M. R., & Nematollahi, D. (2022). Effect of different concentrations of substrate in microbial fuel cells toward bioenergy recovery and simultaneous wastewater treatment. *Environmental Technology (United Kingdom)*, *43*(1), 1–9.

Ramirez-Nava, J., Martínez-Castrejón, M., García-Mesino, R. L., López-Díaz, J. A., Talavera-Mendoza, O., Sarmiento-Villagrana, A., Rojano, F., & Hernández-Flores, G. (2021). The implications of membranes used as separators in microbial fuel cells. *Membranes*, *11*(10), 1–27.

Reinhard, S., Sitorus, I., Hani, M., Bakar, A., & Majlan, E. H. (2020). Review on High-Performance Air Cathode Microbial Fuel Cell for Power Generation and COD Reduction. *Jurnal Kejuruteraan*, *32*(4), 569–577.

Rohma, N. A., Suhartini, S., & Nurika, I. (2021). Chemical pre-treatments on oil palm empty fruit bunches: Impacts on characteristics and methane potential. *IOP Conference Series: Earth and Environmental Science*, *924*(1).

Rosli, N. S., Harun, S., Jahim, J. M., & Othaman, R. (2017). Chemical and Physical Characterization of Oil Palm Empty Fruit Bunch. *Malaysian Journal of Analytical Sciences*, *21*(1), 188–196.

Rozendal, R. A., Hamelers, H. V. M., Rabaey, K., Keller, J., & Buisman, C. J. N. (2008). Towards practical implementation of bioelectrochemical wastewater treatment. *Trends in Biotechnology*, *26*(8), 450–459.

Ruscalleda Beylier, M., Balaguer, M. D., Colprim, J., Pellicer-Nàcher, C., Ni, B. J., Smets, B. F., Sun, S. P., & Wang, R. C. (2019). Biological nitrogen removal from domestic wastewater. *Comprehensive Biotechnology*, *6*, 285–296.

Rusyn, I. B., Medvediev, O. V., & Valko, B. T. (2021). Enhancement of bioelectric parameters of multi-electrode plant–microbial fuel cells by combining of serial and parallel connection. *International Journal of Environmental Science and Technology*, *18*(6), 1323–1334.

Saba, B., Christy, A. D., Yu, Z., Co, A. C., Islam, R., & Tuovinen, O. H. (2017). Characterization and performance of anodic mixed culture biofilms in submersed microbial fuel cells. *Bioelectrochemistry*, *113*, 79–84.

Saha, M. S., Neburchilov, V., Ghosh, D., & Zhang, J. (2013). Nanomaterials-supported Pt catalysts for proton exchange membrane fuel cells. *Wiley Interdisciplinary Reviews: Energy and Environment*, *2*(1), 31–51.

Saravanan, N., & Karthikeyan, M. (2018). Study of Single Chamber and Double Chamber Efficiency and Losses of Wastewater Treatment. *International Research Journal of Engineering and Technology*, *5*(3), 1225–1230.

Sarmin, S., Ideris, A. B., Ethiraj, B., Amirul Islam, M., Yee, C. S., & Rahman Khan, M. M. (2020). Potentiality of petrochemical wastewater as substrate in microbial fuel cell. *IOP Conference Series: Materials Science and Engineering*, *736*(3).

Sayed, E. T., Tsujiguchi, T., & Nakagawa, N. (2012). Catalytic activity of baker's yeast in a mediatorless microbial fuel cell. *Bioelectrochemistry*, *86*, 97–101.

Schoemaker, H. E., & Leisola, M. S. A. (1990). Degradation of lignin by Phanerochaete chrysosporium. *Journal of Biotechnology*, *13*, 101–109.

Shabani, M., Pontié, M., Younesi, H., Nacef, M., Rahimpour, A., Rahimnejad, M., & Bouchenak Khelladi, R. M. (2021). Biodegradation of acetaminophen and its main by-product 4-aminophenol by Trichoderma harzianum versus mixed biofilm of Trichoderma harzianum/Pseudomonas fluorescens in a fungal microbial fuel cell. *Journal of Applied Electrochemistry*, *51*(4), 581–596.

Shantaram, A., Beyenal, H., Veluchamy, R. R. A., & Lewandowski, Z. (2005). Wireless sensors powered by microbial fuel cells. *Environmental Science and Technology*, *39*(13), 5037–5042.

Sharma, Y., & Li, B. (2010). The variation of power generation with organic substrates in single-chamber microbial fuel cells (SCMFCs). *Bioresource Technology*, *101*(6), 1844–1850.

Shen, J., Hou, L., Sun, H., Hu, M., Zang, L., Zhang, Z., Ji, D., & Zhang, F. (2020). Effect of an electro-Fenton process on the biodegradation of lignin by Trametes versicolor. *BioResources*, *15*(4), 8039–8050.

Shimoyama, T., Komukai, S., Yamazawa, A., Ueno, Y., Logan, B. E., & Watanabe, K. (2008). Electricity generation from model organic wastewater in a cassette-electrode microbial fuel cell. *Applied Microbiology and Biotechnology*, *80*(2), 325–330.

Shu, C., Wang, E., Jiang, L., & Sun, G. (2013). High performance cathode based on carbon fiber felt for magnesium-air fuel cells. *International Journal of Hydrogen Energy*, *38*(14), 5885–5893.

Sigoillot, J. C., Berrin, J. G., Bey, M., Lesage-Meessen, L., Levasseur, A., Lomascolo, A., Record, E., & Uzan-Boukhris, E. (2012). Fungal Strategies for Lignin Degradation. In *Advances in Botanical Research* (1st ed., Vol. 61). Elsevier Ltd.

Singh, D., & Chen, S. (2008). The white-rot fungus Phanerochaete chrysosporium: Conditions for the production of lignin-degrading enzymes. *Applied Microbiology and Biotechnology*, *81*(3), 399–417.

Singh, K., Risse, M., Das, K. C., & Worley, J. (2009). Determination of composition of cellulose and lignin mixtures using thermogravimetric analysis. *Journal of Energy Resources Technology, Transactions of the ASME*, *131*(2), 0222011–0222016.

Sonawane, J. M., Pant, D., Ghosh, P. C., & Adeloju, S. B. (2019). Fabrication of a Carbon Paper/Polyaniline-Copper Hybrid and Its Utilization as an Air Cathode for Microbial Fuel Cells [Research-article]. *ACS Applied Energy Materials*, *2*(3), 1891–1902.

Strycharz, S. M., Glaven, R. H., Coppi, M. V., Gannon, S. M., Perpetua, L. A., Liu, A., Nevin, K. P., & Lovley, D. R. (2011). Gene expression and deletion analysis of mechanisms for electron transfer from electrodes to Geobacter sulfurreducens. *Bioelectrochemistry*, *80*(2), 142–150.

Sukri, A., Othman, R., Abd-Wahab, F., & Noor, N. M. (2021). Self-sustaining bioelectrochemical cell from fungal degradation of lignin-rich agrowaste. *Energies*, *14*(8).

Tanaka, K., Yokoe, S., Igarashi, K., Takashino, M., Ishikawa, M., Hori, K., Nakanishi, S., & Kato, S. (2018). Extracellular electron transfer via outer membrane cytochromes in a methanotrophic bacterium methylococcus capsulatus (Bath). *Frontiers in Microbiology*, *9*(NOV), 1–7.

Tandukar, M., Huber, S. J., Onodera, T., & Pavlostathis, S. G. (2009). Biological chromium(VI) reduction in the cathode of a microbial fuel cell. *Environmental Science and Technology*, *43*(21), 8159–8165.

Tang, X., Guo, K., Li, H., Du, Z., & Tian, J. (2010). Microfiltration membrane performance in two-chamber microbial fuel cells. *Biochemical Engineering Journal*, *52*(2–3), 194–198.

Tien, M., & Kirk, T. K. (1984). Lignin-degrading enzyme from Phanerochaete chrysosporium : Purification, characterization, and catalytic properties of a unique H 2 O 2 -requiring oxygenase. *Proceedings of the National Academy of Sciences*, *81*(8), 2280–2284.

Tiwari, S., Koreti, D., Kosre, A., Mahish, P. K., Jadhav, S. K., & Chandrawanshi, N. K. (2021). Fungal Microbial Fuel Cells, an Opportunity for Energy Sources. *Energy*, *March 2022*, 250–273.

Tomboc, G. M., Yu, P., Kwon, T., Lee, K., & Li, J. (2020). Ideal design of air electrode-A step closer toward robust rechargeable Zn-air battery. *APL Materials*, *8*(5).

Tront, J. M., Fortner, J. D., Plötze, M., Hughes, J. B., & Puzrin, A. M. (2008). Microbial fuel cell biosensor for in situ assessment of microbial activity. *Biosensors and Bioelectronics*, *24*(4), 586–590.

Ullah, Z., & Zeshan, S. (2020). Effect of substrate type and concentration on the performance of a double chamber microbial fuel cell. *Water Science and Technology*, *81*(7), 1336–1344.

Umar, M. F., Abbas, S. Z., Mohamad Ibrahim, M. N., Ismail, N., & Rafatullah, M. (2020). Insights into advancements and electrons transfer mechanisms of electrogens in benthic microbial fuel cells. *Membranes*, *10*(9), 1–18.

Ungan, H., & Bayrakçeken Yurtcan, A. (2019). PEMFC catalyst layer modification with the addition of different amounts of PDMS polymer in order to improve water management. *International Journal of Energy Research*, *43*(11), 5946–5958.

Vasileva, E., Parvanova-Mancheva, T., Beschkov, V., Alexieva, Z., Gerginova, M., & Peneva, N. (2021). Effects of constant electric field on biodegradation of phenol by free and immobilized cells of bradyrhizobium japonicum 273. *ChemEngineering*, *5*(4).

Velasquez-Orta, S. B., Head, I. M., Curtis, T. P., & Scott, K. (2011). Factors affecting current production in microbial fuel cells using different industrial wastewaters. *Bioresource Technology*, *102*(8), 5105–5112.

Venkata Mohan, S., Saravanan, R., Raghavulu, S. V., Mohanakrishna, G., & Sarma, P. N. (2008). Bioelectricity production from wastewater treatment in dual chambered microbial fuel cell (MFC) using selectively enriched mixed microflora: Effect of catholyte. *Bioresource Technology*, *99*(3), 596–603.

Verboven, P., Pedersen, O., Ho, Q. T., Nicolai, B. M., & Colmer, T. D. (2014). The mechanism of improved aeration due to gas films on leaves of submerged rice. *Plant Cell and Environment*, *37*(10), 2433–2452.

Wang, B., & Han, J. I. (2009). A single chamber stackable microbial fuel cell with air cathode. *Biotechnology Letters*, *31*(3), 387–393.

Wang, C. T., Huang, Y. S., Sangeetha, T., Chen, Y. M., Chong, W. T., Ong, H. C., Zhao, F., & Yan, W. M. (2018). Novel bufferless photosynthetic microbial fuel cell (PMFCs) for enhanced electrochemical performance. *Bioresource Technology*, *255*(October 2017), 83–87.

Wang, Y., & Leung, D. Y. C. (2017). Optimization of Cathode Flooding in Scaled-up Microfluidic Fuel Cells. *Energy Procedia*, *105*, 1454–1460.

Watson, V. J., Nieto Delgado, C., & Logan, B. E. (2013). Influence of chemical and physical properties of activated carbon powders on oxygen reduction and microbial fuel cell performance. *Environmental Science and Technology*, *47*(12), 6704–6710.

Wei, J., Liang, P., & Huang, X. (2011). Recent progress in electrodes for microbial fuel cells. *Bioresource Technology*, *102*(20), 9335–9344.

Whiddon, E., Zhu, H., & Zhu, X. (2019). Sodium-ion concentration flow cell stacks for salinity gradient energy recovery: Power generation of series and parallel configurations. *Journal of Power Sources*, *435*.

Winkel, A., Colmer, T. D., & Pedersen, O. (2011). Leaf gas films of Spartina anglica enhance rhizome and root oxygen during tidal submergence. *Plant, Cell and Environment*, *34*(12), 2083–2092.

Winkel, A., Pedersen, O., Ella, E., Ismail, A. M., & Colmer, T. D. (2014). Gas film retention and underwater photosynthesis during field submergence of four contrasting rice genotypes. *Journal of Experimental Botany*, *65*(12), 3225–3233.

Winkel, A., Visser, E. J. W., Colmer, T. D., Brodersen, K. P., Voesenek, L. A. C. J., Sand-Jensen, K., & Pedersen, O. (2016). Leaf gas films, underwater photosynthesis and plant species distributions in a flood gradient. *Plant, Cell and Environment*, *39*(7), 1537–1548.

Wong, D. W. S. (2009). Structure and action mechanism of ligninolytic enzymes. *Applied Biochemistry and Biotechnology*, *157*(2), 174–209.

Wu, M. S., Lin, C. Y., Wang, Y. Y., Wan, C. C., & Yang, C. R. (2006). Numerical simulation for the discharge behaviors of batteries in series and/or parallel-connected battery pack. *Electrochimica Acta*, *52*(3), 1349–1357.

Wu, S., Li, H., Zhou, X., Liang, P., Zhang, X., Jiang, Y., & Huang, X. (2016). A novel pilot-scale stacked microbial fuel cell for efficient electricity generation and wastewater treatment. *Water Research*, *98*, 396–403.

Xu, F., & Li, Y. (2017). Biomass Digestion. *Encyclopedia of Sustainable Technologies*, *3*(2015), 197–204.

Yadav, M., & Vivekanand, V. (2019). Chaetomium globosporum: A novel laccase producing fungus for improving the hydrolyzability of lignocellulosic biomass. *Heliyon*, *5*(3), e01353.

Yang, S., Jia, B., & Liu, H. (2009). Effects of the Pt loading side and cathode-biofilm on the performance of a membrane-less and single-chamber microbial fuel cell. *Bioresource Technology*, *100*(3), 1197–1202.

Yang, Wei, Fu, Q., Zhang, L., & Zhu, X. (2019). Waste to Sustainable Energy. In *Waste to Sustainable Energy* (Issue March). Taylor & Francis.

Yang, Wei, Li, J., Fu, Q., Zhang, L., Zhu, X., & Liao, Q. (2019). Cost-effective Carbon Catalysts and Related Electrode Designs for the Air Cathode of Microbial Fuel Cells. In *Waste to Sustainable Energy* (Issue March). Taylor & Francis.

Yang, Wulin, He, W., Zhang, F., Hickner, M. A., & Logan, B. E. (2014). Single-Step Fabrication Using a Phase Inversion Method of Poly(vinylidene fluoride) (PVDF) Activated Carbon Air Cathodes for Microbial Fuel Cells. *Environmental Science and Technology Letters*, *1*(10), 416–420.

Yang, Wulin, Kim, K. Y., & Logan, B. E. (2015). Development of carbon free diffusion layer for activated carbon air cathode of microbial fuel cells. *Bioresource Technology*, *197*, 318–322.

Yang, Y., Yan, L., Lin, X., Li, P., & Xu, M. (2019). Effects of unit distance and number on sediment microbial fuel cell stacks for practical power supply. *International Journal of Energy Research*, *43*(13), 7287–7295.

Yi, Y., Xie, B., Zhao, T., Li, Z., Stom, D., & Liu, H. (2019). Effect of external resistance on the sensitivity of microbial fuel cell biosensor for detection of different types of pollutants. *Bioelectrochemistry*, *125*, 71–78.

Youn, H. D., Hah, Y. C., & Kang, S. O. (1995). Role of laccase in lignin degradation by white-rot fungi. *FEMS Microbiology Letters*, *132*(3), 183–188.

Yuan, H., Hou, Y., Abu-Reesh, I. M., Chen, J., & He, Z. (2016). Oxygen reduction reaction catalysts used in microbial fuel cells for energy-efficient wastewater treatment: A review. *Materials Horizons*, *3*(5), 382–401.

Zhang, J., Zhang, B., Tian, C., Ye, Z., Liu, Y., Lei, Z., Huang, W., & Feng, C. (2013). Simultaneous sulfide removal and electricity generation with corn stover biomass as co-substrate in microbial fuel cells. *Bioresource Technology*, *138*, 198–203.

Zhang, Y., Min, B., Huang, L., & Angelidaki, I. (2009). Generation of electricity and analysis of microbial communities in wheat straw biomass-powered microbial fuel cells. *Applied and Environmental Microbiology*, *75*(11), 3389–3395.

Zhong, C., Zhang, B., Kong, L., Xue, A., & Ni, J. (2010). Electricity generation from molasses wastewater by an anaerobic baffled stacking microbial fuel cell. *Journal of Chemical Technology and Biotechnology*, *86*(3), 406–413.

Zhou, M., Yang, J., Wang, H., Jin, T., Hassett, D. J., & Gu, T. (2014). Bioelectrochemistry of Microbial Fuel Cells and their Potential Applications in Bioenergy. In *Bioenergy Research: Advances and Applications*. Elsevier.

Zhuang, L., Zheng, Y., Zhou, S., Yuan, Y., Yuan, H., & Chen, Y. (2012). Scalable microbial fuel cell (MFC) stack for continuous real wastewater treatment. *Bioresource Technology*, *106*, 82–88.

Zou, L., Qiao, Y., Zhong, C., & Li, C. M. (2017). Enabling fast electron transfer through both bacterial outer-membrane redox centers and endogenous electron mediators by polyaniline hybridized large-mesoporous carbon anode for high-performance microbial fuel cells. *Electrochimica Acta*, *229*, 31–38.

APPENDICES

APPENDIX-A: EXPERIMENTAL SETUP FOR PARALLEL AND OPEN-PARALLE UNIT-CELL CONFIGURATION

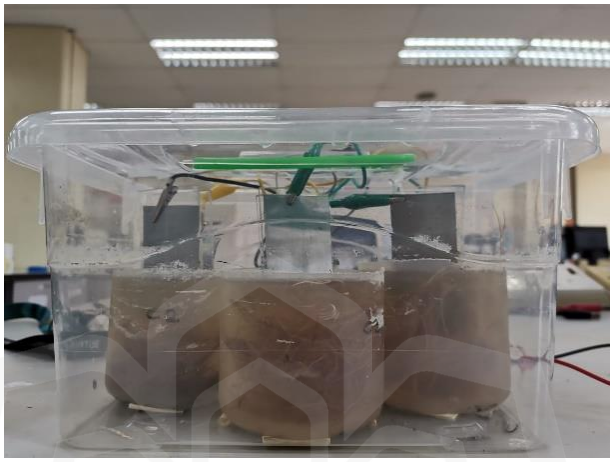

(a)

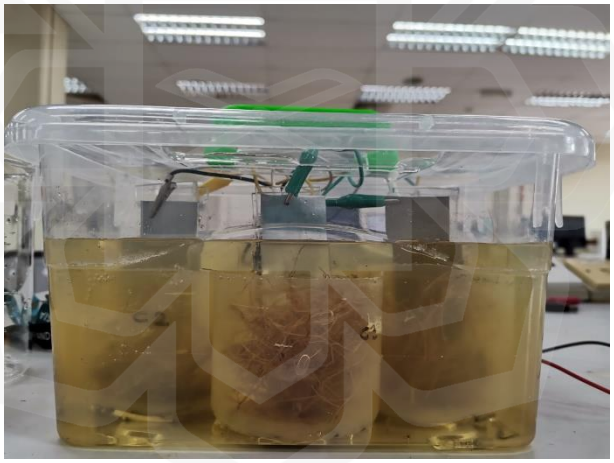

(b)

Figure show setup for the measurement of parasitic current during open circuit voltage (OCV): (a) parallel MFC and (b) open-parallel unit cell configuration after parallel MFC stack filled up with PDB electrolyte until all mini cells were totally submerged.

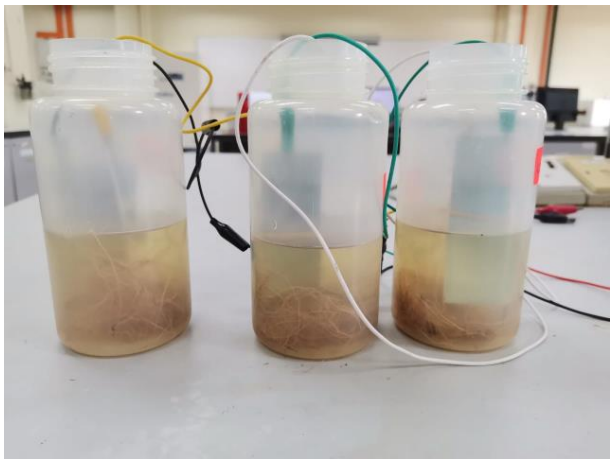

Figure show setup for parallel MFC

APPENDIX-B: EXPERIMENTAL SETUP FOR A LOW-COST, EASY TO FABRICATE CARBON-BASED AIR CATHODE FOR MFC

Figure show components of air cathode

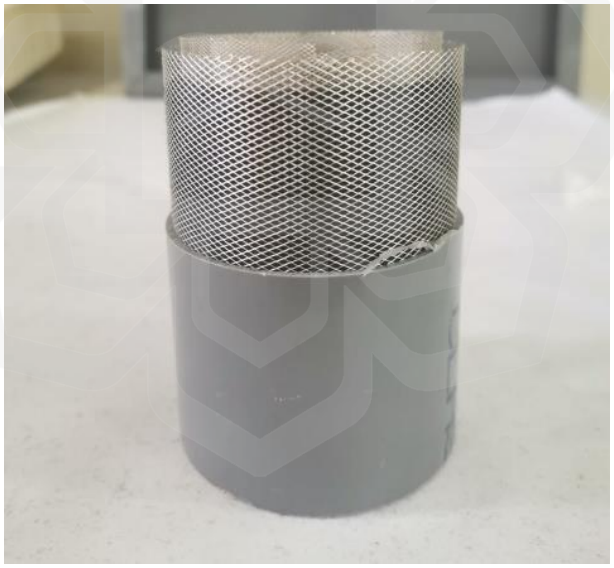

Figure show assembled air cathode

Figure show setup for zinc/air MFC with fabricated air cathode

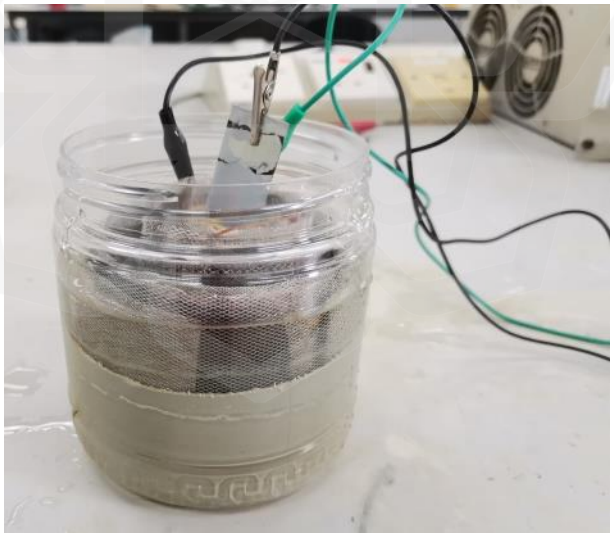

Figure show setup for zinc/air MFC with bipolar configuration

LIST OF PUBLICATION

Sukri, A., Othman, R., Sarifuddin, N. (2023), An Effective, Easy-to-Fabricate Submerged Carbon-Based Air Cathode for Biofuel Cells, IIUM Engineering Journal [Under review]

Raihan Othman, Asiah Sukri, Nurfazwani Ain Nur Ahmad and Firdaus Abd-Wahab, “Microbial Fuel Unit-Cell with Open-Parallel Configuration” Malaysian Patent (PI2021006687)